

HYDROFOIL SIMULATION IN SIX
DEGREES OF FREEDOM

DEC 75

Jose A. G. Salinas Moreira Ribeiro

DUDLEY KNOX LIBRARY
NAVAL POSTGRADUATE SCHOOL
MONTEREY, CALIFORNIA 93940

NAVAL POSTGRADUATE SCHOOL

Monterey, California



THESIS

HYDROFOIL SIMULATION IN
SIX DEGREES OF FREEDOM

by

Jose A. G. Salinas Moreira Ribeiro

December 1975

Thesis Advisor:

G. J. Thaler

Approved for public release; distribution unlimited.

T171663

REPORT DOCUMENTATION PAGE		READ INSTRUCTIONS BEFORE COMPLETING FORM
1. REPORT NUMBER	2. GOVT ACCESSION NO.	3. RECIPIENT'S CATALOG NUMBER
4. TITLE (and Subtitle) HYDROFOIL SIMULATION IN SIX DEGREES OF FREEDOM		5. TYPE OF REPORT & PERIOD COVERED Master's Thesis December 1975
		6. PERFORMING ORG. REPORT NUMBER
7. AUTHOR(s) Jose A. G. Salinas Moreira Ribeiro		8. CONTRACT OR GRANT NUMBER(s)
9. PERFORMING ORGANIZATION NAME AND ADDRESS Naval Postgraduate School Monterey, California 93940		10. PROGRAM ELEMENT, PROJECT, TASK AREA & WORK UNIT NUMBERS
11. CONTROLLING OFFICE NAME AND ADDRESS Naval Postgraduate School Monterey, California 93940		12. REPORT DATE December 1975
		13. NUMBER OF PAGES 127
14. MONITORING AGENCY NAME & ADDRESS (if different from Controlling Office) Naval Postgraduate School Monterey, California 93940		15. SECURITY CLASS. (of this report) Unclassified
		15a. DECLASSIFICATION/DOWNGRADING SCHEDULE
16. DISTRIBUTION STATEMENT (of this Report) Approved for public release. Distribution unlimited.		
17. DISTRIBUTION STATEMENT (of the abstract entered in Block 20, if different from Report)		
18. SUPPLEMENTARY NOTES		
19. KEY WORDS (Continue on reverse side if necessary and identify by block number) Hydrofoil Freedom		
20. ABSTRACT (Continue on reverse side if necessary and identify by block number) The heeling behavior of a fully-submerged foil hydrofoil craft turning, has been studied by producing a digital computer simulation program, using a Digital Simulation Language on the digital computer IBM system 360/67. The High Point PC(H)-1 is used as the model of this simulation.		

Hydrofoil Simulation in
Six Degrees of Freedom

by

Jose A. G. Salinas Moreira Ribeiro
Lieutenant, Portuguese Navy

Submitted in partial fulfillment of the
requirements for the degree of

MASTER OF SCIENCE IN ELECTRICAL ENGINEERING

from the

NAVAL POSTGRADUATE SCHOOL
December 1975

ABSTRACT

The heeling behavior of a fully-submerged foil hydrofoil craft turning, has been studied by producing a digital computer simulation program, using a Digital Simulation Language on the digital computer IBM system 360/67. The High Point PC(H)-1 is used as the model of this simulation.

TABLE OF CONTENTS

I.	INTRODUCTION-----	12
II.	HYDROFOIL EQUATIONS STUDY-----	13
	A• FOIL TYPES AND FOIL ARRANGEMENT-----	13
	B• COORDINATE SYSTEMS-----	18
	C• EQUATIONS OF MOTION-----	22
	D• CALCULATION OF VELOCITY COMPONENTS-----	25
	E• ANGLE OF ATTACK AND ANGLE OF SIDE SLIP-----	28
	F• EXPANSION OF FORCES AND MOMENT TERMS-----	30
III.	HYDROFOIL SIMULATION-----	32
	A• SIMULATION OBJECTIVES-----	32
	B• COMPUTER SIMULATION-----	33
	C• AUTOMATIC CONTROL-----	35
	1. Vertical Gyros-----	35
	2. Rate Gyros-----	35
	3. Accelerometers-----	35
	4. Height Sensors-----	36
IV.	HYDROFOIL TURNING CHARACTERISTICS STUDY-----	38
	A• RUDDER EFFECTS-----	38
	1. Speed=30 Knots-----	38
	2. Speed=36 Knots, Rudder to Starboard-----	40
	3. Speed=36 Knots, Rudder to Port-----	41
	4. Speed=40 Knots-----	42
	5. Speed=50 Knots-----	43
	B• EFFECTS OF A HELM STEP COMMAND-----	70
	1. Speed=30 Knots-----	71
	2. Speed=36 Knots-----	72
	3. Speed=40 Knots-----	73
	4. Speed=50 Knots-----	73
	C• RESULTS WITH THE SPLITTING OF THE FORWARD FOIL---	95
	D• CALCULATION OF THE CORRECT ROLL ANGLE-----	97

V. CONCLUSIONS AND RECOMMENDATIONS FOR FURTHER STUDIES	104
APPENDIX A SUMMARY OF COMPLETE EQUATIONS-----	105
COMPUTER PROGRAMS-----	110
LIST OF REFERENCES-----	126
INITIAL DISTRIBUTION LIST-----	127

TABLE OF SYMBOLS

A_F	Feet ²	Area of foil
A_S	Feet ²	Area of strut
CG		Center of gravity
C_{DF}	Dimensionless	Drag coefficient of a foil
C_{DS}	Dimensionless	Drag coefficient of a strut
C_L	Dimensionless	Lift coefficient
C_S	Dimensionless	Side force coefficient
F_{CENT}	Pounds	Craft's centrifugal force
F_{DiF}	Pounds	Drag force on a foil (water axes)
F_{DiS}	Pounds	Drag force on a strut (water axes)
F_{LiF}	Pounds	Lift force on a foil (water axes)
F_{NET}	Pounds	Perpendicular force to craft's deck
F_{SiS}	Pounds	Side force on a strut (water axes)
F_X	Pounds	Force in direction of body X-axis
F_{XiF}	Pounds	Force on a foil in body X-axis
F_Y	Pounds	Force in direction of body Y-axis
F_{YiF}	Pounds	Force on a foil in body Y-axis
F_{YiS}	Pounds	Force on a strut in body Y-axis

F_Z	Pounds	Force in direction of body Z-axis
F_{ZiF}	Pounds	Force on a foil in body Z-axis
F_{ZiS}	Pounds	Force on a strut in body Z-axis
g_X	Feet/Second ²	Component of gravity in body X-axis
g_Y	Feet/Second ²	Component of gravity in body Y-axis
g_Z	Feet/Second ²	component of gravity in body Z-axis
Helm _r	Radians	Helm angle
h_S	Feet	Height of Height Sensor above instantaneous water surface
I_{XX}	Slug-Foot ²	Moment of inertia about body X-axis
I_{YY}	Slug-Foot ²	Moment of inertia about body Y-axis
I_{ZZ}	Slug-Foot ²	Moment of inertia about body Z-axis
L	Foot-Pound	Moment acting to produce roll about body X-axis
L_{XiF}	Feet	Distance from CG. along body X-axis to a point of application of foil force
L_{YiF}	Feet	Distance from CG. along body Y-axis to a point of application of foil force

L_{ZiF}	Feet	Distance from CG. along body Z-axis to a point of application of foil force
L_{ZiS}	Feet	Distance from CG. along body Z-axis to a point of application of strut force
M	Foot-Pound	Moment acting to produce pitch about body Y-axis
m	Slugs	Mass of the craft
N	Foot-Pound	Moment acting to produce yaw about body Z-axis
P	Radians/Second	Roll rate about body X-axis
Q	Radians/Second	Pitch rate about body Y-axis
R	Radians/Second	Yaw rate about body Z-axis
Rgir	Feet	Craft's turning radius
Rudr	Radians	Rudder angle
S_{EiF}	Feet	Submergence of a foil in earth axes
S_{EiS}	Feet	Submergence in earth axes of the assumed point of application of strut force
T_X	Pounds	Thrust in direction of body X-axis
U	Feet/Second	Velocity in direction of body X-axis
U_E	Feet/Second	Velocity along earth X-axis
U_i	Feet/Second	Foil velocity in direction of body X-axis
V	Feet/Second	Velocity in direction of body Y-axis
V_E	Feet/Second	Velocity along earth Y-axis
V_i	Feet/Second	Foil velocity in direction of

		body Y-axis
W	Feet/Second	Velocity in direction of body Z-axis
W_E	Feet/Second	Velocity along earth Z-axis
W_i	Feet/Second	Foil velocity in direction of body Z-axis
X_E	Feet	Distance along earth X-axis from reference origin
Y_E	Feet	Distance along earth Y-axis from reference origin
Z_E	Feet	Distance along earth Z-axis from reference origin
α_i	Radians	Angle of attack of a foil
β_i	Radians	Angle of side slip of a strut
ρ	Slugs/Foot ³	Water density
Φ	Radians	Roll angle
Ψ	Radians	Yaw angle
θ	Radians	Pitch angle

Subscripts

C	Refers to center foil or strut
P	Refers to port foil or strut
S	Refers to starboard foil or strut
M	Refers to mid foil section
F	Refers to foil
S	Refers to strut
i	When i appears in the subscript to a symbol, it indicates that the symbol is to be repeated with i succesfully replaced by C,P,S and M, as indicated.

ACKNOWLEDGEMENTS

I wish to express my sincere appreciation to Prof. George J. Thaler of the Naval Postgraduate School. His knowledge, dedication, patience, continuous advice and orientation provided the necessary help to the realization of this paper.

To Lt. John J. Uhrin III, USN, for his help on the computer programming work.

To my wife, Alice, who, while competing with the computer, due to my long periods of absence, gave me the necessary moral support to finish this job.

I• INTRODUCTION

This thesis deals with the yaw motion and turning characteristics, in calm water, of the hydrofoil craft PC(H)-1 High Point. This will be the model used in the computer simulation program for this study.

In previous theses, the system was made conditionally stable in two modes, the pitch-heave mode and the roll mode. In this thesis, keeping the system stable and working in six degrees of freedom, its behavior will be analyzed in three modes, pitch mode, roll mode and yaw mode, when the simulated model is turning by the effects of a helm step command, acting on the astern flaps. This analysis will also include the study of rudder effects, aft starboard and aft port flaps effects and the heeling behavior of the system. In a further investigation the forward flap will be split in two parts and pitching and rolling effects will be analyzed.

Since slight changes in the manual control of the system occur in such short time intervals and provoke tremendous effects, the system necessitates an automatic control that will provide the necessary outputs to operate the model according to the given inputs. This automatic control, already existent, will be improved and adapted to the new motion of the craft.

Finally the favourable roll angle for a certain speed and a certain helm step command will be calculated and compared with the actual roll angle of the craft.

II. HYDROFOIL EQUATIONS STUDY

A. FOIL TYPES AND FOIL ARRANGEMENT

There are two principal foil types used in the construction of hydrofoil crafts, the surface-piercing foil and the fully-submerged foil, as shown in Figure 1.

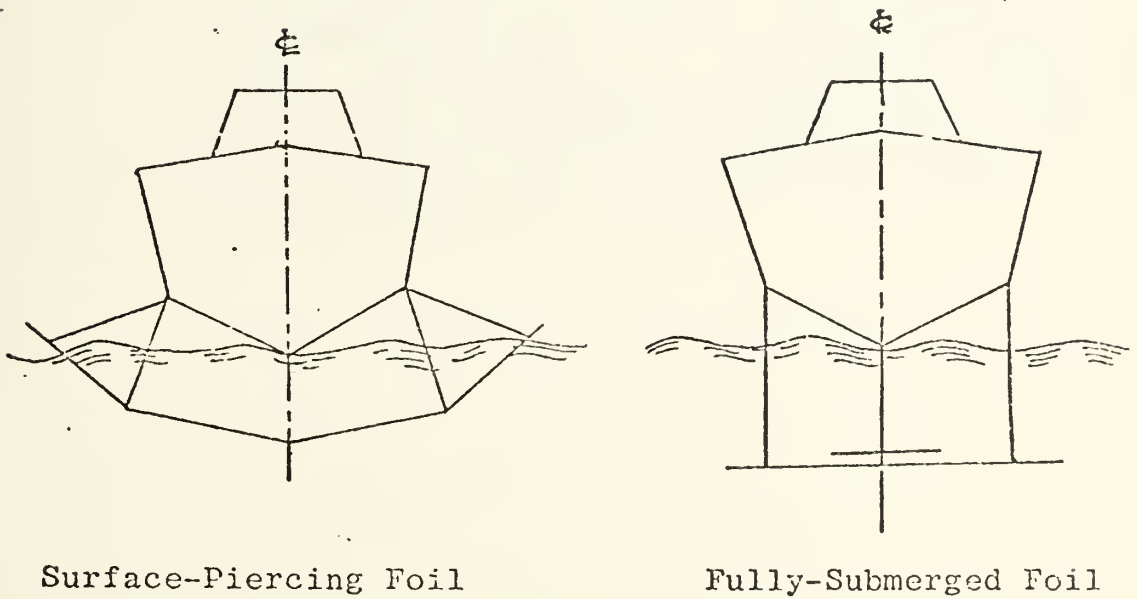


FIGURE 1

TYPE OF HYDROFOIL CRAFT

The surface-piercing foil provides a self-stabilization for the craft in pitch, height and roll. On the other hand the fully-submerged foil cannot adjust itself to a changing lift. This can only be achieved by a change in incidence angle of the foil flaps. The fully-submerged foil requires a more sophisticated sensing arrangement to control that incidence. But the fully-submerged foil has a great advantage, when the craft is operating in heavy sea. The surface-piercing foil responds to relatively small changes in the surface of the sea and gives a very rough ride. On the other hand, the fully-submerged foil is much less affected by the effects of the surface of the sea. This paper will only deal with the fully-submerged foil craft.

The model for this simulation, the High Point PC(H)-1, uses the foils in canard arrangement, which has a secondary foil as forward foil and a main foil as aft foil. Both foils are supported by vertical struts. Figure 2, important for the understanding of the digital computer simulation program, shows the configuration of the forward and aft foil. The drawing and the dimensions of the craft and the foils are shown in Figures 3A and 3B.

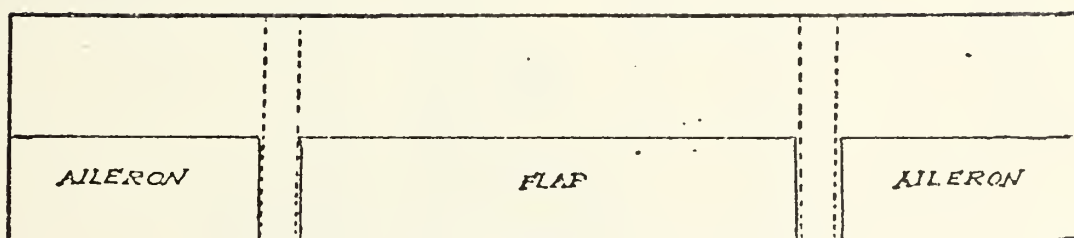
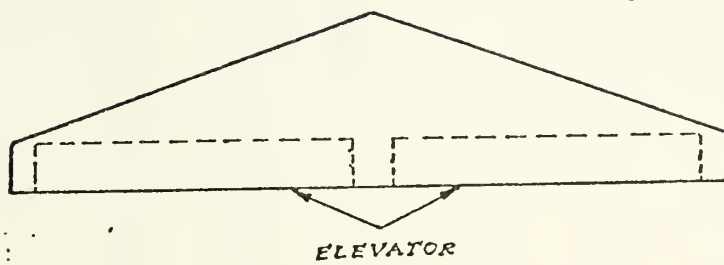


FIGURE 2
FOILS CONFIGURATION

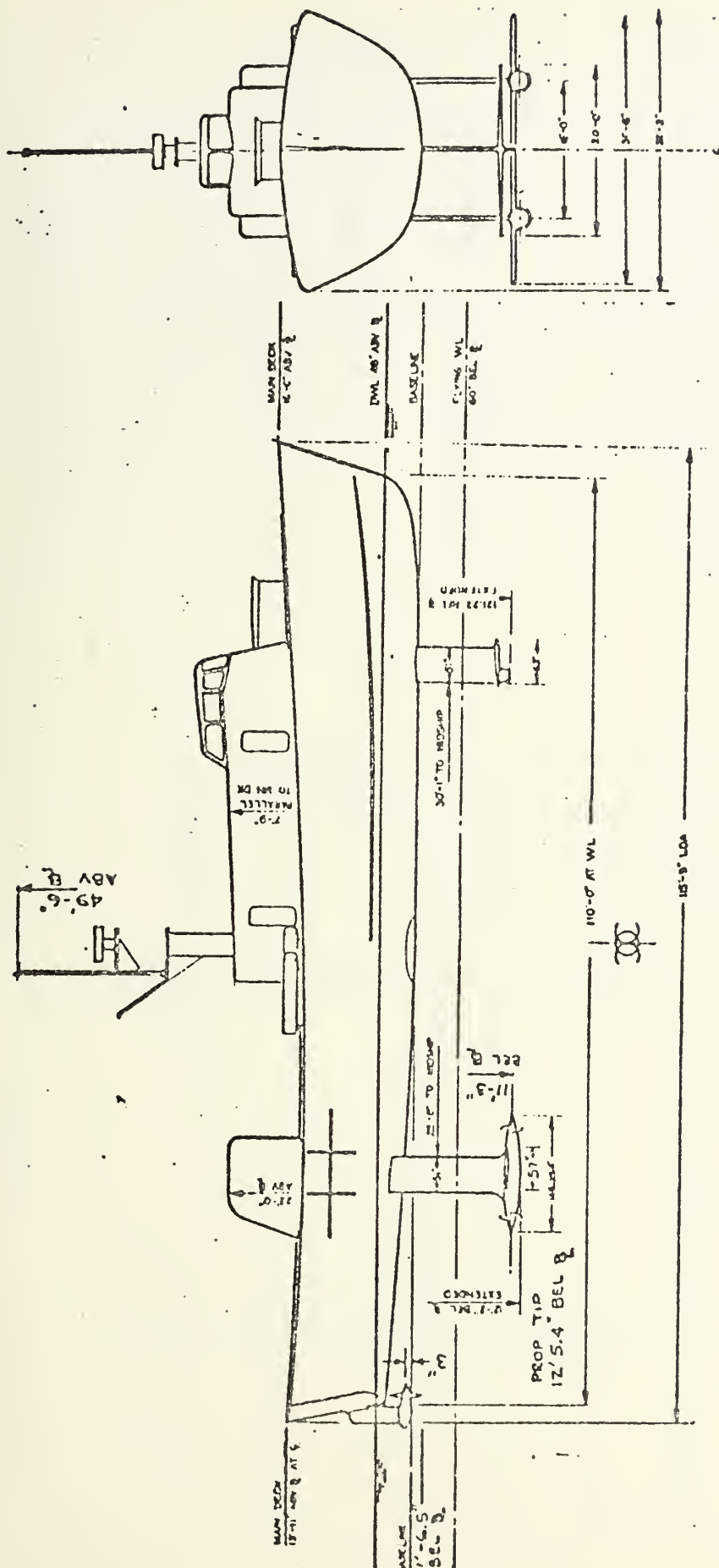
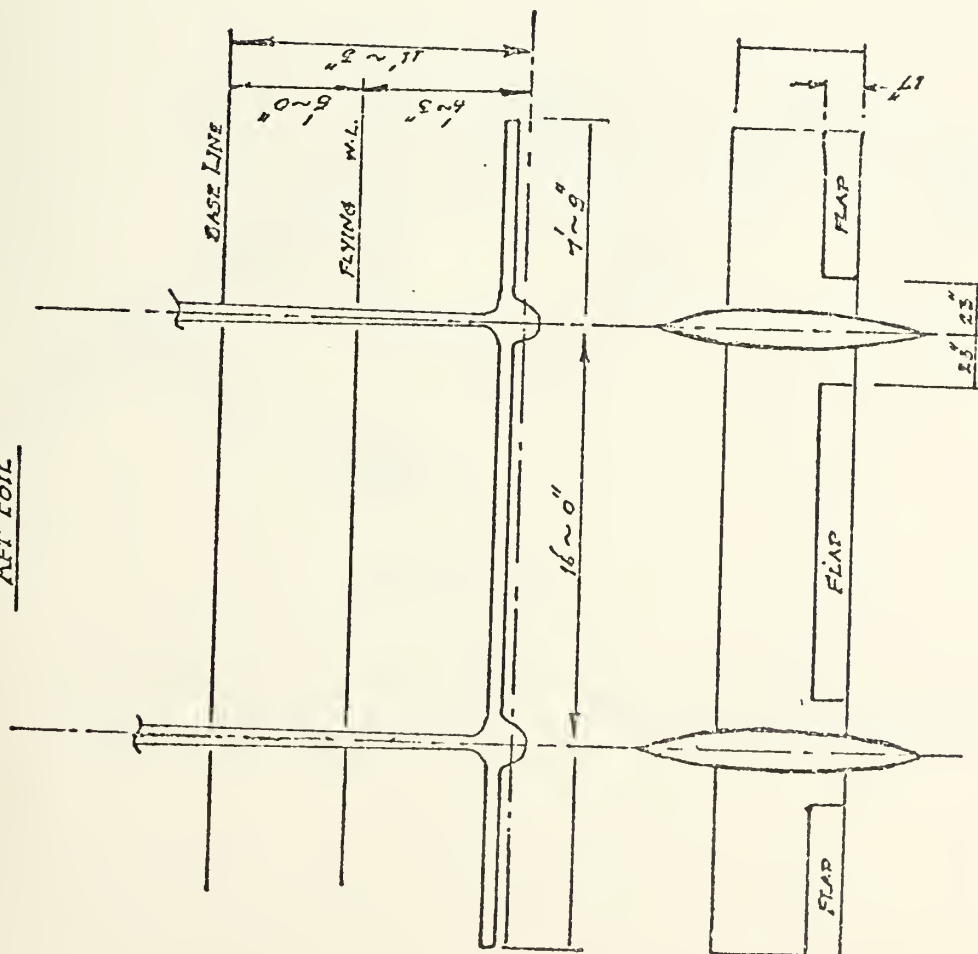


FIGURE 3A
PRINCIPAL DIMENSIONS OF PC(H)-1

AFT FOIL



FORWARD FOIL

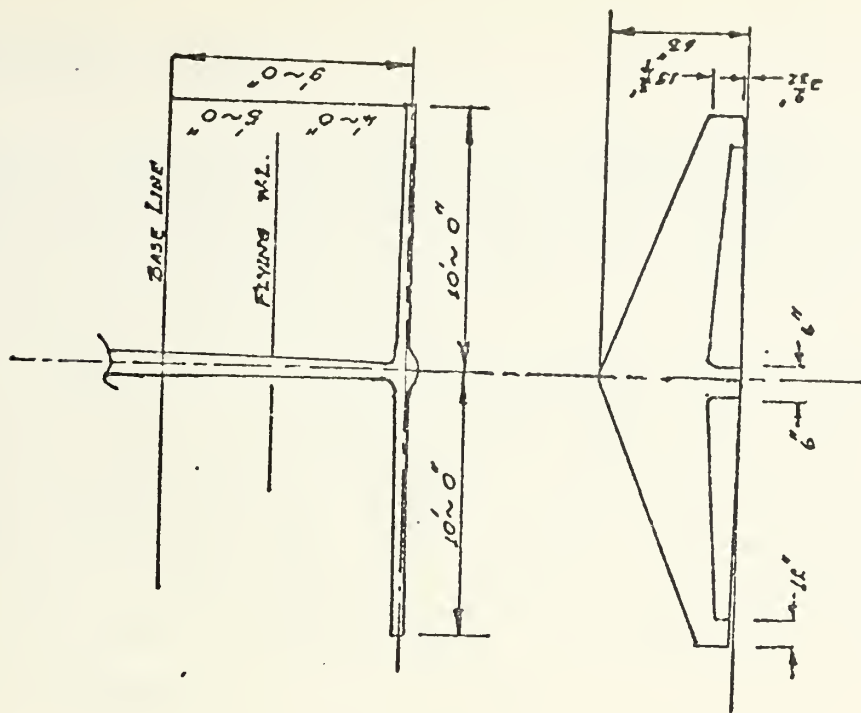


FIGURE 3B
DRAWING OF FOILS AND FLAP CONFIGURATION

B. COORDINATE SYSTEMS

Three coordinate systems will be used in this study of the hydrofoil craft dynamics. They are : the Body Axes, the Earth Axes and the Water Axes. Each of these systems is a right hand orthogonal system.

The body axes coordinate system (X,Y,Z) , shown in Figure 4, has its origin at the center of gravity of the craft and is fixed relative to the craft with the X axis running longitudinally through the craft. This system is initially coincident with the origin of the earth axes system, but it moves with the craft as time progresses. X is positive forward, Y is positive to starboard and Z is positive downward.

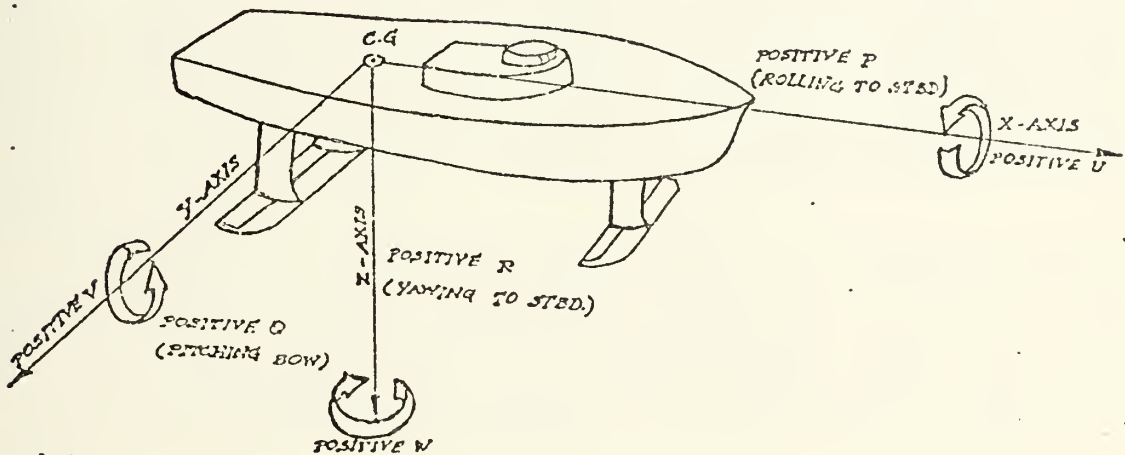


FIGURE 4

ORIENTATION OF THE BODY AXES WITH RESPECT TO THE
CRAFT AND DIRECTIONS OF THE POSITIVE VELOCITIES

The earth axes coordinate system (X_E, Y_E, Z_E) is fixed relative to the earth's surface. The origin may be at any convenient location, provided the body system origin is initially at the same point. The X_E axis lies in the horizontal plane ; it is initially coincident with, and positive in the same direction as, the body X axis. The Y_E lies in the horizontal plane and is positive to starboard when the observer is facing the positive X_E direction. The Z_E axis is normal to the horizontal plane and is positive downward. The craft's motion relative to the calm water surface, (constraint of this paper), is described in terms of this coordinate system.

In general, the body axes are displaced from the fixed earth axes by the three Euler angles, θ (pitch angle), ϕ (roll angle) and ψ (yaw angle). Figure 6 defines the positive directions of the Euler angles. The transformations between earth and body axes are outlined in Ref.3, by transformation matrices, however, only the results will be considered here.

The water axes coordinate system is aligned with the relative water velocity vector and resolves into lift, drag and side force directions. All hydrodynamic model test data is taken and presented as plots in terms of this coordinate system.

The hydrodynamic force and moment data are obtained in a water axis system which is always oriented with respect to the relative water velocity. These data must be transformed into the body axes in order that their effect will be properly included in the equations of craft motions.

In general, the water axis orientation is always changing with respect to the body axes. This leads to the need for a transformation matrix, also outlined in Ref.3, to

resolve the lift, drag and side force values in the body axes. The orthogonal water axis coordinate system is defined in Figure 5. The angles of rotation between water and body axes are α and β and will be defined later.

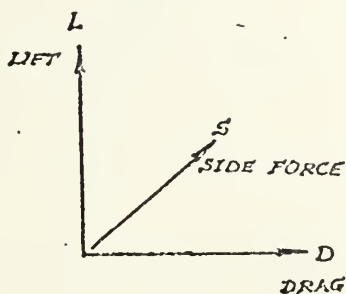


FIGURE 5

ORIENTATION OF WATER AXES COORDINATE SYSTEM

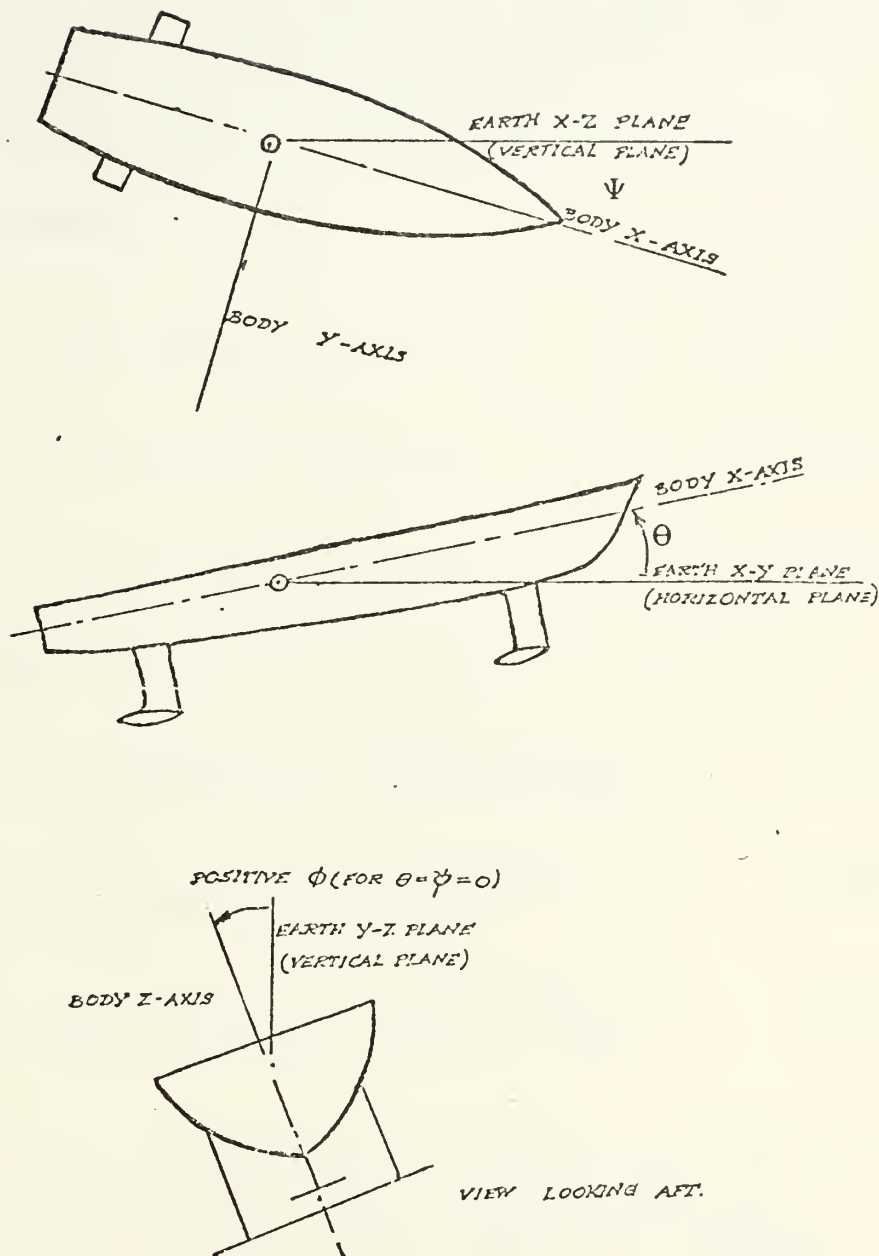


FIGURE 6

DEFINITION OF POSITIVE DIRECTIONS OF EULER ANGLE

C. EQUATIONS OF MOTION

The development of the six equations of motion for a hydrofoil follows the same procedure as those for a displacement type hull. This development is clearly outlined in Ref.3 and therefore will not be done here.

The equations of motion are summarized in this form :

Translation

$$\dot{U} = (1/m) F_X - QW + RV \quad (2-1)$$

$$\dot{V} = (1/m) F_Y + PW - RU \quad (2-2)$$

$$\dot{W} = (1/m) F_Z + QU - PV \quad (2-3)$$

Rotation

$$\dot{P} = 1/I_{XX} \left[L - QR(I_{ZZ} - I_{YY}) + (\dot{R} + QP) I_{XZ} \right] \quad (2-4)$$

$$\dot{Q} = 1/I_{YY} \left[M - RP(I_{XX} - I_{ZZ}) - (P^2 - R^2) I_{XZ} \right] \quad (2-5)$$

$$\dot{R} = 1/I_{ZZ} \left[N - PQ(I_{YY} - I_{XX}) - (QR - \dot{P}) I_{XZ} \right] \quad (2-6)$$

Investigations with the craft simulation show that the terms RV, PV, and PW are very small and may be neglected. Similarly, the term I_{XZ} is less than 10% of I_{XX} and less than 4% of I_{ZZ} . Consequently, the terms containing I_{XZ} may be neglected for this craft.

Equations (2-1) through (2-6) are linear and rotational accelerations in body axes.

Given the previous equations, the velocity terms in

body axes are obtained by integrating each equation one time.

$$U = \int \dot{U} dt \quad (2-7)$$

$$V = \int \dot{V} dt \quad (2-8)$$

$$W = \int \dot{W} dt \quad (2-9)$$

$$P = \int \dot{P} dt \quad (2-10)$$

$$Q = \int \dot{Q} dt \quad (2-11)$$

$$R = \int \dot{R} dt \quad (2-12)$$

In order to calculate the craft's position in earth axes coordinates, these velocity outputs must be transformed from body axes coordinates into earth axes coordinates. The transformation of the linear equations become :

$$\begin{aligned} U_E &= U \cos \theta \cos \psi + V (\cos \psi \sin \theta \sin \phi - \sin \psi \cos \phi) \\ &\quad + W (\cos \psi \sin \theta \cos \phi + \sin \psi \sin \phi) \end{aligned} \quad (2-13)$$

$$\begin{aligned} V_E &= U \cos \theta \sin \psi + V (\cos \psi \cos \phi + \sin \psi \sin \theta \sin \phi) \\ &\quad + W (\sin \psi \sin \theta \cos \phi - \cos \psi \sin \phi) \end{aligned} \quad (2-14)$$

$$W_E = -U \sin \theta + V \cos \theta \sin \phi + W \cos \theta \cos \phi \quad (2-15)$$

Only the craft's velocity in the downward direction, Z_E , is required to calculate its height above the water surface. That is, the vertical position in earth axes follows:

$$Z_E = \int W_E dt \quad (2-16)$$

The craft's position in earth axes coordinates is obtained from :

$$X_E = \int U_E dt \quad (2-17)$$

$$Y_E = \int V_E dt \quad (2-18)$$

The Euler angles, ϕ , θ and ψ are also of interest and can be found by integration of Euler rates $\dot{\phi}$, $\dot{\theta}$ and $\dot{\psi}$. The rates in turn must be derived from the body angular rates. The Euler rates are not easily obtained because they occur about axes which are not orthogonal. This fact can be appreciated by referring to Figure 6 and recalling how the angles were defined. ψ is a rotation about the Z axis, θ is a rotation about the Y axis, and ϕ is a rotation about the X axis. They result in the following set of equations :

$$\dot{\phi} = P + \dot{\psi} \sin \theta \quad (2-19)$$

$$\dot{\theta} = Q \cos \phi - R \sin \phi \quad (2-20)$$

$$\dot{\psi} = (Q \sin \phi + R \cos \phi) \cos \theta + (\dot{\phi} - P) \sin \theta \quad (2-21)$$

The Euler angles are obtained by integration of these equations.

Studies of this craft indicated that during abnormal situations, roll angles of 15 degrees and larger may occur, but under normal operating conditions, roll angles will not exceed 10 degrees and pitch angles are not expected to reach 3 degrees. Therefore, the following assumptions are justified :

$$\sin \theta = 0 \quad (2-22)$$

$$\cos \theta = 1 \quad (2-23)$$

D. CALCULATION OF VELOCITY COMPONENTS

The various foil velocity components must be determined at this point in order to calculate the angles of attack and side slip. The total velocity components of each foil in body axes can be expressed in terms of the craft linear and angular velocities by considering the craft geometry as represented in Figure 7 and Table I.

Center Foil

$$U_C = U + L_{ZCF} \cdot Q \quad (2-24)$$

$$V_C = V - L_{ZCF} \cdot P + L_{XCF} \cdot R \quad (2-25)$$

$$W_C = W - L_{XCF} \cdot Q \quad (2-26)$$

Port Foil

$$U_P = U + L_{ZPF} \cdot Q - L_{YPF} \cdot R \quad (2-27)$$

$$V_P = V - L_{ZPF} \cdot P + L_{XPF} \cdot R \quad (2-28)$$

$$W_P = W + L_{YPF} \cdot P - L_{XPF} \cdot Q \quad (2-29)$$

Starboard Foil

$$U_S = U + L_{ZSF} \cdot Q - L_{YSF} \cdot R \quad (2-30)$$

$$V_S = V - L_{ZSF} \cdot P + L_{XSF} \cdot R \quad (2-31)$$

$$W_S = W + L_{YSF} \cdot P - L_{XSF} \cdot Q \quad (2-32)$$

Mid-Foil Segment

$$U_M = U + L_{ZMF} \cdot Q \quad (2-33)$$

$$V_M = V - L_{ZMF} \cdot P + L_{XMF} \cdot R \quad (2-34)$$

$$W_M = W - L_{XMF} \cdot Q$$

(2-35)

●=Point of application of foil forces

○=Point of application of strut forces

$$L_{XCF} = L_{XCS}$$

$$L_{XPF} = L_{XPS} = L_{XSF} = L_{XSS} = L_{XMF}$$

$$L_{YSF} = L_{YSS} = L_{YPF} = L_{YPS}$$

$$L_{ZPF} = L_{ZSF} = L_{ZMF}$$

L_{ZPS} and L_{ZSS} are variables and in general will not be equal.

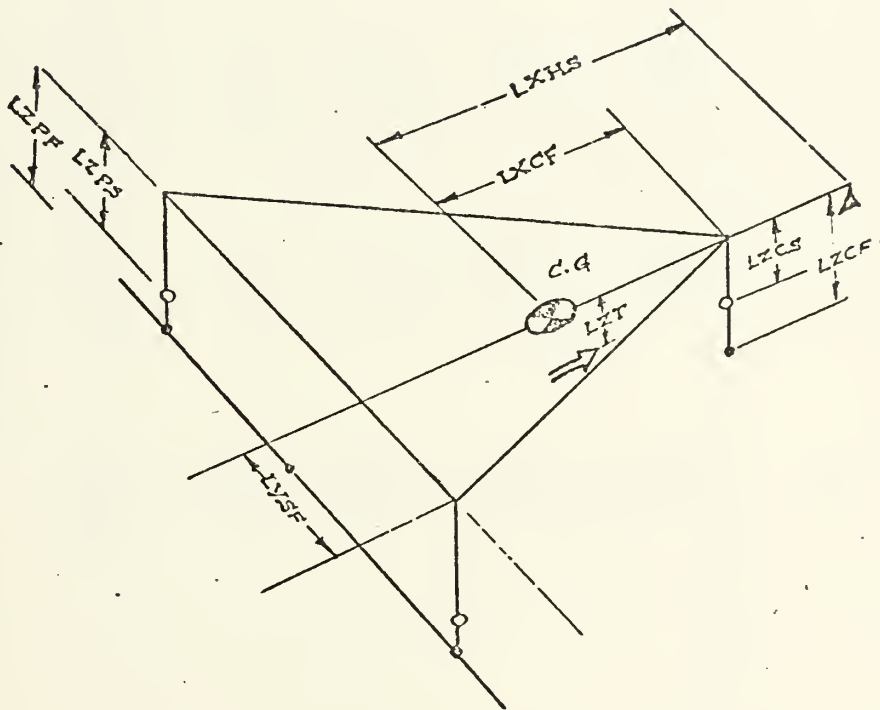


FIGURE 7

DEFINITION OF SYMBOLOGY

TABLE I

Point of Application of Force	Symbol for Force Along or Parallel to			Coordinate From CG to Point of Application Relative to		
	X-Axis	Y-Axis	Z-Axis	X-Axis	Y-Axis	Z-Axis
Center Foil	F_{XCF}	F_{YCF}	F_{ZCF}	L_{XCF}	L_{YCF}	L_{ZCF}
Center Strut	F_{XCS}	F_{YCS}	F_{ZCS}	L_{XCS}	L_{YCS}	L_{ZCS}
Port Foil	F_{XPF}	F_{YPF}	F_{ZPF}	L_{XPF}	L_{YPF}	L_{ZPF}
Port Strut	F_{XPS}	F_{YPS}	F_{ZPS}	L_{XPS}	L_{YPS}	L_{ZPS}
Starboard Foil	F_{XSF}	F_{YSF}	F_{ZSF}	L_{XSF}	L_{YSF}	L_{ZSF}
Starboard Strut	F_{XSS}	F_{YSS}	F_{ZSS}	L_{XSS}	L_{YSS}	L_{ZSS}
Mid Foil Segment	F_{XMF}	F_{YMF}	F_{ZMF}	L_{XMF}	L_{YMF}	L_{ZMF}
Effective Point of Application of Prop. Thrust	T_X	0	T_Z	L_{XT}	0	L_{ZT}

E. ANGLE OF ATTACK AND ANGLE OF SIDE SLIP

The angle of attack of a foil is shown in Figure 8A and is defined as the angle whose tangent is the total relative velocity between the foil and water in the body Z direction, divided by the total relative velocity between the foil and water in the body X direction.

$$\alpha = \arctan \left(\frac{W_r}{U_r} \right) \quad (2-36)$$

If the foil is not aligned with the body X axis, then the foil has a fixed incidence angle and the total angle of attack becomes :

$$\alpha_{\text{total}} = \alpha_{\text{fixed}} + \alpha \quad (2-37)$$

The side slip angle is shown in Figure 8B and can be represented by :

$$\beta_i = \arctan \left[\frac{V_{ri}}{\sqrt{(U_{ri}^2 + V_{ri}^2 + W_{ri}^2)}} \right] \quad (2-38)$$

During actual craft operations the angles will be less than 10 degrees, so that the inverse trigonometric functions can be replaced by quotients. Except at low craft speeds, the forward velocity of the craft, U , is much greater than the velocities, V and W . Applying these simplifications, the equations become :

$$\alpha_i = (W_{ri}/U) + \alpha_{i\text{-fixed}}$$

$$\beta_i = V_{ri}/U$$

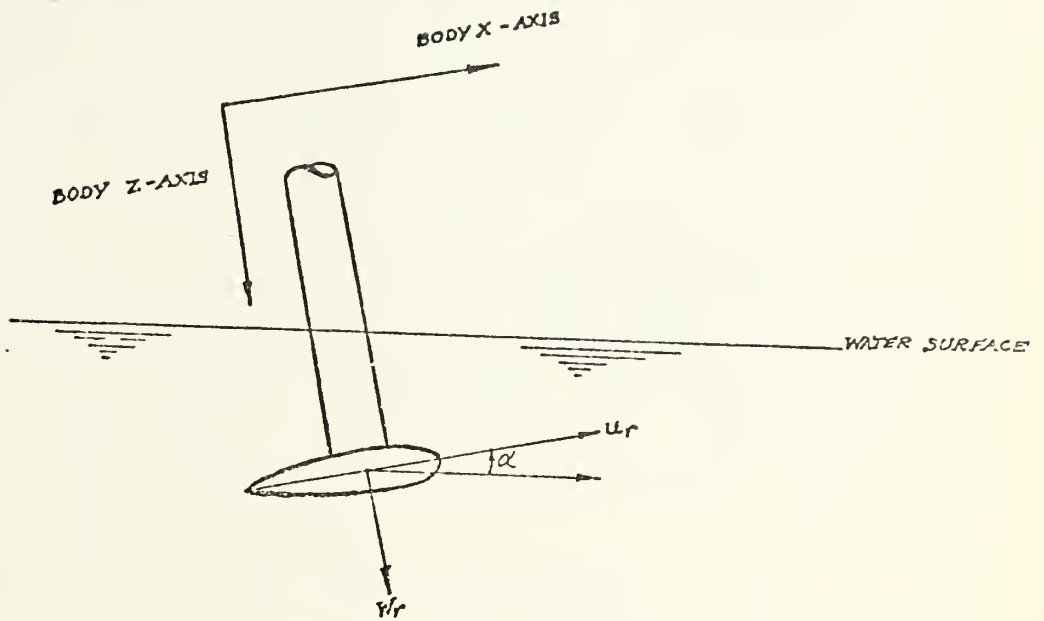


FIGURE 8A
ANGLE OF ATTACK

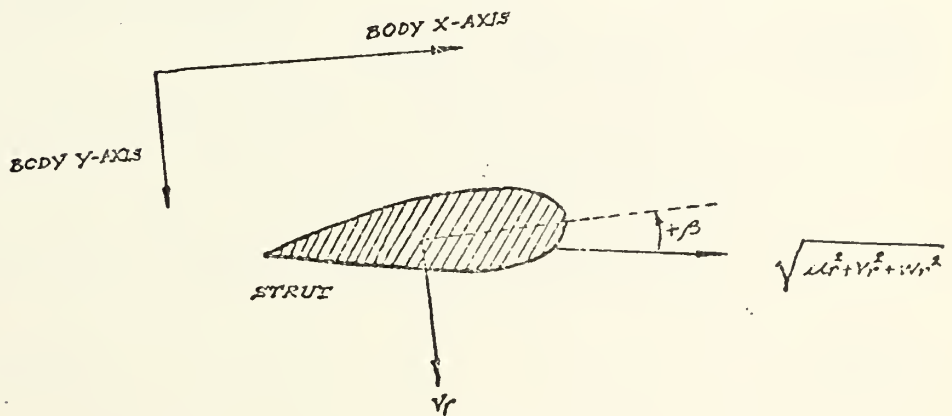


FIGURE 8B
ANGLE OF SIDE SLIP

F. EXPANSION OF FORCES AND MOMENT TERMS

With the aid of Figure 7 and Table I, the forces and moments for the craft are easily written. It is important to note that when a numerical value is inserted for one of the alphabetical dimensions, the sign of the value must be positive or negative according to positive and negative directions from the axis system origin at the C.G. One of the assumptions made upon commencing simulation was that the struts contributed with zero lift and that the foils contributed with zero side force. Also note that horizontal foils make no contribution to the body Y force and vertical struts do not contribute to the body Z force. Therefore, all body Y motion originates at the struts and all body Z motion originates at the foils.

The forces and moment equations become :

$$F_X = F_{XCF} + F_{XPF} + F_{XSF} + F_{XMF} + F_{XCS} + F_{XPS} + F_{XSS} + mg_X + T_X \quad (2-39)$$

$$F_Y = F_{YCS} + F_{YPS} + F_{YSS} + mg_Y \quad (2-40)$$

$$F_Z = F_{ZCF} + F_{ZPF} + F_{ZSF} + F_{ZMF} + mg_Z \quad (2-41)$$

$$L = (F_{ZY} L_{PF}) + (F_{ZY} L_{SF}) - (F_{YZ} L_{PS}) - (F_{YZ} L_{SS}) - (F_{YZ} L_{CS}) \quad (2-42)$$

$$M = - (F_{ZX} L_{CF}) - (F_{ZX} L_{PF}) - (F_{ZX} L_{SF}) - (F_{ZX} L_{MF}) + (F_{XZ} L_{CF})$$

$$+ (F_{XZ} L_{PF}) + (F_{XZ} L_{SF}) + (F_{XZ} L_{MF}) + (F_{XZ} L_{CS}) + (F_{XZ} L_{PS})$$

$$+ (F_{XZ} L_{SS}) + T_{XZ} L_{XT} \quad (2-43)$$

$$N = (F_{YX} L_{CS}) + (F_{YX} L_{PS}) + (F_{YX} L_{SS}) \quad (2-44)$$

All of these forces have a hydrodynamic origin except for the thrust and gravity terms. The thrust is always

associated with the body axis and requires no further expansion. The gravity terms can be simplified using small angle approximations for the Euler angles.

The standard expression for hydrodynamic forces in water axis coordinates is :

$$F_i = qAC_i \quad i=L,D,S \quad (2-45)$$

Where L,D,S represent lift,drag and side force respectively. The lift, drag and side force coefficients vary as functions of angle of attack, angle of side slip, submergence, velocity, flap deflections, elevator deflections and rudder deflections.

Ideally, mathematical expressions would have been developed to correctly depict the interrelation of all variables which affect the force coefficients. However, except for the conditions when relationships are linear, hydrofoil technology has not advanced to a position which would yield such expressions. The difficulties which are encountered in deriving a mathematical expression include :

- 1) The occurrence of cavitation and ventilation, which are not completely predictable.
- 2) The even more unpredictable cessation of cavitation and ventilation.
- 3) The nonlinearity of the hydrodynamic coefficients.
- 4) Lack of sufficient test data to completely describe all of the above.

III• HYDROFOIL SIMULATION

A. SIMULATION OBJECTIVES

The objective of this simulation was to study the dynamic characteristics of motion along and about each body axis. That is, perturbations should be introduced to separately excite :

- 1) Motion along the X-axis
- 2) Motion about the X-axis
- 3) Motion along the Y-axis
- 4) Motion about the Y-axis
- 5) Motion along the Z-axis
- 6) Motion about the Z-axis

The following assumptions were made prior to beginning simulation :

- 1) Craft equations of motion are valid only for the foilborne mode.
- 2) Weight of the craft remains constant.
- 3) Hydrodynamic coefficients are based on fully wetted surfaces, i.e. no cavitation or ventilation.
- 4) The craft may be operated in calm water or in a seaway.

B. COMPUTER SIMULATION

The computer program used was based on the computer programs of Ref.1 and Ref.2.

As in the preceding References, before the main program could be assembled, Fortran subroutines were used to find the hydrodynamic coefficients of foil lift and drag, and strut drag and side slip. The SETUP subroutine stored as data points the simulation curves of Ref.4. The subroutines INTERP and INTRP1 are interpolation subroutines to obtain the proper coefficient from the above simulation curves. For INTERP, values of angle of attack and forward flap angle were used to enter the curves and obtain a value of foil drag. Angle of side slip and submergence were used to enter INTRP1 to obtain strut drag. Listings of the subroutines are shown in the computer program section. The main program was then assembled using Figure 9 as a reference for data flow and is also listed in the computer program section. In one of the parts of this main program, the automatic control block, were introduced some modifications, needed for the main objective of this paper, the study of the craft's turning characteristics. This automatic control block is still open for future studies.

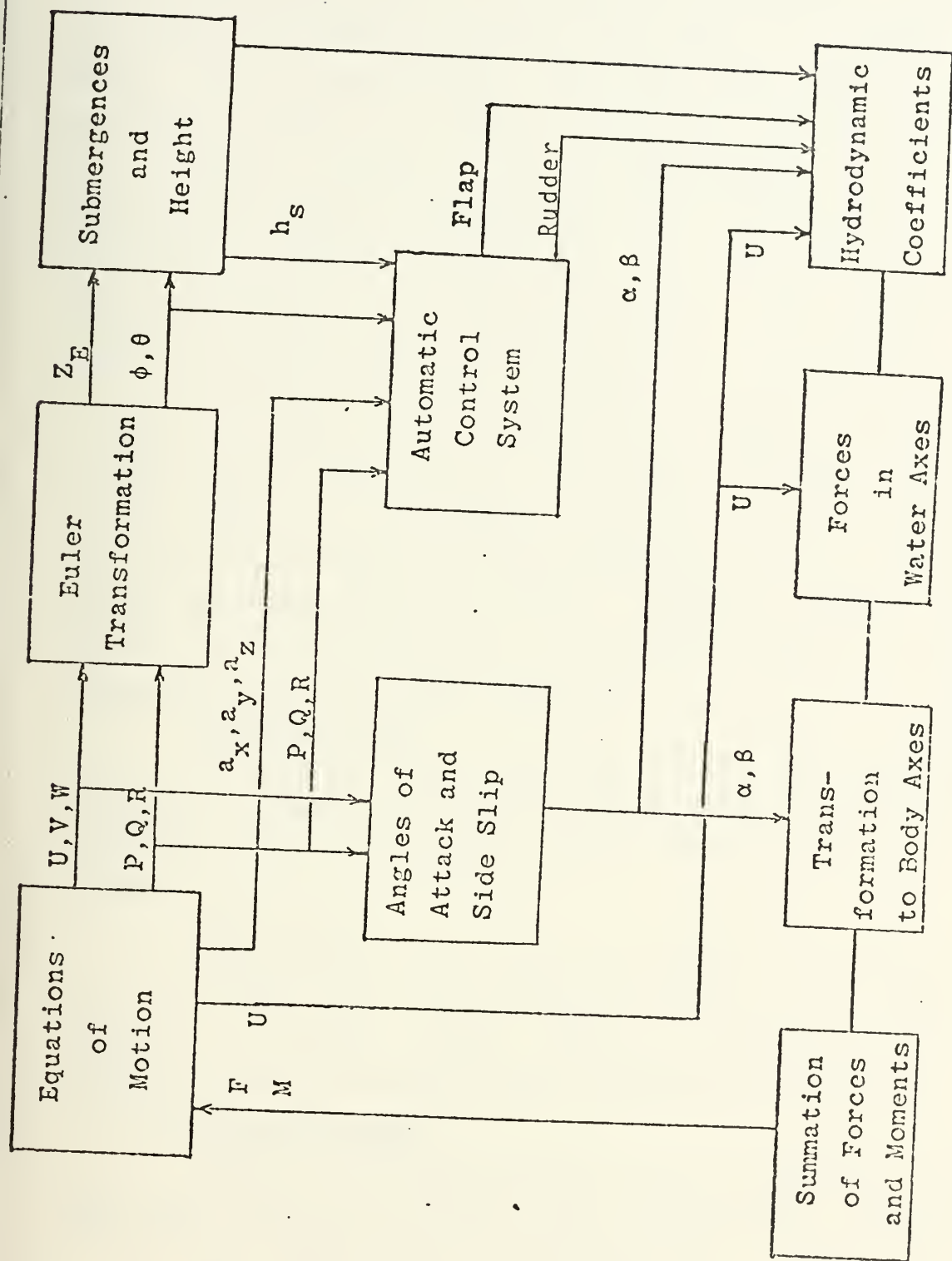


FIGURE 9

BLOCK DIAGRAM OF EQUATION RELATIONSHIPS

C. AUTOMATIC CONTROL

Control signals originate at the pilot's controls, at the motion sensors and at the position transducer. These are combined and processed in the electronics to produce the signal for the servo-valve. The pilot will be able to move the helm, a lever, or a knob to introduce steering, altitude and attitude commands ; the motion sensors sense errors between the commanded and actual craft motions and produce electrical signals proportional to these errors ; the position transducer provides the feedback signal so that the control surface stops moving when it has reached the position corresponding to the processed error signals.

It is now necessary to consider how the control system components affect the equations of motion through the control surface deflections. In general, a signal originated at the pilot or at the motion sensors will be modified by the individual dynamics of the components in the signal path before the control surface motion actually occurs. Motion sensors to be discussed are vertical gyros, rate gyros, accelerometers and height sensors.

1. Vertical Gyros

A vertical gyro here will produce one signal directly proportional to the pitch angle of the craft and one signal directly proportional to the roll angle of the craft.

2. Rate Gyros

A rate gyro will sense an angular rate about one of the three body axes. The dynamics of the gyro are such as to produce an output signal which is related to the actual angular rate by a second order differential equation.

3. Accelerometers

Outputs of accelerometers are also assumed to relate the craft motions by second order differential equations.

To identify the accelerations sensed by the instruments, it will be assumed that there is one accelerometer at the C.G., mounted such as to measure

lateral acceleration, and one accelerometer above each foil mounted in the X-Y plane so as to measure accelerations parallel to the Z-axis.

The lateral acceleration at the C.G. is :

$$a_Y = F_Y/m \quad (3-1)$$

Taking angular accelerations into account, the accelerations in the Z-direction at points above the center, port and starboard foil are :

$$a_{ZC} = (F_Z/m) - L_{XCF} \cdot \dot{Q} \quad (3-2)$$

$$a_{ZP} = (F_Z/m) + L_{XPF} \cdot \dot{Q} - L_{YPF} \cdot \dot{P} \quad (3-3)$$

$$a_{ZS} = (F_Z/m) + L_{XSF} \cdot \dot{Q} + L_{YSF} \cdot \dot{P} \quad (3-4)$$

4. Height Sensor

Ultrasonic and sonar types are either in use or expected to be used. For this study it will be assumed that the dynamic characteristics of the sensor, whatever the type, will be such as to give a direct indication of the instantaneous height of the sensor above the water.

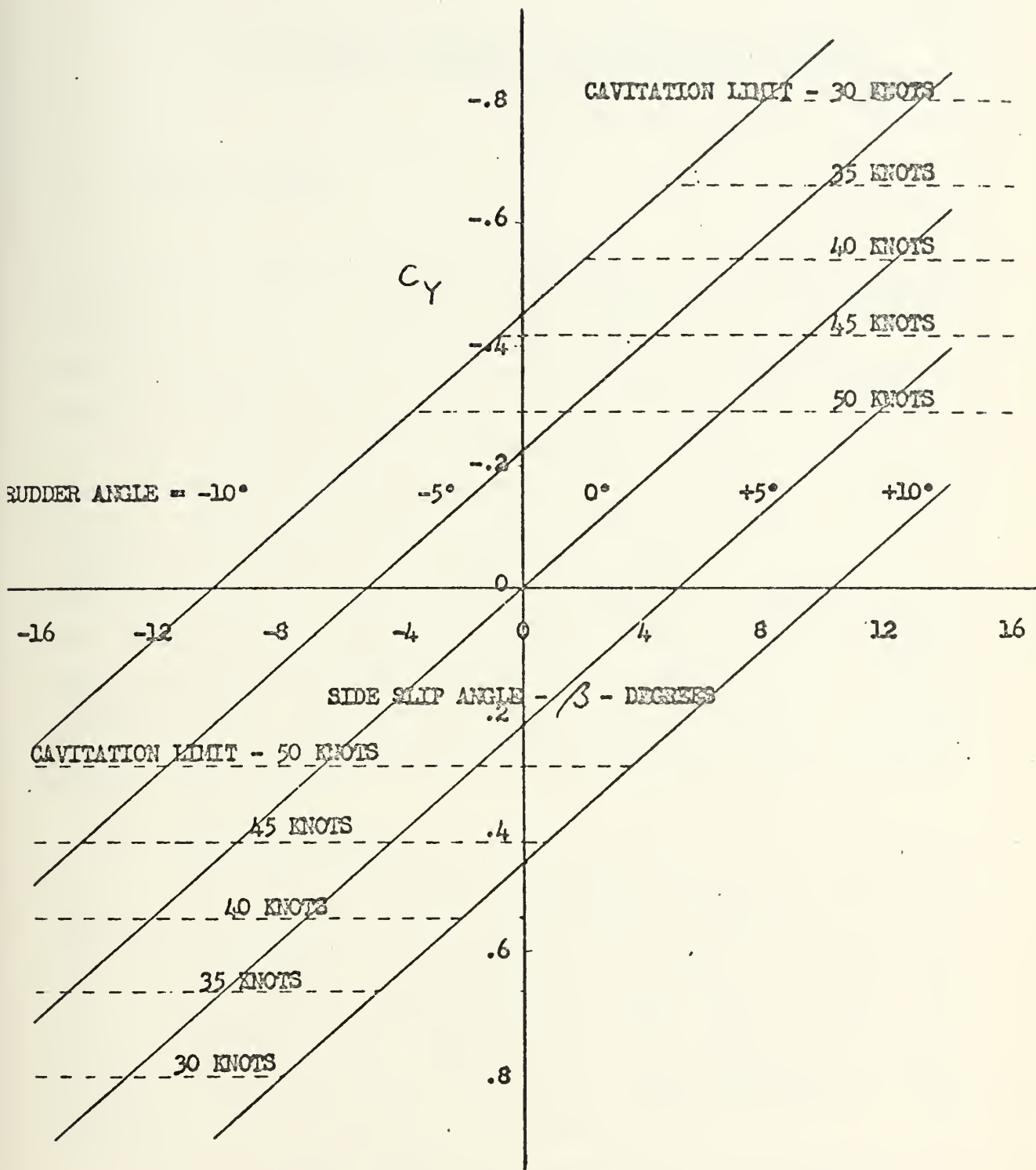


FIGURE 10

SPADE RUDDER CHARACTERISTICS

IV• HYDROFOIL TURNING CHARACTERISTICS STUDY

A. RUDDER EFFECTS

For the hydrofoil steering control, the struts can be viewed as vertical foils so that steering can be achieved by rotating a strut, by rotating a hinged trailing edge or by rotating an extension of a strut below a foil, (spade or ventral rudder), as in the case of the PC(H)-1.

The rudder on the forward strut exerts an influence upon the forward strut side force coefficient. Based on Figure 10 the necessary changes were made in the computer simulation program. To document the rudder's influence in the system and to show the craft's behavior, several figures are presented, corresponding to runs using different speeds and successive rudder angles of 30,25,20,15,10, and 5 degrees at each speed. The craft started moving straight ahead, the rudder angle being introduced after 3 seconds, for all the cases.

1. Speed=30 knots

For a forward speed $U=30$ knots, Figure 11A shows the pitch angle of the craft, which had an oscillation at the beginning of the run, but it went to a steady state value of 1.53 degrees, with the craft's bow up, in 4.5 seconds, for all the six different rudder angles used. The result was natural, because the rudder plays a negligible role in changing the value of the foil lift coefficient and therefore in the craft's pitch motion.

For the same speed, in Figure 11B the different roll angles corresponding to different rudder angles were represented. When the ship went straight ahead, naturally the roll angle was 0 degrees, but as soon as a rudder angle

of 30 degrees was introduced after 3 seconds, the craft started rolling, going to a steady state value of -1.29 degrees for the roll angle in 19.5 seconds. On the other end of the scale for a rudder angle of only 5 degrees, the reaction was smaller, the initial oscillation was also smaller and the craft went to a steady state value of -0.216 degrees for the roll angle in 13 seconds. Comparing with Figure 4, these negative values show a roll to the port side direction, although the ship was turning to starboard. This result would be perfectly acceptable for a conventional ship, but banking in the opposite direction is desired for the hydrofoil because of the high speeds of operation.

In Figure 11C were represented the several heading angles, with positive values, showing that the craft was in fact turning to starboard. At 3 seconds when 30 degrees rudder angle were introduced, the craft had a reaction, reaching a maximum heading angle of 2.02 degrees, but returning to a steady heading value of 1.39 degrees in 23 seconds. For a rudder angle of only 5 degrees the maximum heading of the craft was 0.33 degrees, getting a steady heading of 0.23 degrees in 17.5 seconds, because the rudder change was smaller and then the reaction was smaller.

The craft's height above the water Z_{E1} was represented in Figure 11D. Starting with a value of 0 feet, the craft went to 3.9 feet above the water in 4.5 seconds. Comparing with the dimensions in Figure 3A, it was observed that the foils were well inside the water. Again it was observed that the rudder plays a negligible role on the lift motion of the craft, because the craft's height above the water was the same for all the rudder angles.

The forward flap was represented in Figure 11E. It started with a value of 0 degrees, reaching a peak of 13.9 degrees to help the transient period. After 5 seconds it reached a steady state positive value of 10.8 degrees. This positive value means that the flap was oriented in the down

direction and therefore offering more resistance to the water, provoking more lift on the bow part of the craft. It can be concluded that the main roles of the forward flap are craft's lifting and to keep a stable pitch angle.

In Figure 11F the stern mid foil segment was represented. After a transient period with a maximum value of -1.15 degrees, it reached a value of 2.62 degrees in 4.5 seconds, as in the preceding case it was oriented in the down direction and again its main role is to help the lift motion of the craft.

In Figure 11G the stern starboard flap was represented. Its value was 0 degrees, before the rudder was introduced after 3 seconds. Then for a rudder angle of 30 degrees, the flap had a transient period with a maximum value of -2.33 degrees, going to a steady state value of -1.86 degrees in 16 seconds. For a rudder angle of only 5 degrees, the maximum negative value was only of -0.38 degrees, going to a steady state value of -0.31 degrees in 13 seconds. Having the starboard flap angles different values for different rudder angles, it was concluded that the stern starboard and port flaps have influence in the craft's turns, therefore a completely different conclusion in relation with the conclusion presented for the forward flap and mid aft flap.

On the next groups of figures the same elements as before will be represented. Similar conclusions can be applied, therefore only the data obtained will be reported.

2. Speed=36 knots, rudder to starboard

The pitch angle was represented in Figure 12A. It reached a steady state value of 0.01 degrees in 6.5 seconds.

In Figure 12B were represented the roll angles for the different rudder angles, showing again the banking in the wrong direction. For a rudder angle of 30 degrees, the roll angle had a maximum negative value of -1.29 degrees, going to a steady state value of -1.12 degrees in 15 seconds. For a rudder angle of 5 degrees, the maximum

negative roll angle was of -0.21 degrees, going to a steady state value of -0.18 degrees in 12.5 seconds.

The heading angles represented in Figure 12C reached higher values due to a faster speed, increasing gradually with time, meaning that with the increase of speed the rudder effect on the craft's turning was larger. After 40 seconds of run time with 30 degrees of rudder, the heading angle reached 8.5 degrees and for 5 degrees of rudder, the heading angle reached 1.42 degrees, clearly larger values than for the 30 knots speed.

In Figure 12D the height above the water was represented, with a steady state value of 1.65 feet in 3.5 seconds, after starting on 0 feet.

The forward flap angle was represented in Figure 12E. On the transient period it reached a maximum value of 9.21 degrees, going to a steady state value of 7.7 degrees in 5.5 seconds. These values are smaller than for the speed of 30 knots, because the thrust is bigger and it is easier for the craft to lift.

In Figure 12F the stern mid foil segment was represented. It reached a maximum value of -1.37 degrees in the transient period, jumping to a steady state value of 1.74 degrees in 7.5 seconds. These values are also smaller than for the 30 knots speed by the same reasons of the preceding paragraph.

In Figure 12G the different aft starboard flap angles were represented. For a rudder angle of 30 degrees the flap angle reached a maximum value of -1.94 degrees, going to a steady state value of -1.6 degrees in 16 seconds. For a rudder angle of 5 degrees, when the rudder was introduced the maximum value was -0.324 degrees, reaching a steady state value of -0.27 degrees in 13 seconds.

3. Speed=36 knots, rudder to port

With the same speed but with the rudder oriented to the opposite board, port, there were no changes in the pitch mode, the only changes were verified with the roll angle,

angle, heading angle and aft starboard flap angle, represented in Figures 13A, 13B and 13C. The corresponding figures with the rudder to starboard were Figures 12B, 12C and 12G and comparing these two groups of figures, it can be observed that the roll angle, heading angle and aft starboard flap angle have exactly the same values but with opposite direction, because on the Y body axis direction the craft is perfectly symmetrical.

4. Speed=40 knots

In Figure 14A the several roll angles for different rudder angles were represented. When a rudder angle of 30 degrees was applied after 3 seconds the craft started banking in the wrong direction again, having a transient oscillation with a maximum value of -1.18 degrees. It went to a steady state value of -1.032 degrees in 15 seconds.

In Figure 14B the different heading angles were represented. The craft went straight ahead and started turning when the rudder angle was introduced after 3 seconds. The heading angles increased gradually with time, for a rudder angle of 30 degrees the heading angle reached the value 11.9 degrees after 40 seconds of run time. For a rudder angle of 5 degrees the maximum heading angle reached 1.99 degrees in 40 seconds.

In Figure 14C the height above the water was represented. It went to a steady state value of 0.628 feet above the water in 11 seconds.

In Figure 14D the forward flap was represented. After a transient oscillation, with a maximum value of 6.9 degrees, it dropped to a steady state value of 6.19 degrees in 7 seconds.

The aft starboard flap angles were represented in Figure 14E. For 30 degrees rudder angle, the flap angle reached a maximum negative value of -1.78 degrees and went to a steady state value of -1.48 degrees in 16 seconds. For 5 degrees rudder angle, the flap angle had a maximum negative value of -0.29 degrees and went to a steady state

value of -0.25 degrees in 11.5 seconds.

5. Speed=50 knots

In Figure 15A the different roll angles were represented. For a 30 degrees rudder angle, the roll angle had a maximum value of -0.99 degrees and went to a steady state value of -0.88 degrees in 10.5 seconds. For a 5 degrees rudder angle, the roll angle reached a maximum value of -0.165 degrees and went to a steady state value of -0.147 degrees in 8 seconds.

The heading angles were represented in Figure 15B. For a 30 degrees rudder, the maximum heading angle was 18.3 degrees in 40 seconds of run time. For a 5 degrees rudder, the maximum heading angle was 3 degrees after 40 seconds.

In Figure 15C the forward flap angle was represented. It went to a steady state value of 3.76 degrees in 3.5 seconds.

In Figure 15D the different aft flap angles were represented. For a 30 degrees rudder angle, the starboard flap angle reached a maximum value of -1.51 degrees and went to a steady state value of -1.26 degrees in 14.5 seconds. For a 5 degrees rudder angle, the starboard flap angle reached a maximum value of -0.25 degrees and went to a steady state value of -0.19 degrees in 8 seconds.

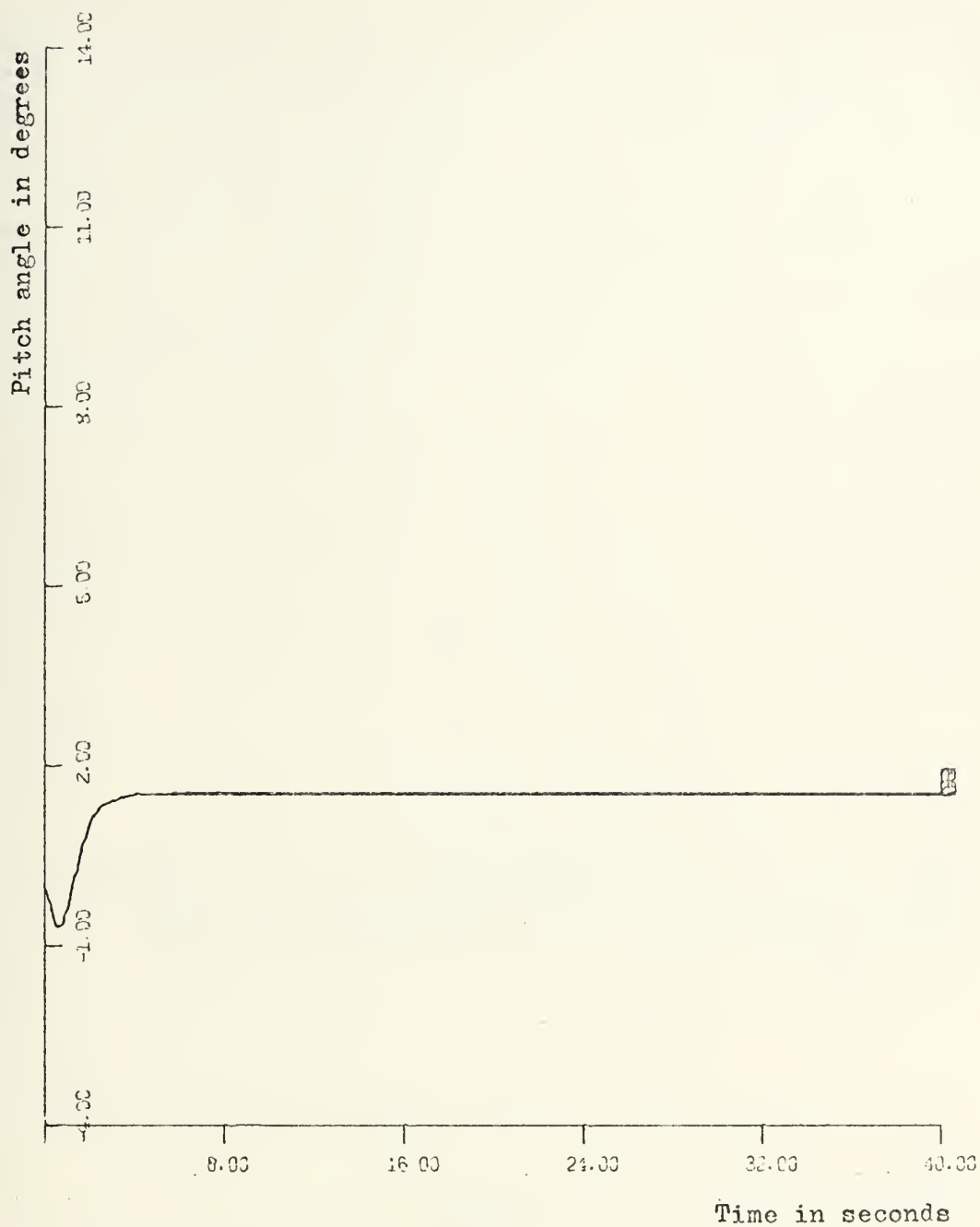


FIGURE 11A
DISTURBANCE : RUDDER SPEED=30 KNOTS

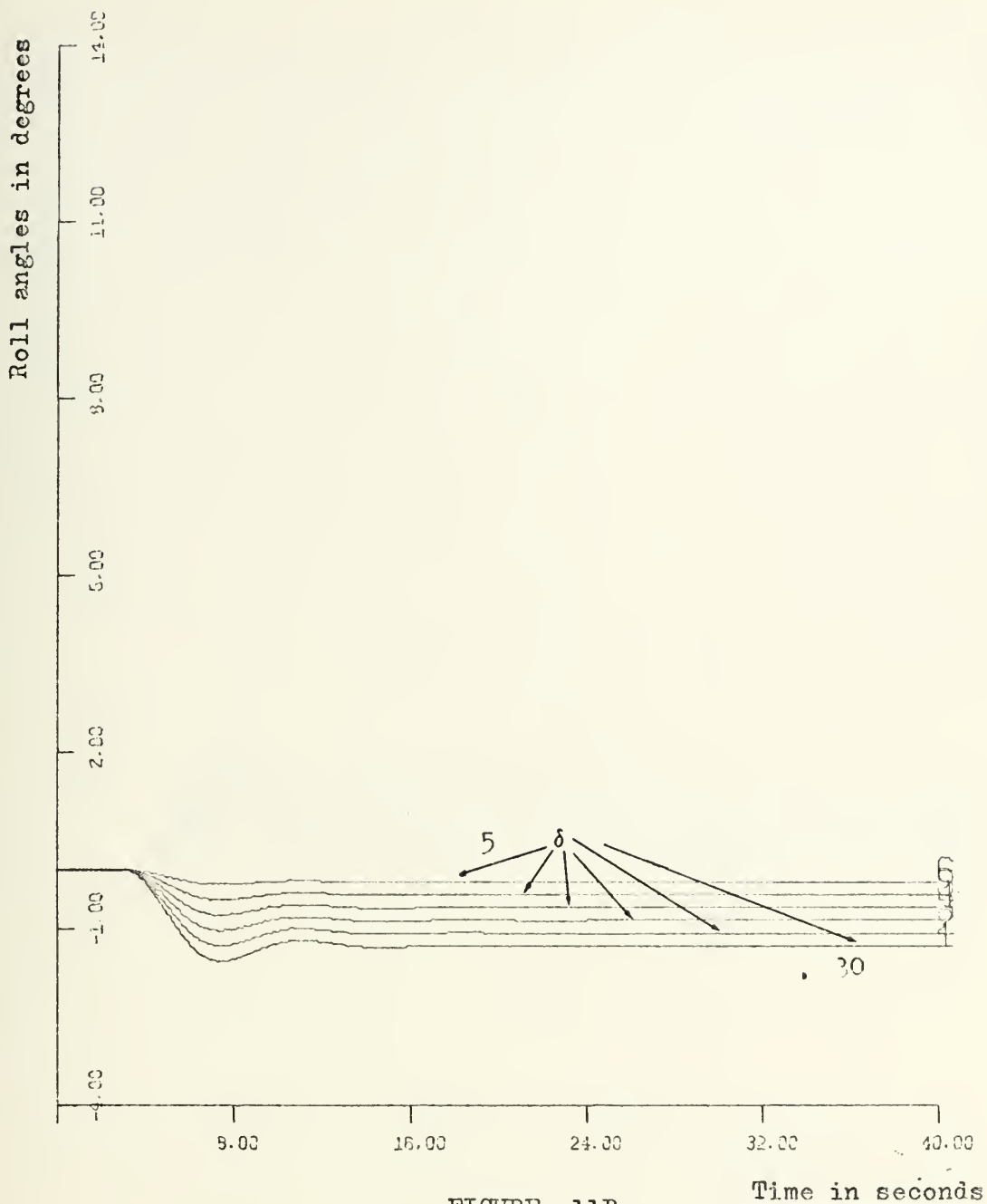


FIGURE 11B
 DISTURBANCE : RUDDER SPEED=30 KNOTS

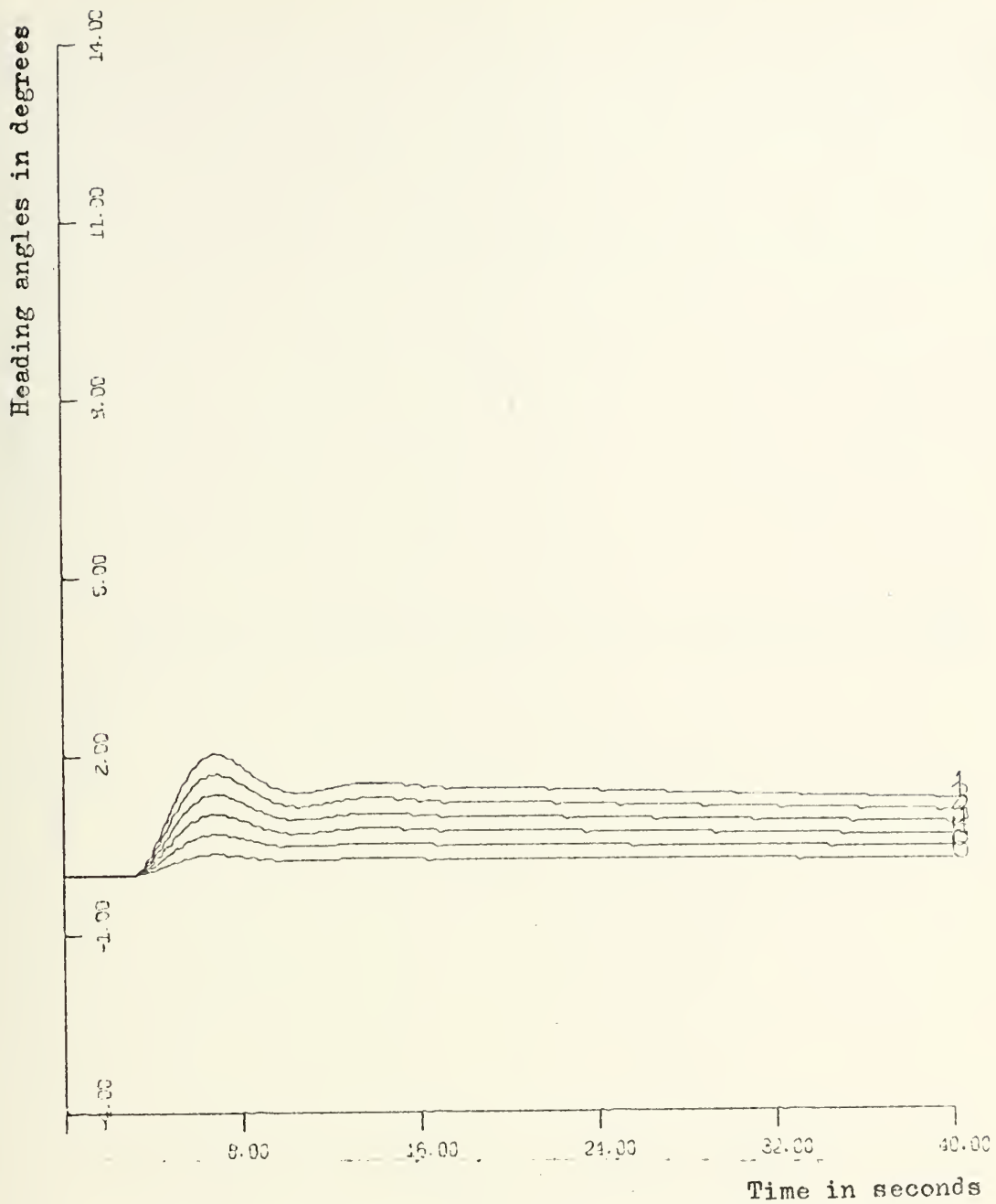


FIGURE 11C

DISTURBANCE : RUDDER

SPEED=30 KNOTS

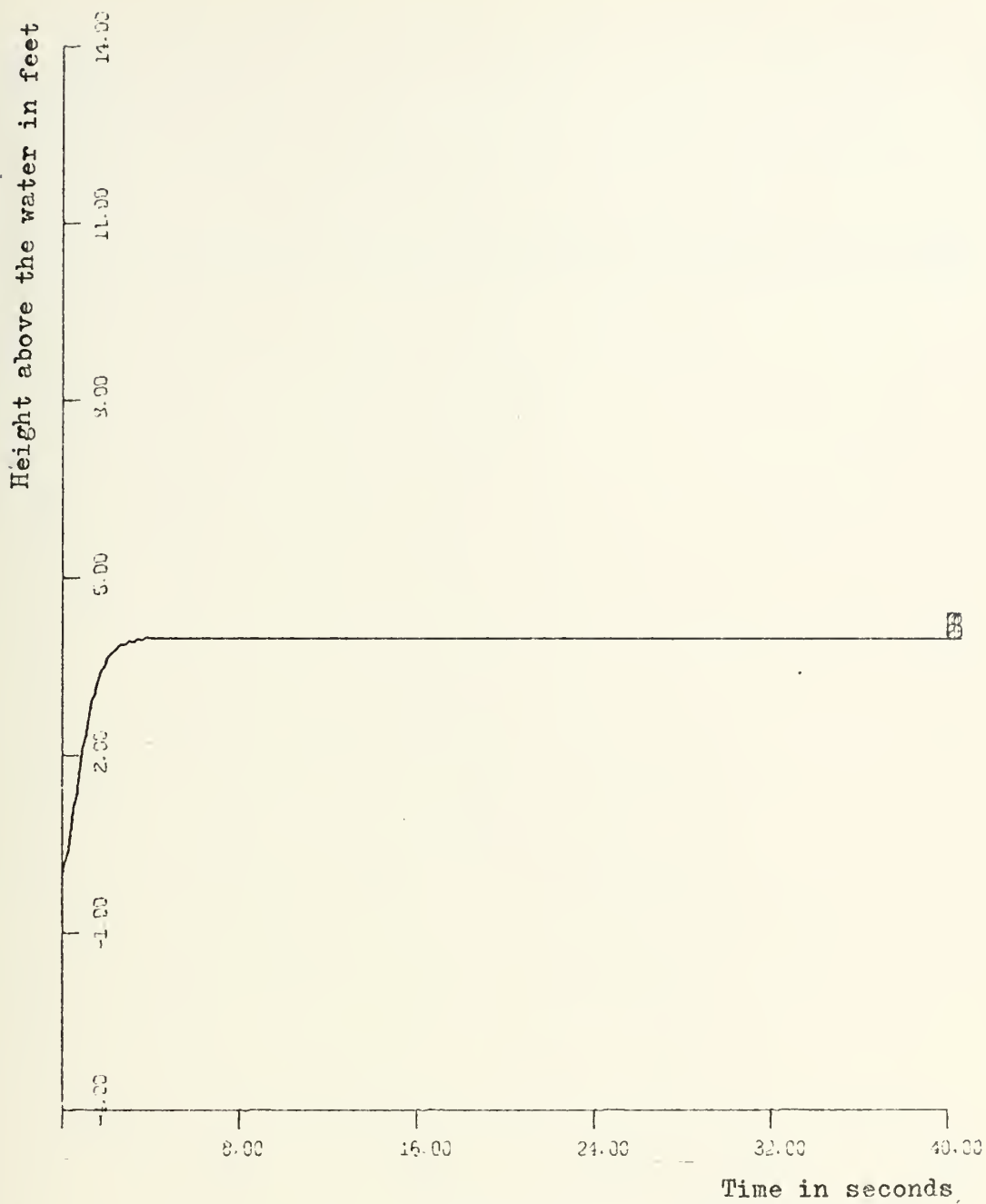


FIGURE 11D

DISTURBANCE : RUDDER

SPEED=30 KNOTS

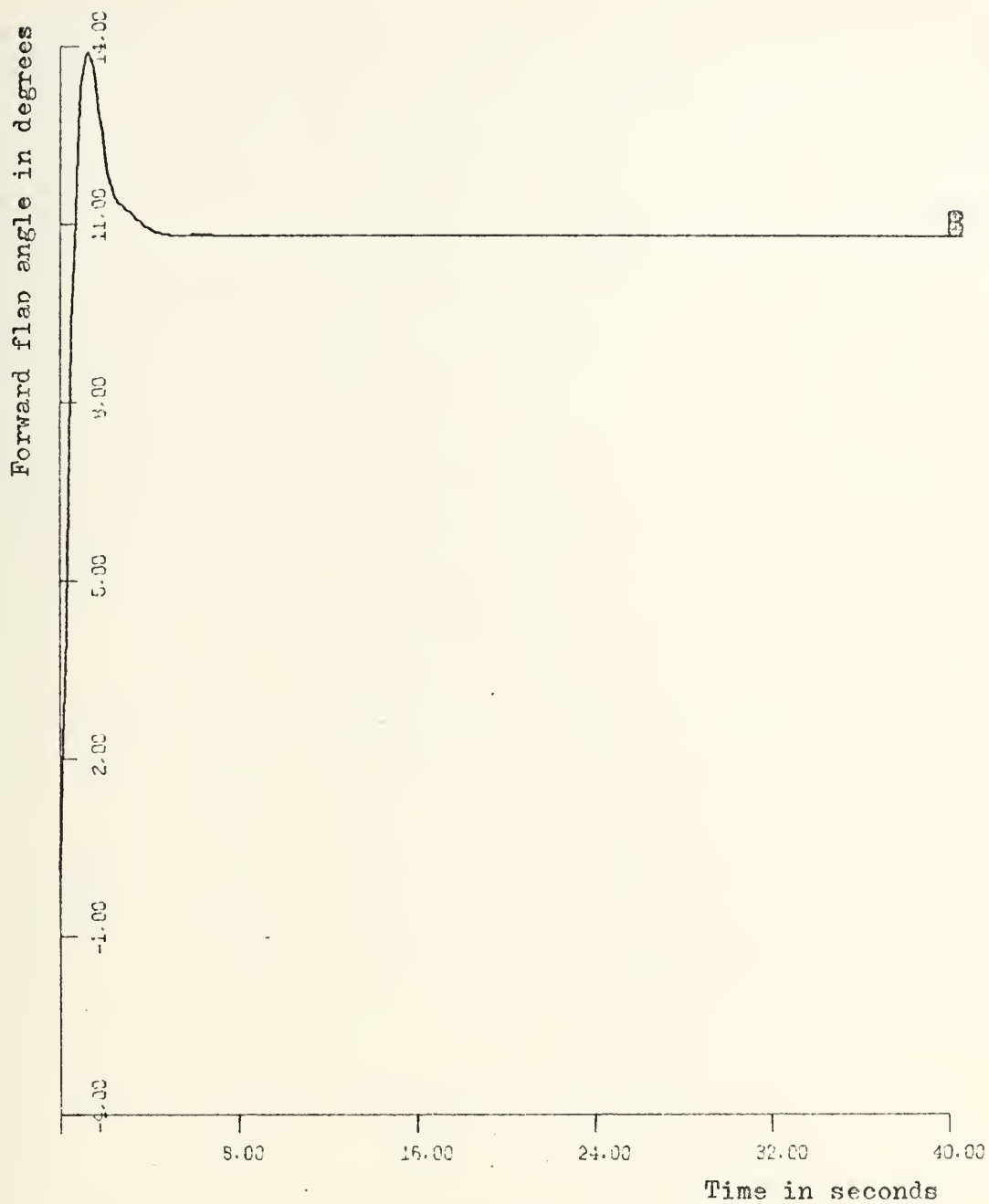


FIGURE 11E

DISTURBANCE : RUDDER

SPEED=30 KNOTS

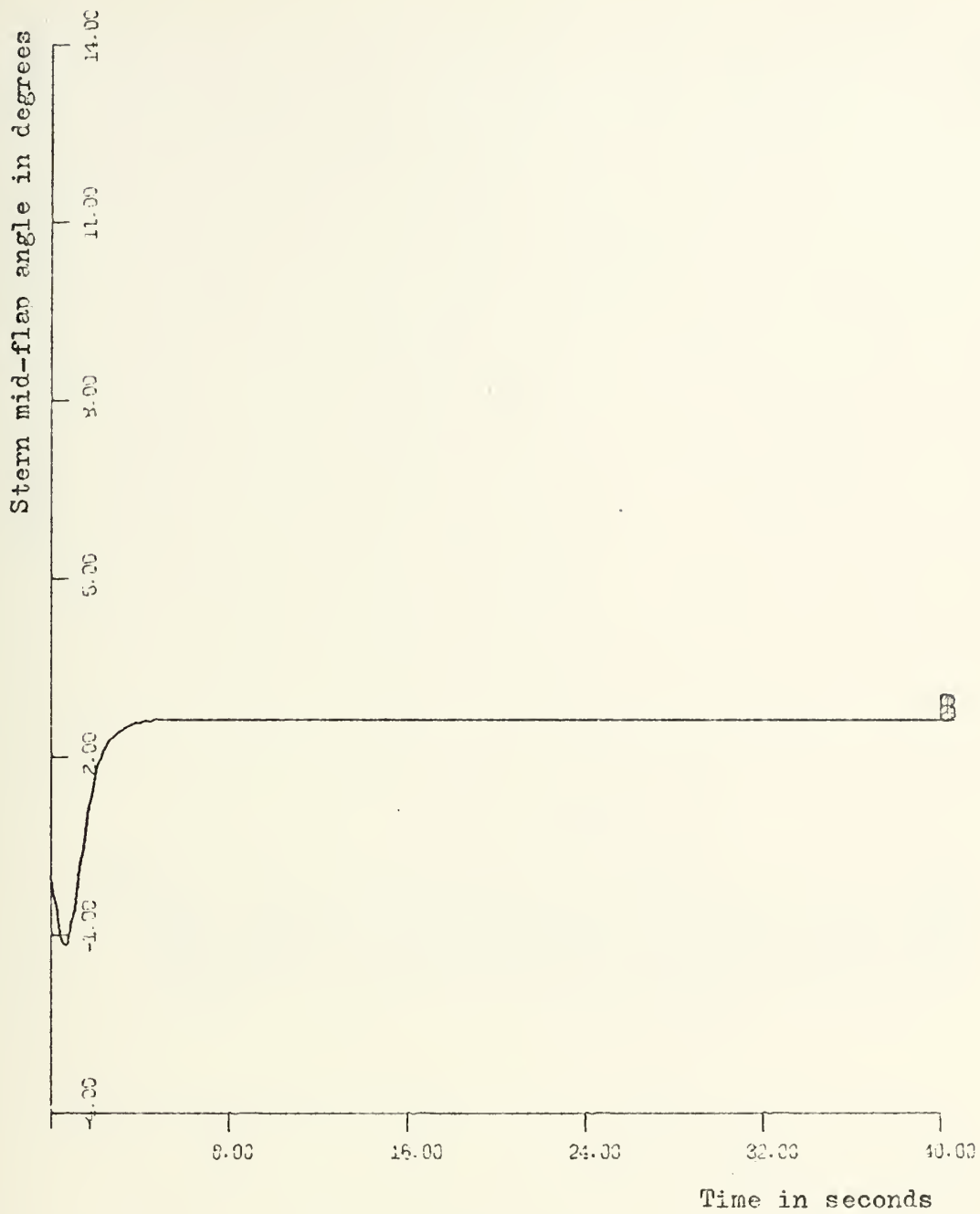


FIGURE 11F

DISTURBANCE : RUDDER

SPEED=30 KNOTS

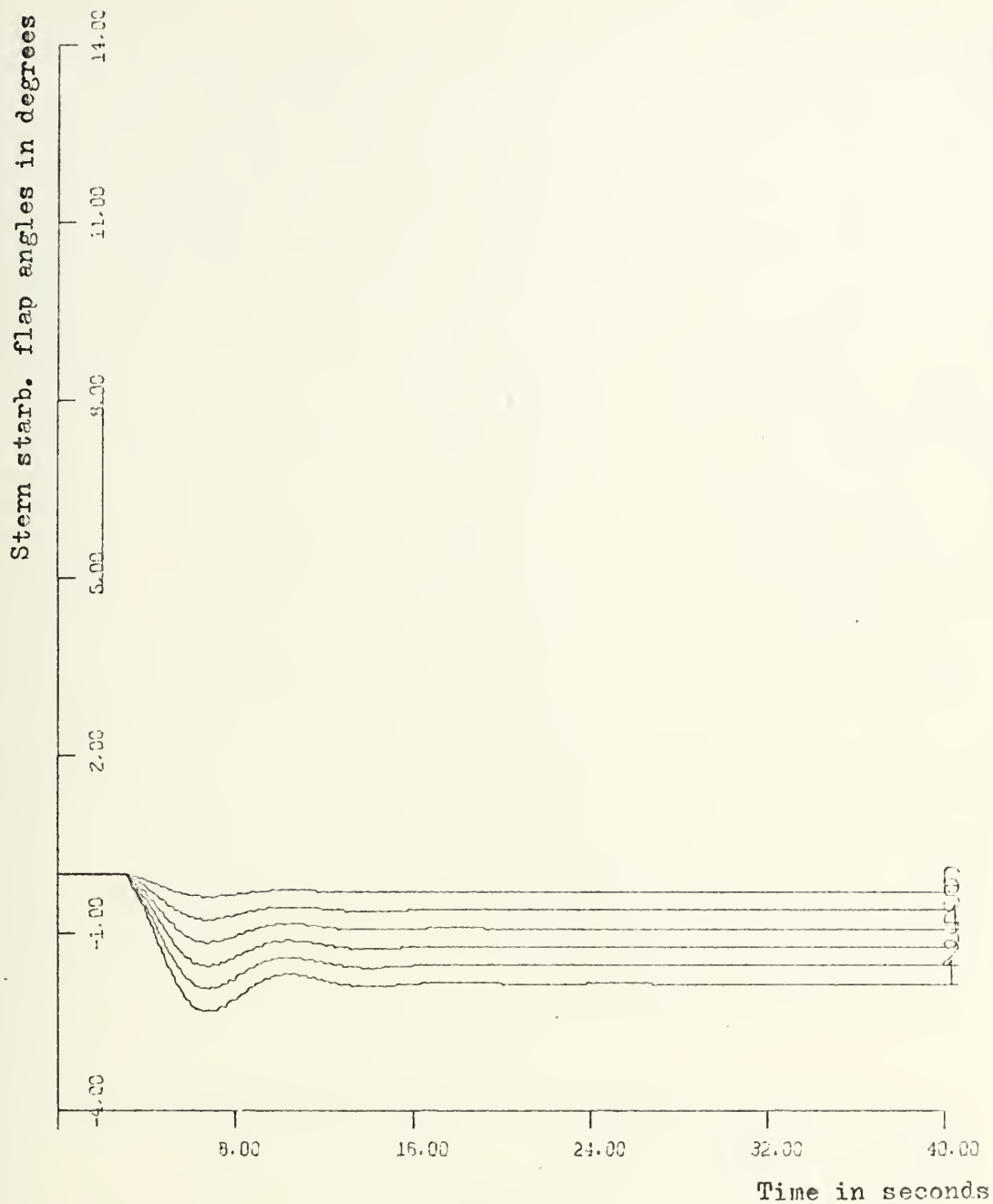


FIGURE 11G

DISTURBANCE : RUDDER

SPEED=30 KNOTS

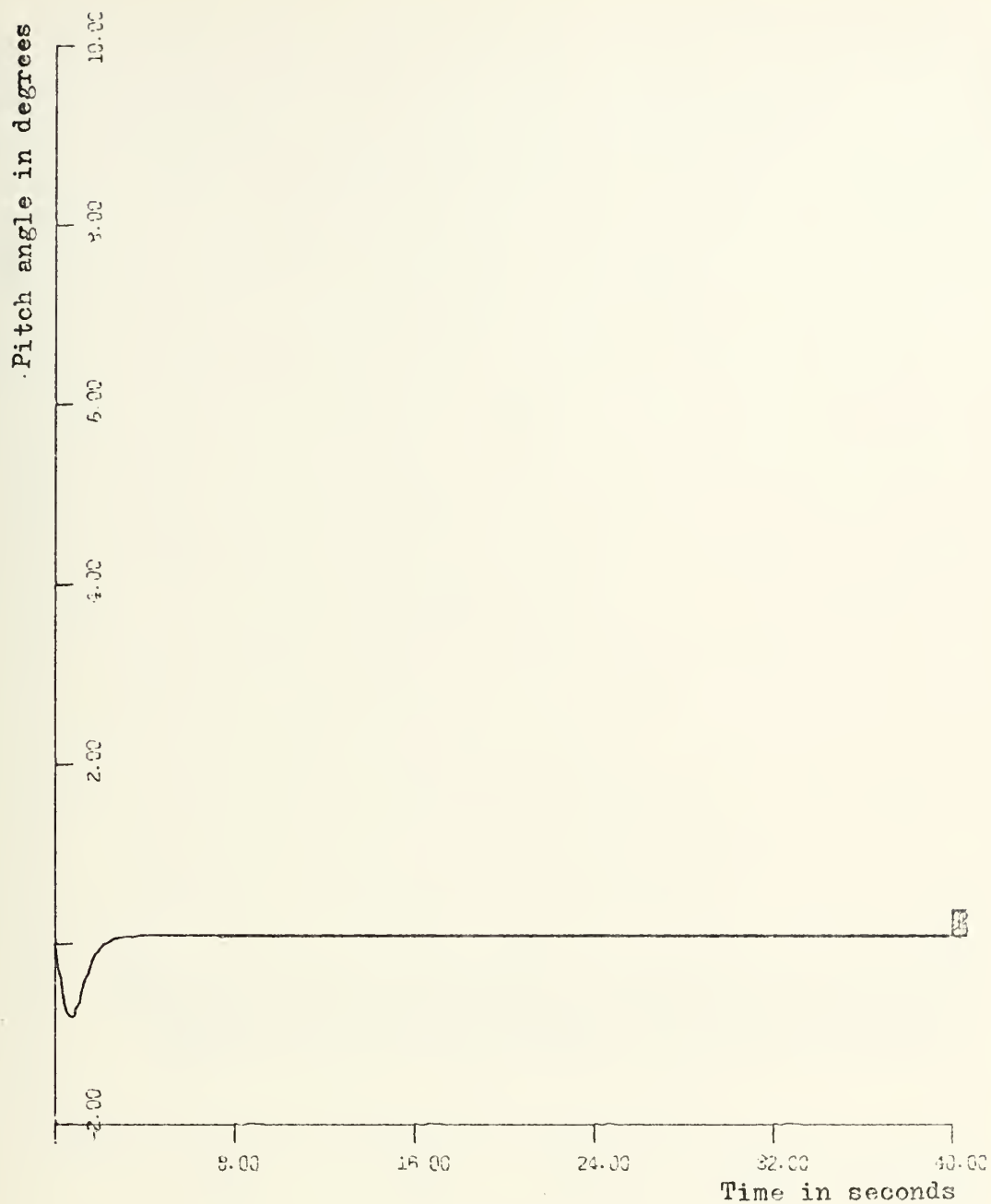


FIGURE 12A

DISTURBANCE : RUDDER TO STARB.

SPEED=36 KNOTS

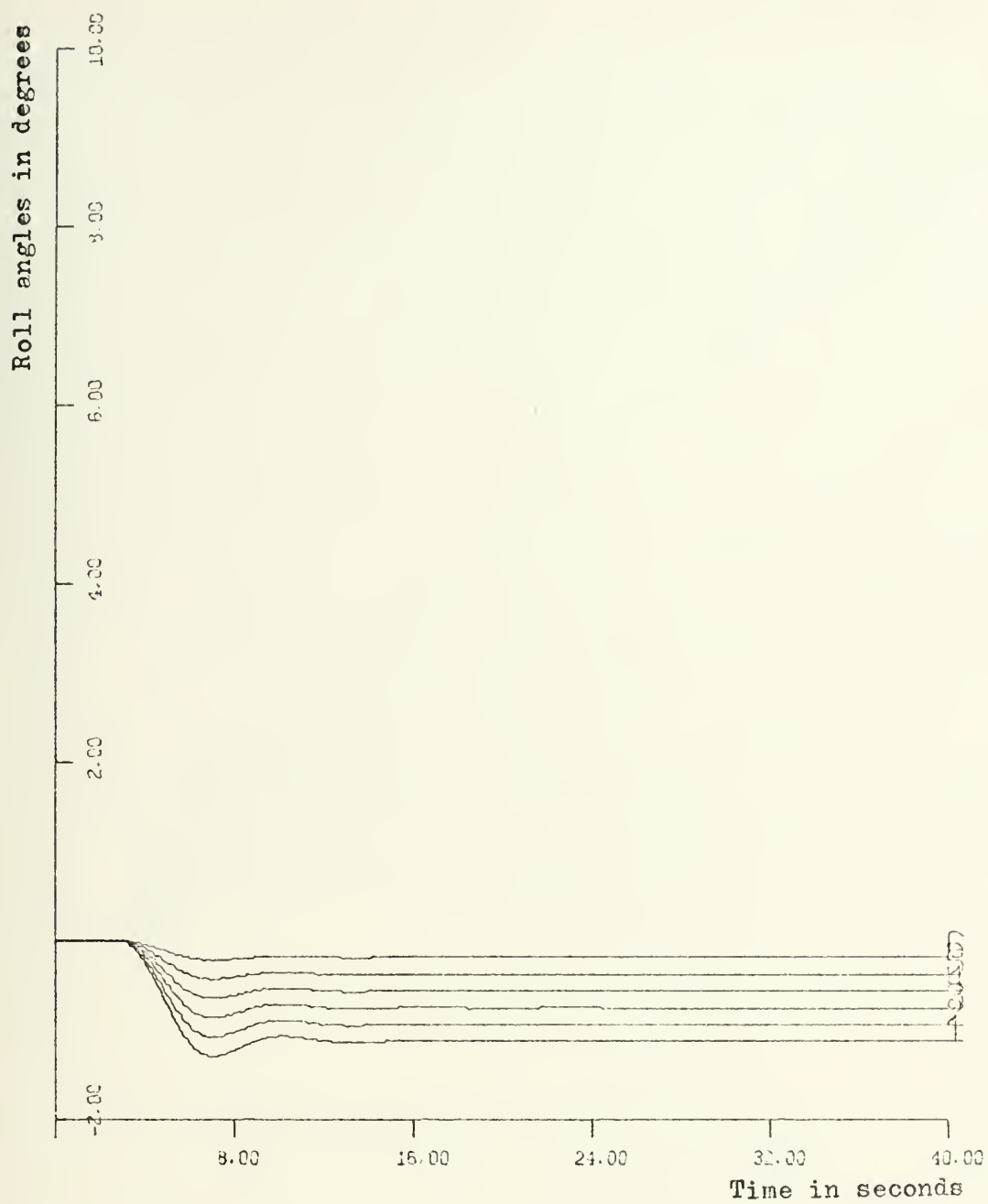


FIGURE 12B

DISTURBANCE : RUDDER TO STARB.

SPEED=36 KNOTS



FIGURE 12C

DISTURBANCE : RUDDER TO STARB.

SPEED=36 KNOTS

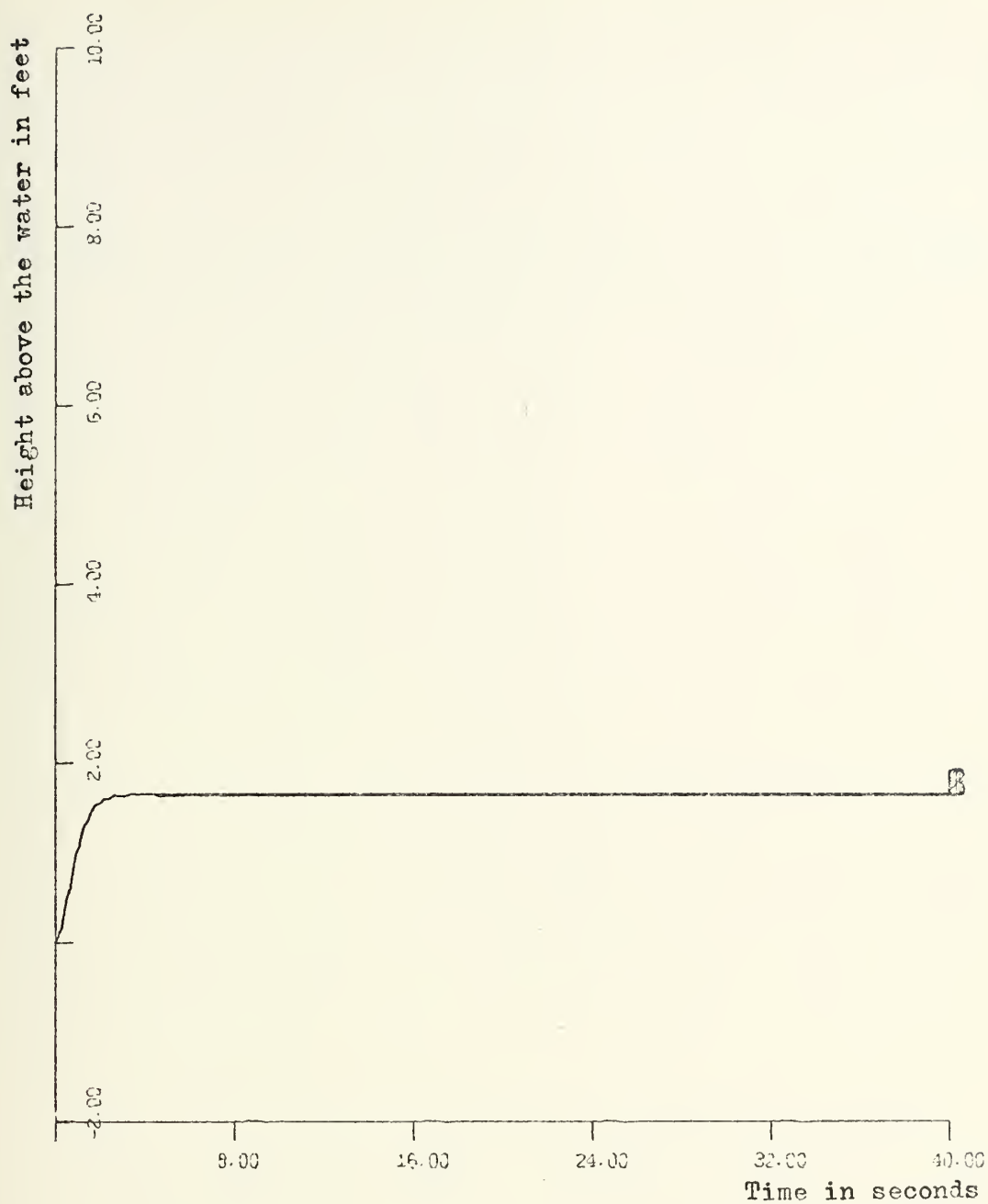


FIGURE 12D

DISTURBANCE : RUDDER TO STARB.

SPEED=36 KNOTS

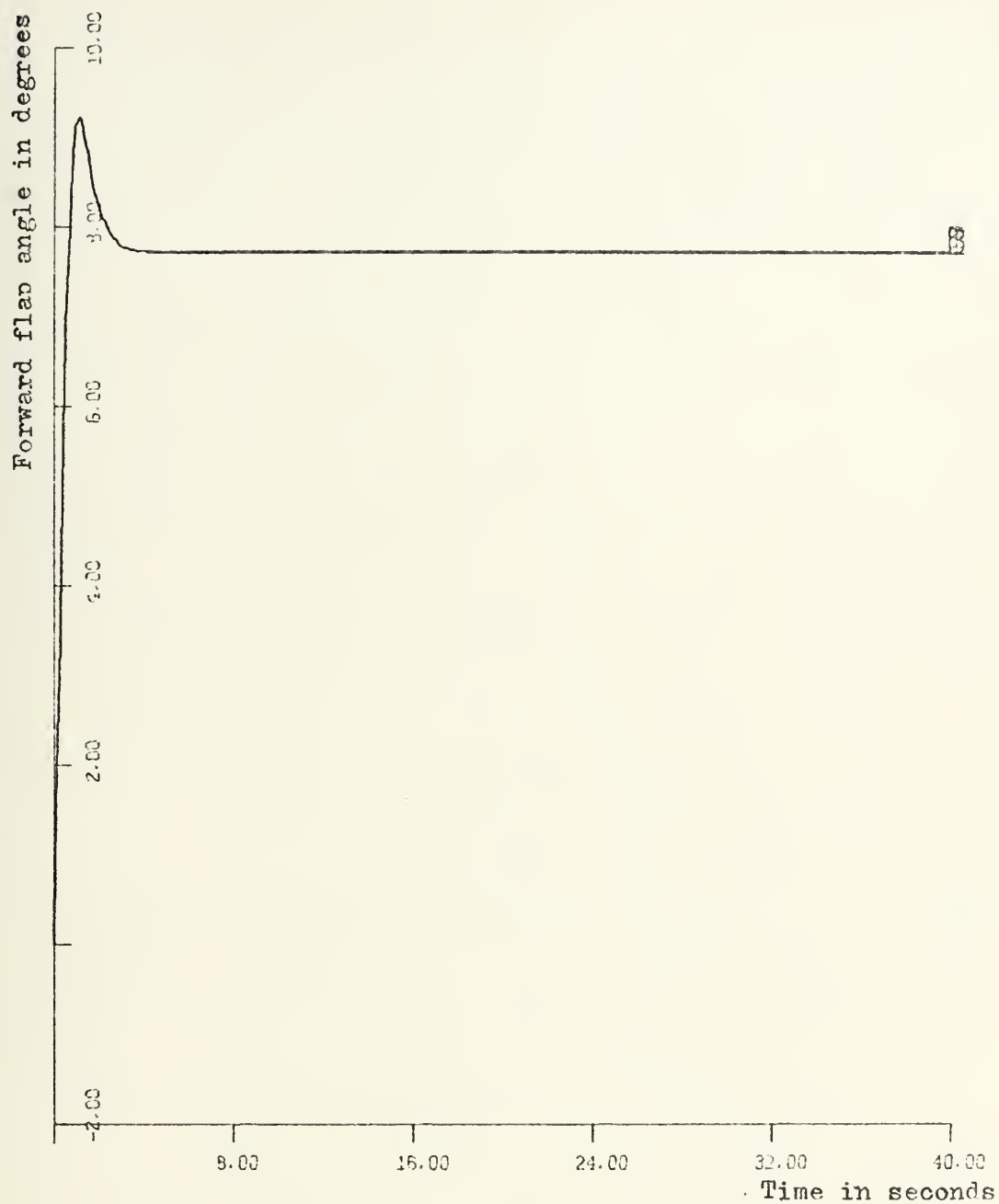


FIGURE 12E

DISTURBANCE: RUDDER TO STARB.

SPEED=36 KNOTS

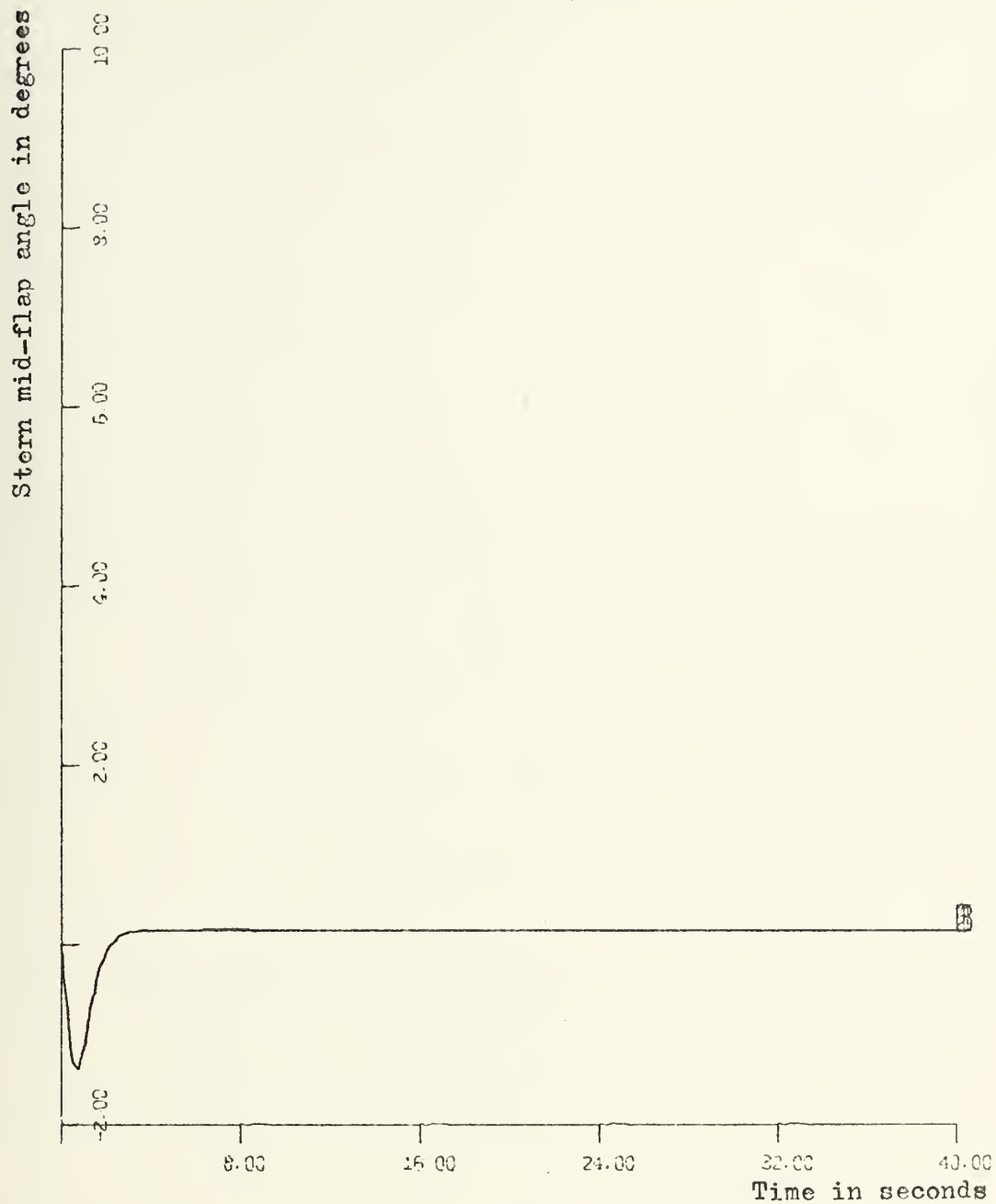


FIGURE 12F

DISTURBANCE : RUDDER TO STARB.

SPEED=36 KNOTS

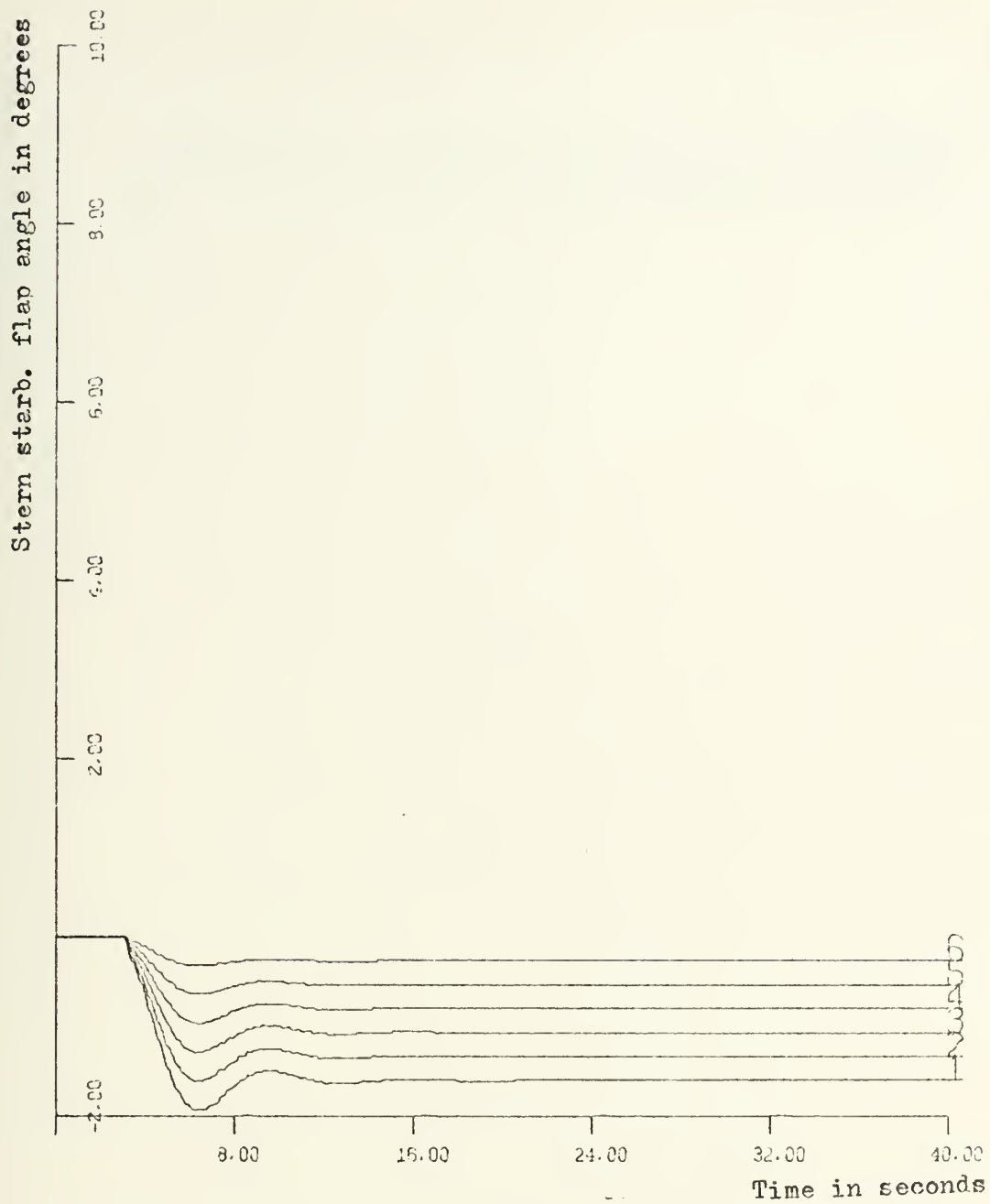


FIGURE 12G

DISTURBANCE : RUDDER TO STARB.

SPEED=36 KNOTS

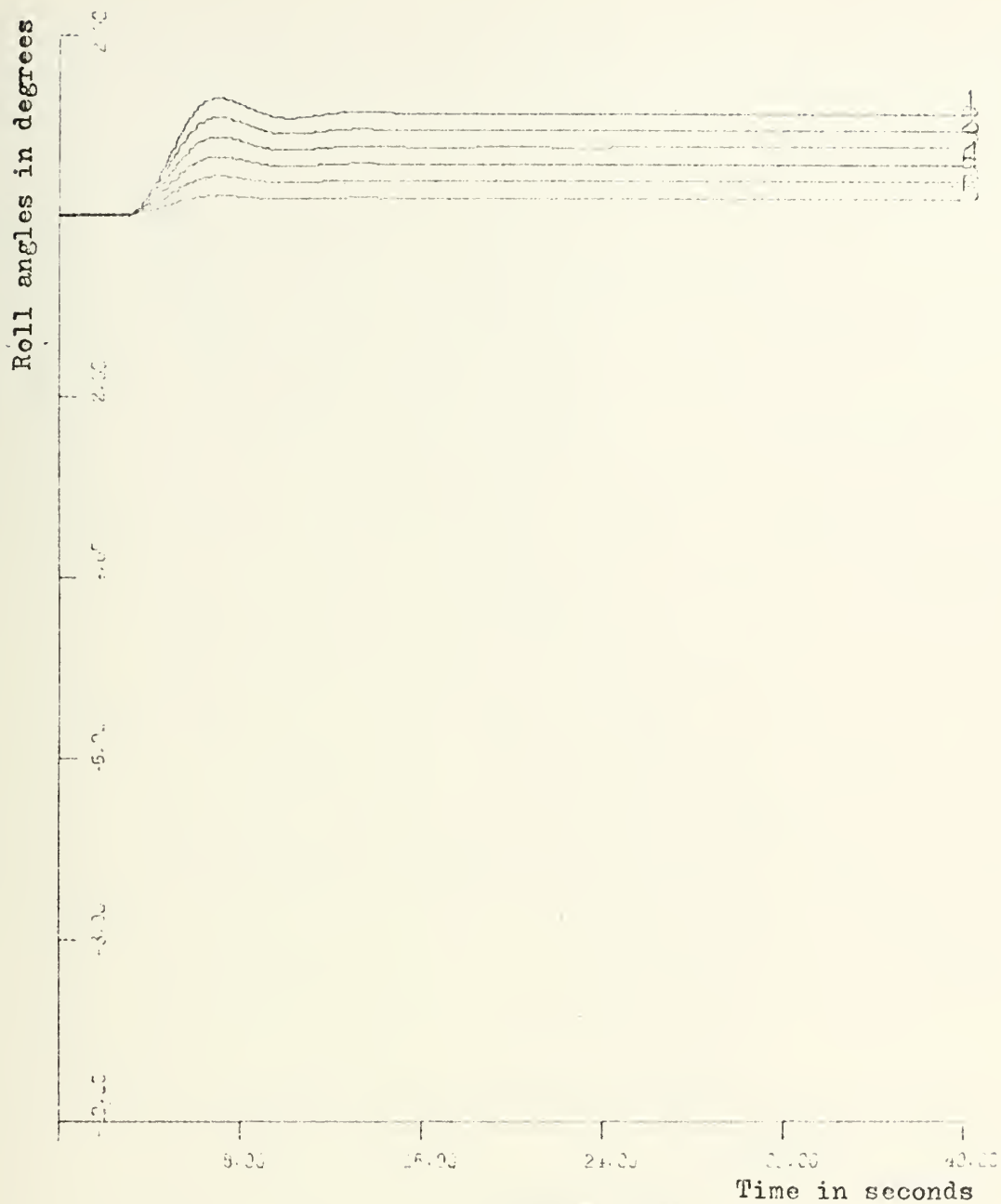


FIGURE 13A

DISTURBANCE : RUDDER TO PORT

SPEED=36 KNOTS



FIGURE 13B

DISTURBANCE : RUDDER TO PORT

SPEED=36 KNOTS

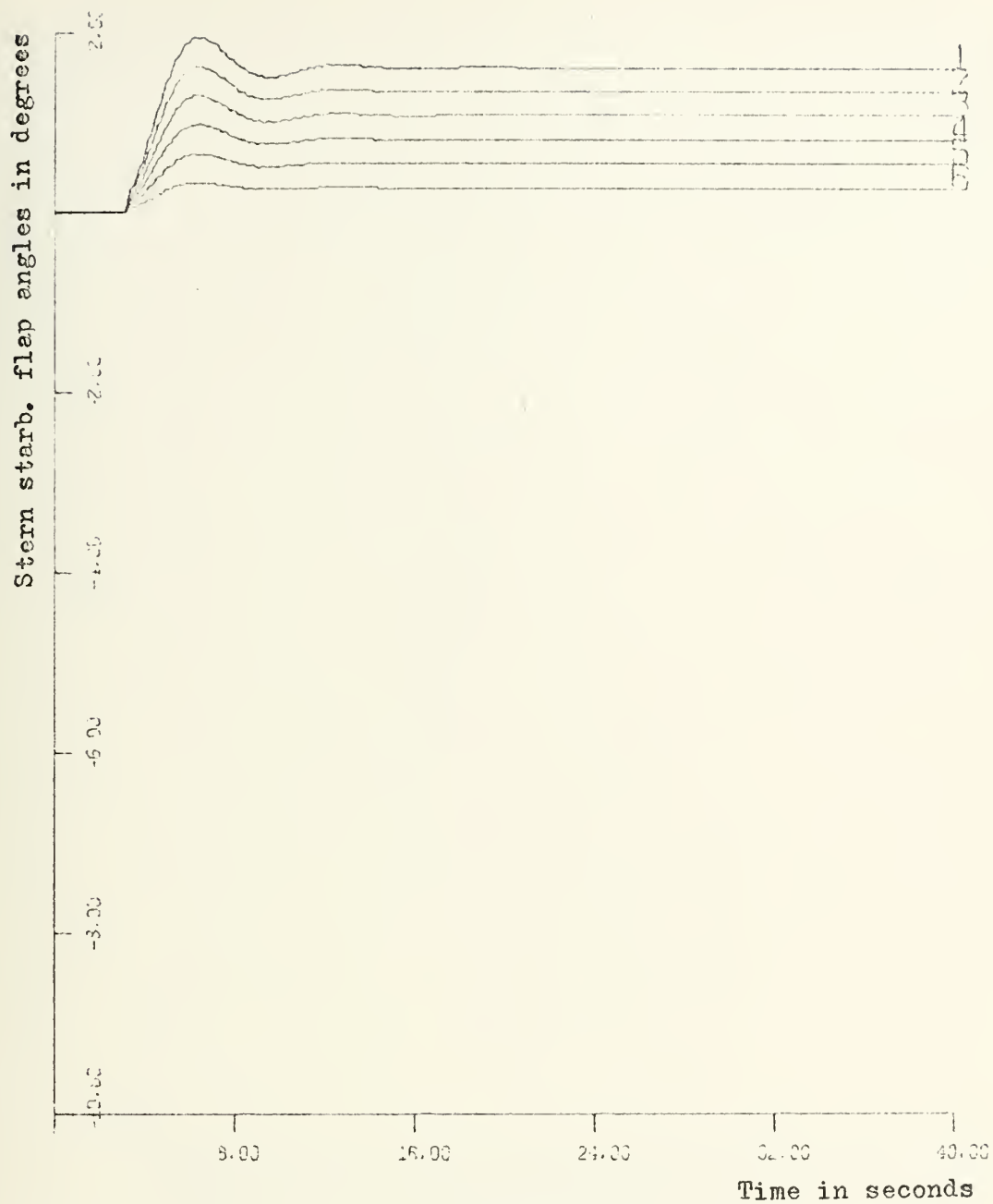


FIGURE 13C

DISTURBANCE : RUDDER TO PORT

SPEED=36 KNOTS

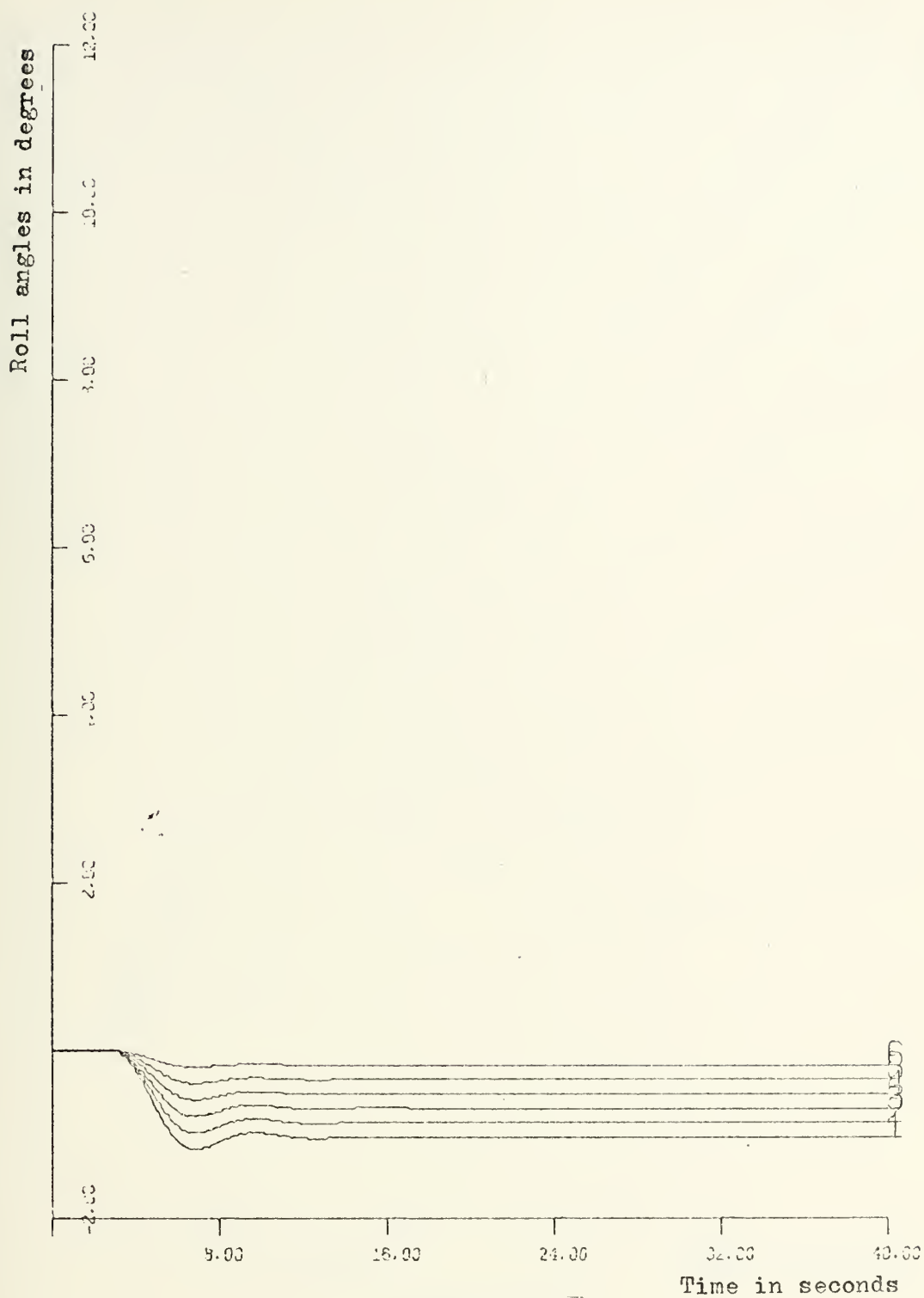


FIGURE 14A

DISTURBANCE : RUDDER

SPEED=40 KNOTS



FIGURE 14B

DISTURBANCE : RUDDER

SPEED=40 KNOTS

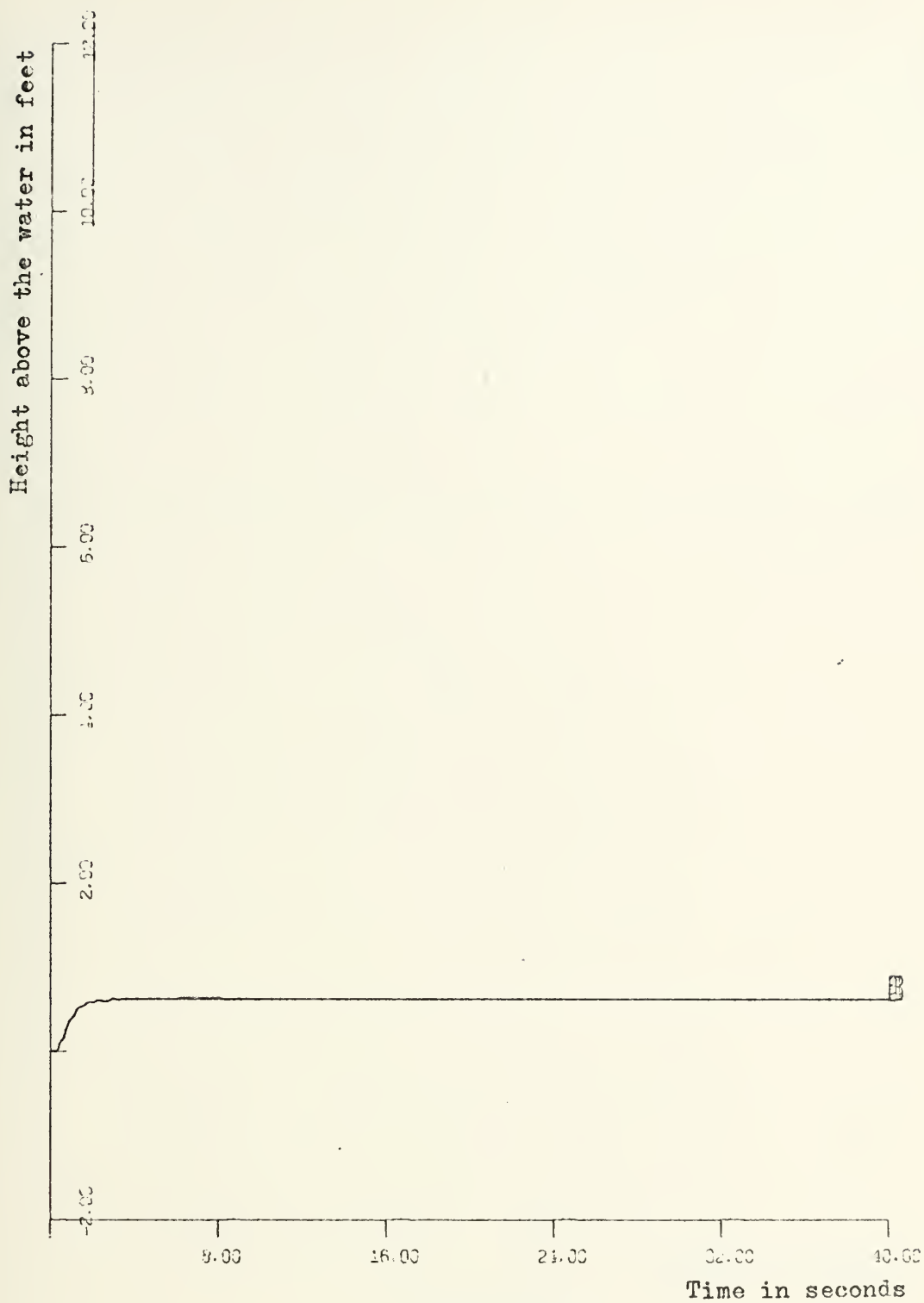


FIGURE 14C

DISTURBANCE : RUDDER

SPEED=40 KNOTS

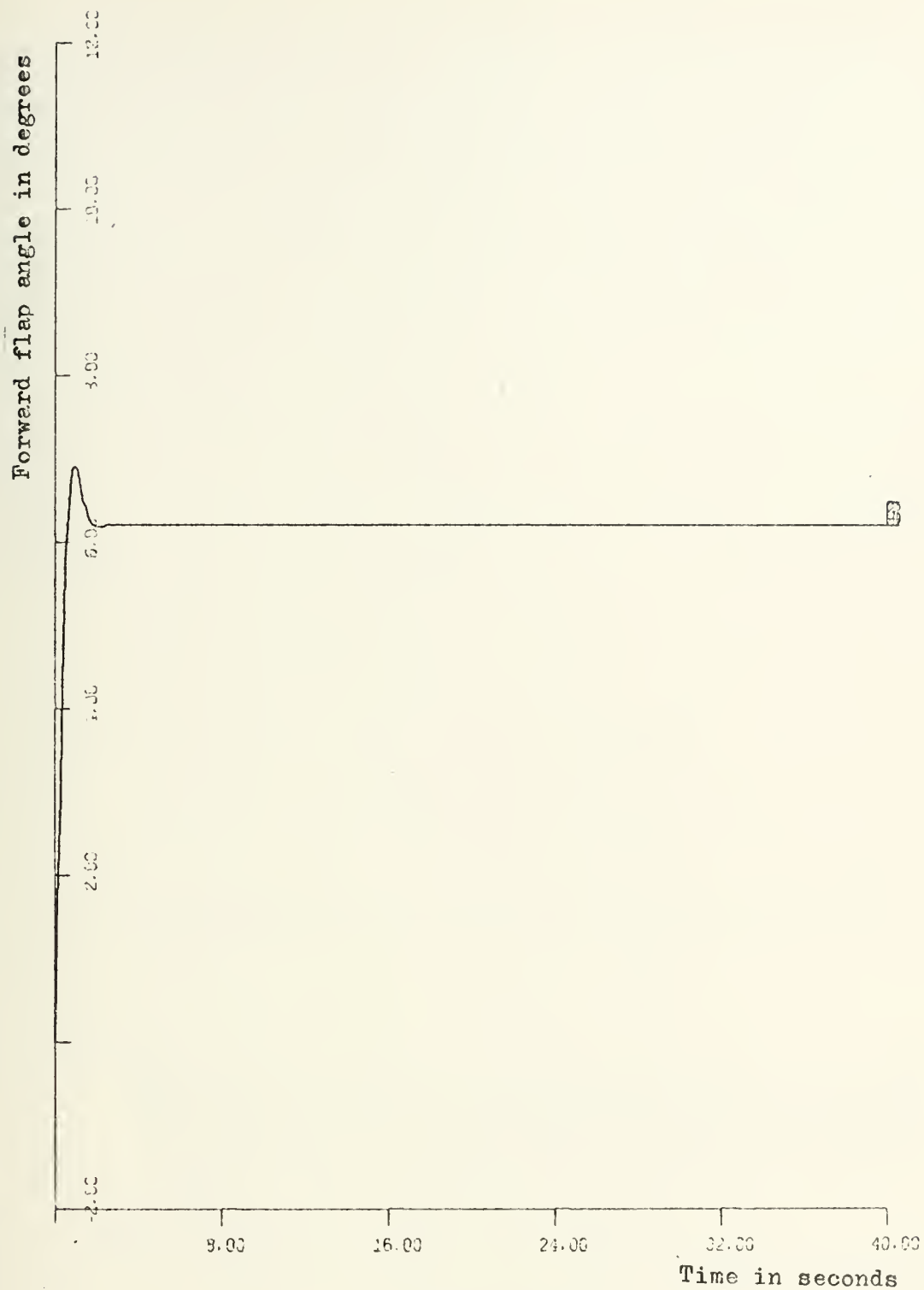


FIGURE 14D

DISTURBANCE : RUDDER

SPEED=40 KNOTS



FIGURE 14E

DISTURBANCE : RUDDER

SPEED=40 KNOTS

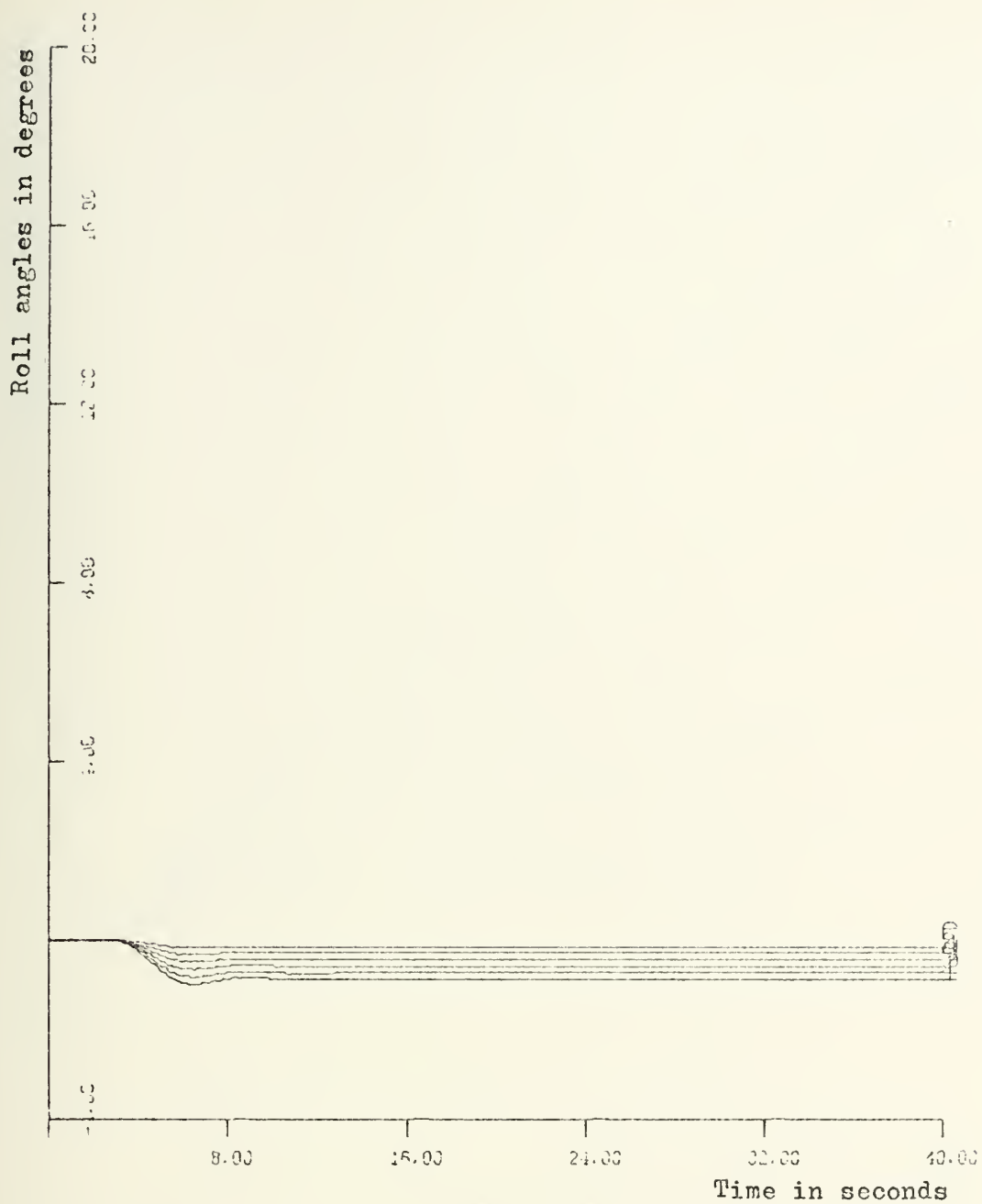


FIGURE 15A

DISTURBANCE : RUDDER

SPEED=50 KNOTS



FIGURE 15B

DISTURBANCE : RUDDER

SPEED=50 KNOTS

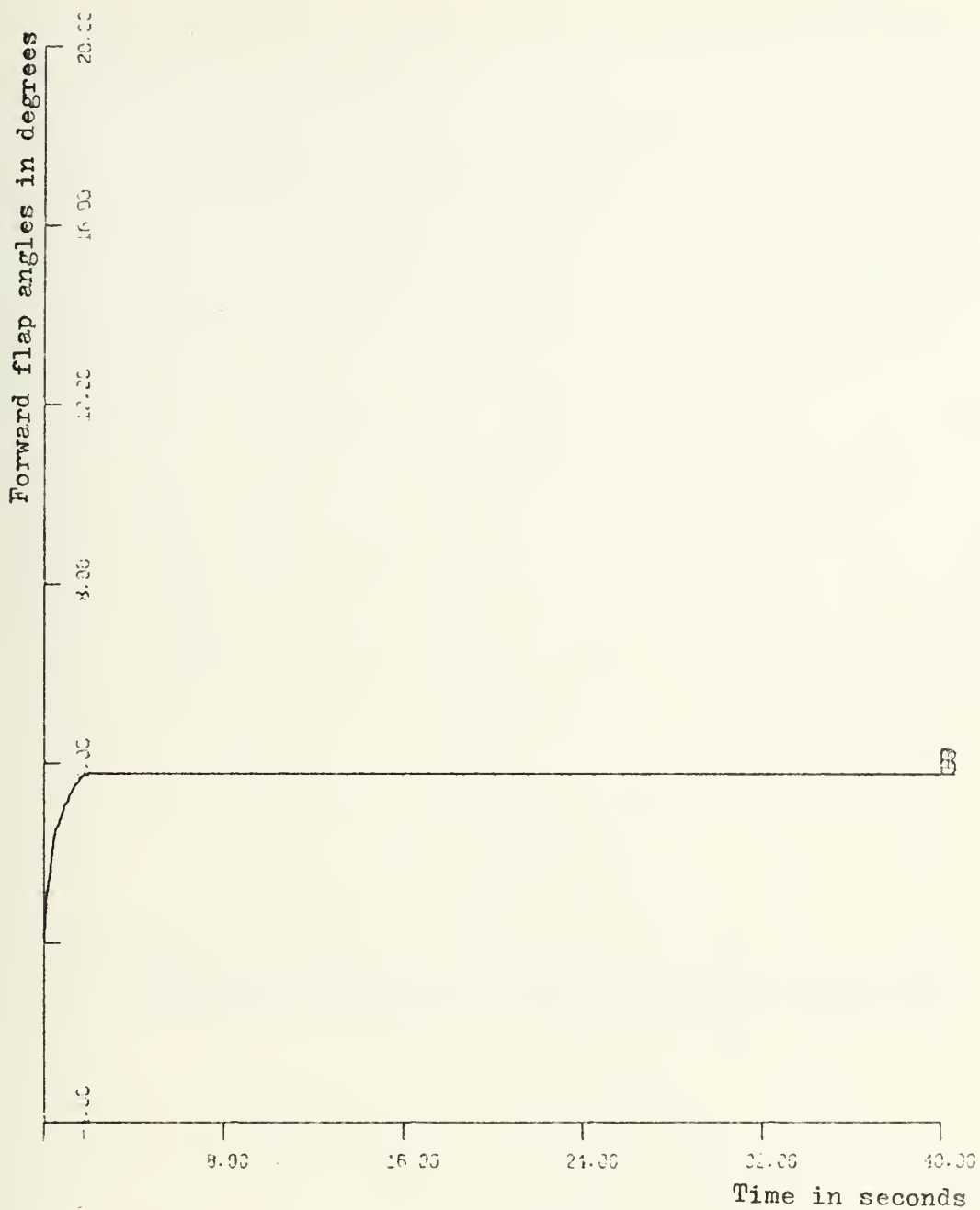


FIGURE 15C

DISTURBANCE : RUDDER

SPEED=50 KNOTS



FIGURE 15D

DISTURBANCE : RUDDER

SPEED=50 KNOTS

B. EFFECTS OF A HELM STEP COMMAND

Improving and completing the automatic control block of References 1 and 2 and based on the block diagram of Figure 6.7 in Ref.5, a simulated automatic control system was built, including the dynamic characteristics of the sensors, the dynamic characteristics of the compensation filters, inputs to the servo valves and the dynamic characteristics of the hydraulic actuators.

There was an important limitation and perhaps a certain inaccuracy in the values used as corner frequencies of the compensation filters and the values used as gains for the control actuation servos, because References 1,2,3 and 4 used the model $PC(H) \rightarrow 1$ for their studies and Ref. 5 used a more recent model, the PHM. Of course there was some lack of information, but some interesting results and some data were obtained for future studies.

As mentioned before, the main function of the forward flap was to lift the craft and keep it stable above the water in the pitch-heave mode. To confirm this, the helm doesn't actuate the forward flap, but only the starboard aft flap and the port aft flap, therefore these two last flaps will be responsible for the craft's turning in conjunction with the rudder and will also be responsible essentially for the craft's rolling and finally for the craft's pitching. The forward flap is only actuated according to its job by the forward accelerometer servo, by the height sensor servo and by the pitch angle servo. The two aft flaps are actuated by the respective accelerometer sensors, by the pitch angle sensor, by the roll angle sensor and by the manual helm control. The rudder servo is actuated by the roll angle servo, by a yaw rate gyro and by a heading command disengaged or engaged. In this last case it will stop and turn back the rudder when the desired heading is reached.

Several figures will be shown with the roll angles,

heading angles, rudder angles, starboard and port flaps angles for different speeds and under the actuation of helm step commands of 150,120,90,60 and 30 degrees to the starboard side, at each speed.

1. Speed=30 knots

In Figure 16A the roll angles corresponding to different helm angles were represented. The helm was moved to starboard after 12 seconds of straight ahead motion, then the craft started turning in the right direction, also to starboard. For a helm angle of 150 degrees the roll angle was 9 degrees after 24 seconds and for a helm angle of only 30 degrees the roll angle was 3 degrees after 30 seconds.

In Figure 16B the heading angles were represented. The craft started straight ahead and when a starboard helm was introduced, the craft started turning to starboard, reaching 21.2 degrees to starboard after 30 seconds for a helm angle of 150 degrees and only 3.4 degrees to starboard in the same amount of time for a helm angle of 30 degrees.

Figure 16C shows the different rudder angles due to a helm step command. While the ship went straight ahead the rudder was also straight ahead, but when the helm was introduced after 12 seconds, the rudder turned to starboard on the craft's turning direction. Finally when the helm was removed after 28 seconds, the rudder went back to its normal position. For a helm angle of 150 degrees the rudder reached a value of 5.1 degrees to starboard and for a helm angle of 30 degrees it only reached 0.78 degrees to starboard.

In Figure 16D and 16E the port aft flap and the starboard aft flap were respectively represented. When a helm angle was introduced after 12 seconds, the craft started turning and banking. After those 12 seconds the port aft flap had positive values, (down direction) and the starboard flap had negative values, (up direction). When the craft is turning to starboard, it must roll to starboard, therefore a lift on the port side must exist. The port flap being down, when the craft advances more force is exerted on

that flap by the water and there is a lift force on that side. The starboard flap is up and on that side there is a down force. When the helm goes to zero degrees after 28 seconds, the craft rolls in the opposite direction and it can be verified by the figures that the flaps have also moved in opposite directions.

2. Speed=36 knots

In Figure 17A the roll angles corresponding to different helm angles were represented. When the helm was introduced after 10 seconds, the craft started rolling to starboard. For a helm angle of 150 degrees the roll angle reached 6.2 degrees in 18 seconds and for a helm angle of 30 degrees the roll angle reached 2.55 degrees after 27 seconds and it started banking in the opposite direction when the helm went again to 0 degrees.

The heading angles were represented in Figure 17B. When a helm angle of 150 degrees was introduced after 10 seconds, the craft started turning to starboard, reaching a maximum heading angle value of 37.3 degrees after 28 seconds and for a helm angle of 30 degrees, the craft reached a maximum heading angle value of 6.9 degrees after 28 seconds.

The rudder angles were represented in Figure 17C. For a helm angle of 150 degrees, the rudder angle reached a value of 5.37 degrees to starboard after 24 seconds, then it started going back in the opposite direction when the helm was removed. For a helm angle of 30 degrees the maximum rudder angle value was 1.44 degrees to starboard after 24 seconds, then, as before, it started returning in the opposite direction.

In Figure 17D and 17E the port and starboard flaps were represented. As before when the craft was banking to starboard, the port flap had positive values (down direction) and the starboard flap negative values (up direction). Both flaps reversed the motions when the craft rolled back to its normal position after 24 seconds.

3. Speed=40 knots

In Figure 18A the roll angles for different helm angles were represented. For a helm angle of 150 degrees, the roll angle reached a value of 9.38 degrees after 19 seconds. For a helm angle of 30 degrees the roll angle reached a maximum value of 2.43 degrees after 23 seconds.

In Figure 18B the different heading angles were represented. For a helm angle of 150 degrees the heading angle reached 26.3 degrees in 24 seconds and for a helm angle of 30 degrees the heading angle reached 12.12 degrees in 24 seconds.

In Figure 18C the different rudder angles were represented. For a helm angle of 150 degrees the rudder angle had a maximum value of 5.83 degrees to starboard after 21 seconds and for a helm angle of 30 degrees, the rudder angle had a maximum value of 1.16 degrees to starboard after 21 seconds.

In Figures 18D and 18E the port and starboard flaps were shown. Their movements were the same as before, according to the craft's rolling motion.

4. Speed=50 knots

In Figure 19A the roll angles for different helm angles were represented. For a helm angle of 150 degrees the roll angle had a value of 9.45 degrees after 15 seconds and for a helm angle of 30 degrees the roll angle had a maximum value of 2.45 degrees after 20 seconds, then it started decreasing because the craft rolled in the opposite direction due to the removal of the helm command.

In Figure 19B the heading angles were represented. For a helm angle of 150 degrees, the heading angle reached a value of 38.7 degrees to starboard after 25 seconds. For a helm angle of 30 degrees the heading angle reached a value of 11.1 degrees to starboard after 25 seconds.

In Figure 19C the rudder angles were represented. For a helm angle of 150 degrees, the rudder angle reached a maximum value of 7.78 degrees after 21 seconds and then it

started decreasing, moving in the opposite direction due to the removal of the helm command. For a helm angle of 30 degrees, the rudder angle reached a value of 1.54 degrees after 21 seconds and again it started decreasing.

In Figures 19D and 19E, the port and starboard flaps were represented. Their motions are the same as before, but with different values.

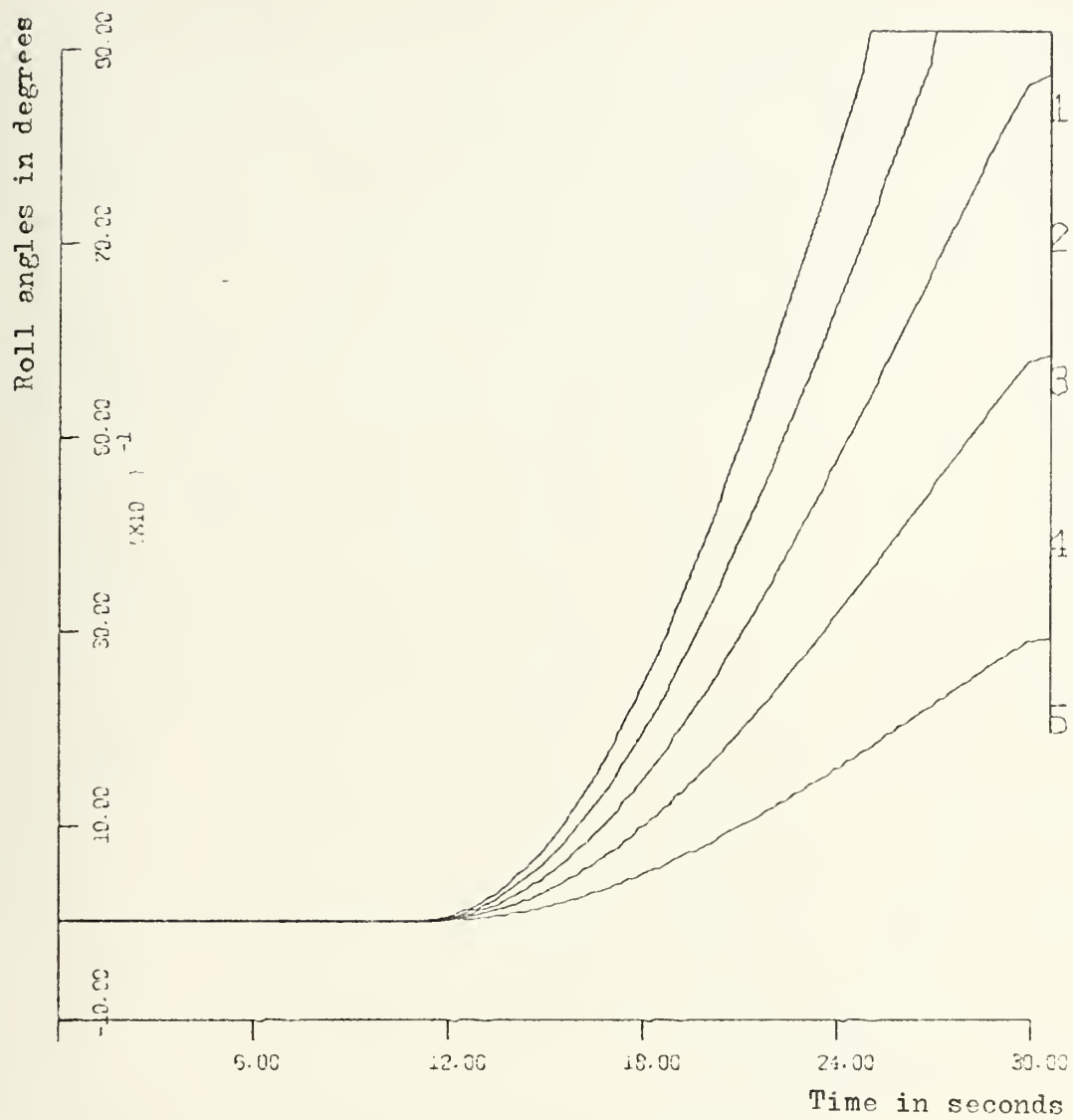


FIGURE 16A

DISTURBANCE : HELM

SPEED=30 KNOTS

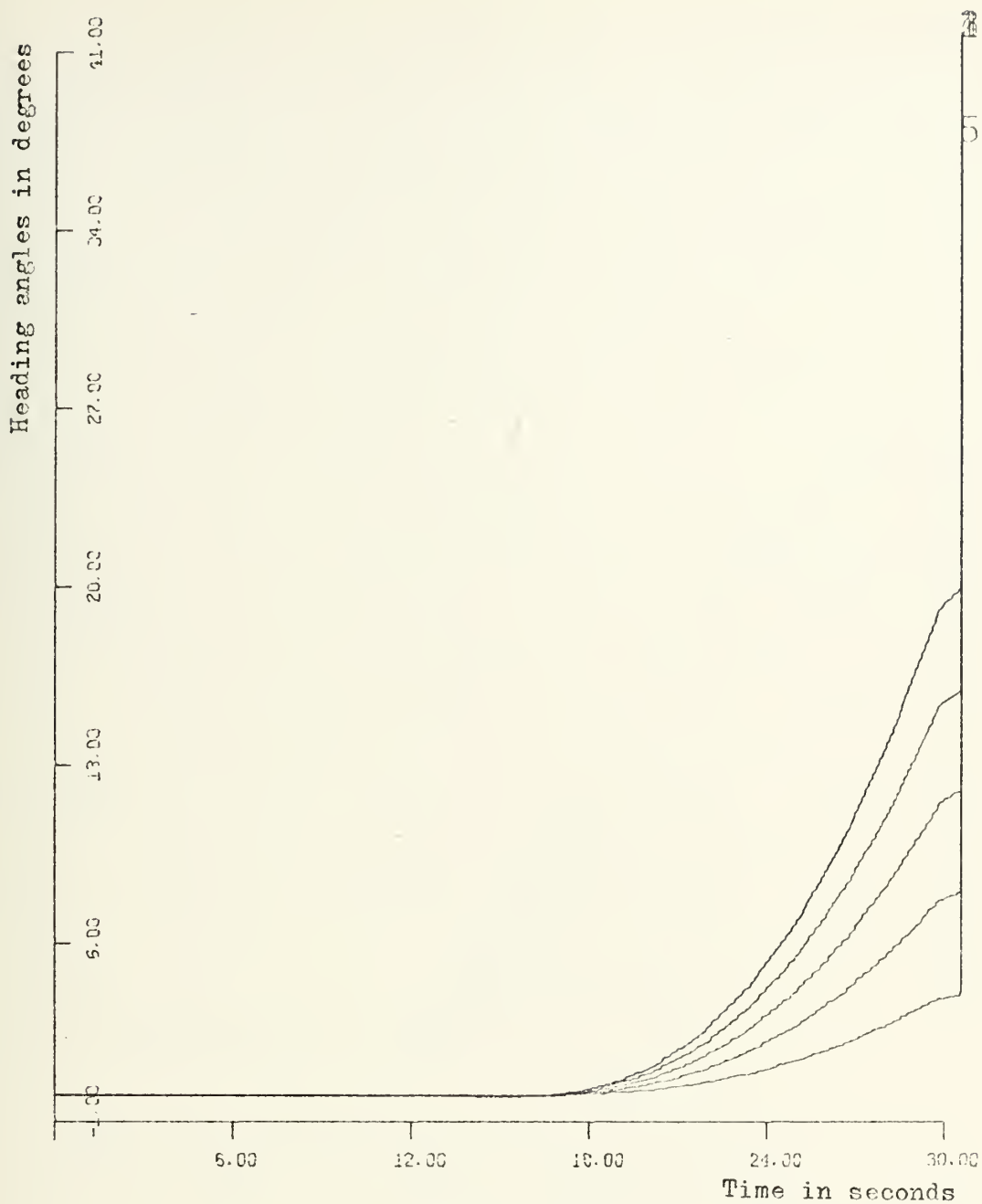


FIGURE 16B

DISTURBANCE : HELM

SPEED=30 KNOTS



FIGURE 16C

DISTURBANCE : HELM

SPEED=30 KNOTS



FIGURE 16D

DISTURBANCE : HELM

SPEED=30 KNOTS

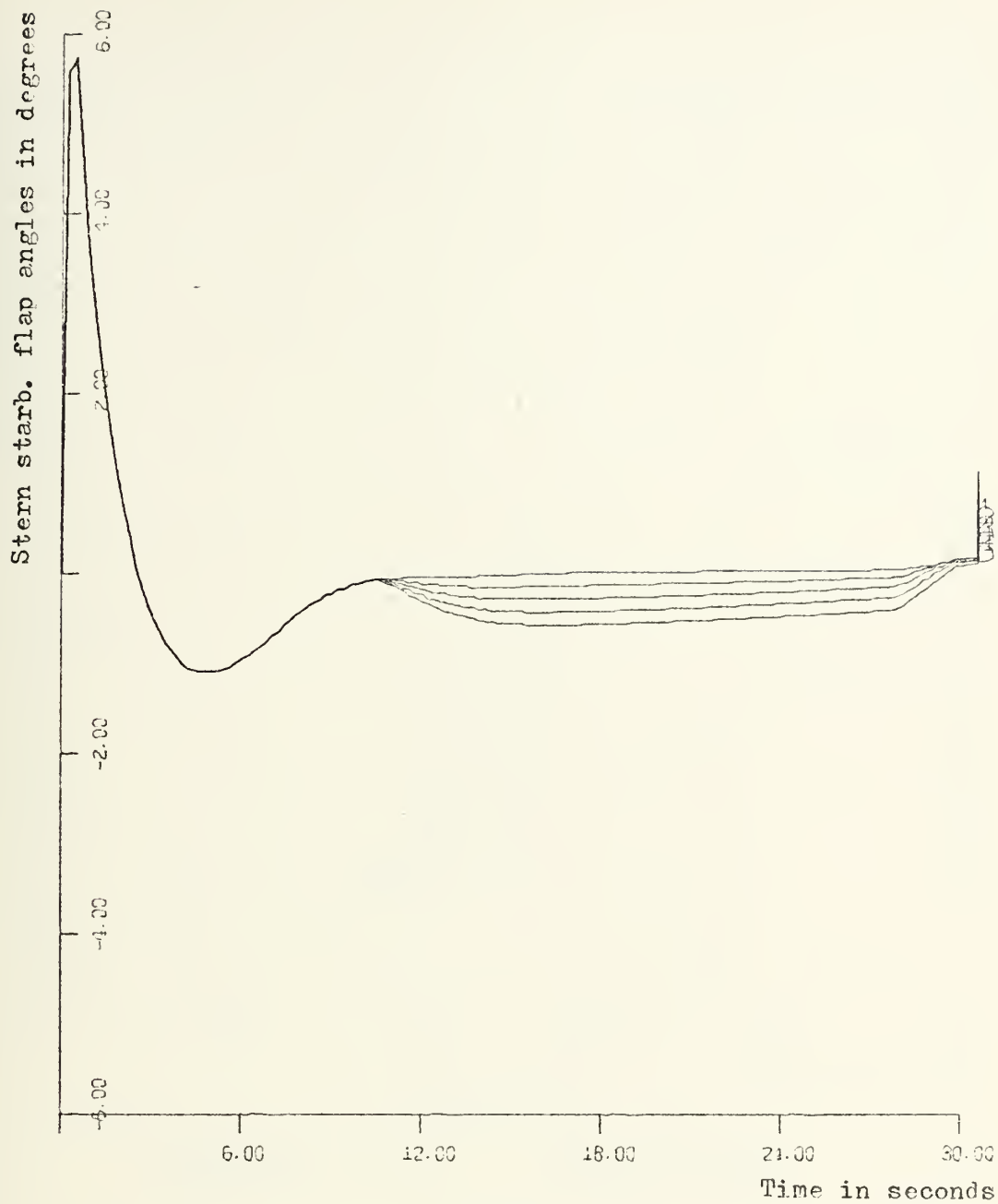


FIGURE 16E

DISTURBANCE : HELM

SPEED=30 KNOTS

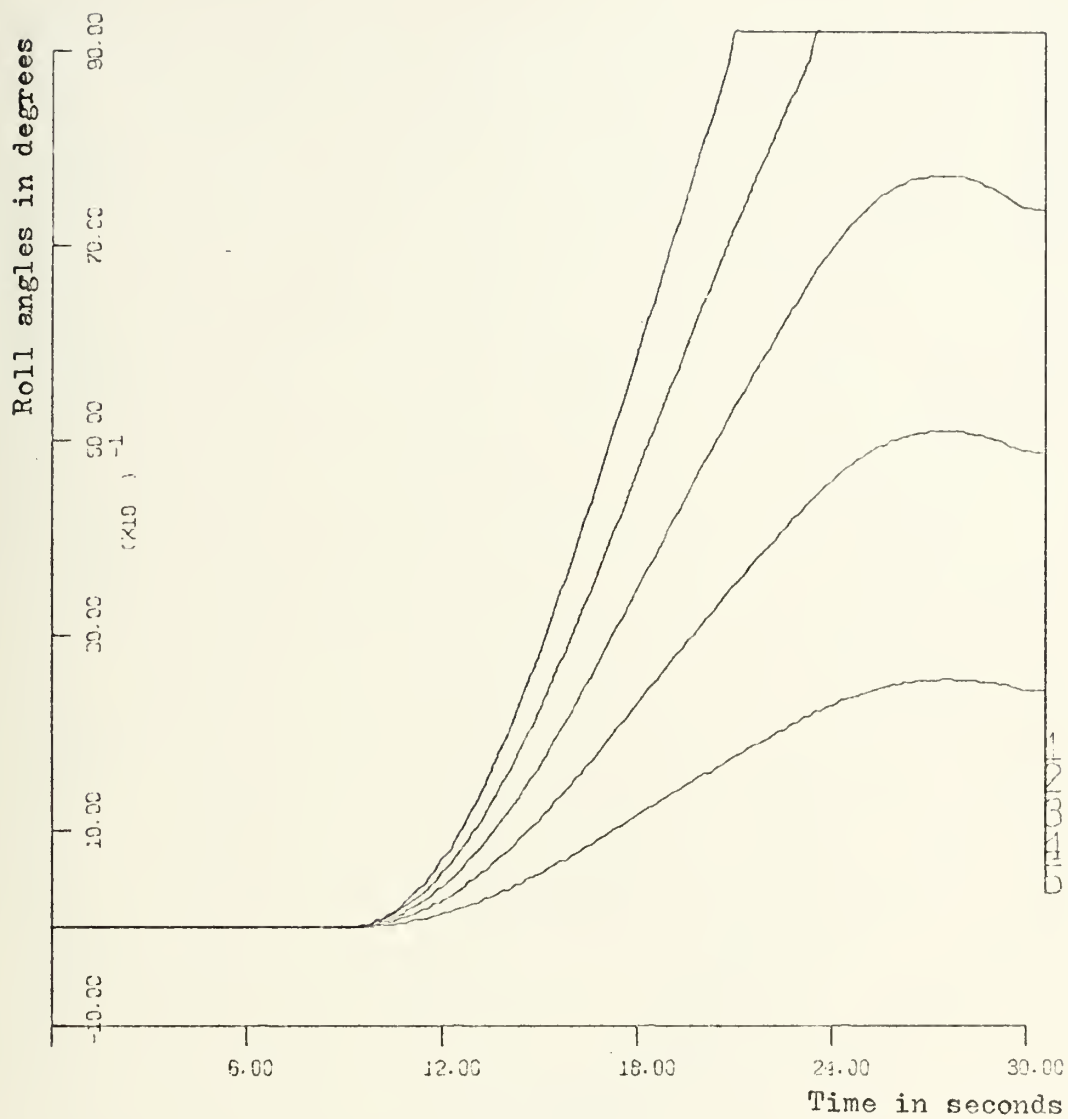


FIGURE 17A

DISTURBANCE : HELM

SPEED=36 KNOTS

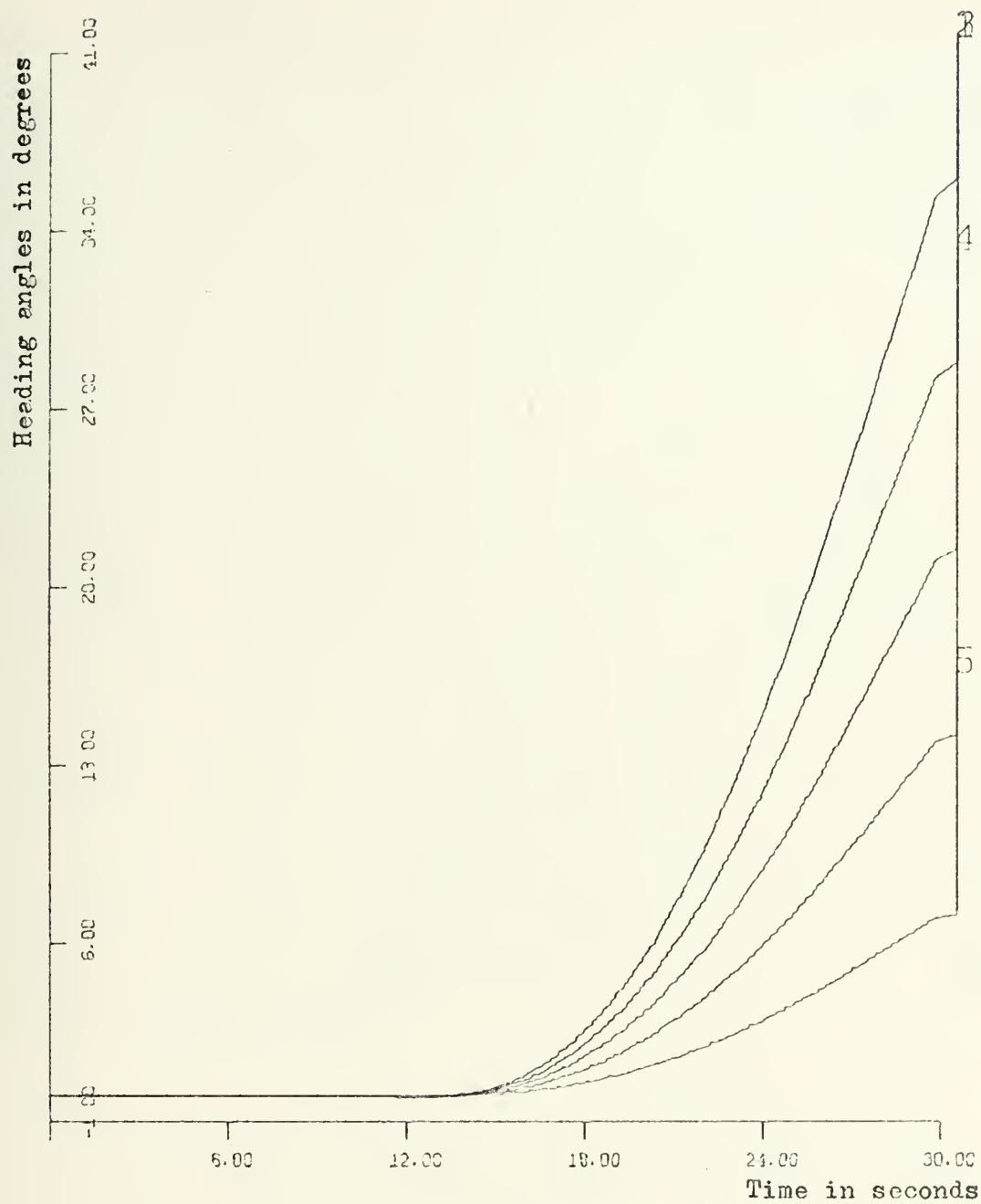


FIGURE 17B'

DISTURBANCE : HELM

SPEED=36 KNOTS



FIGURE 17C

DISTURBANCE : HELM

SPEED=36 KNOTS

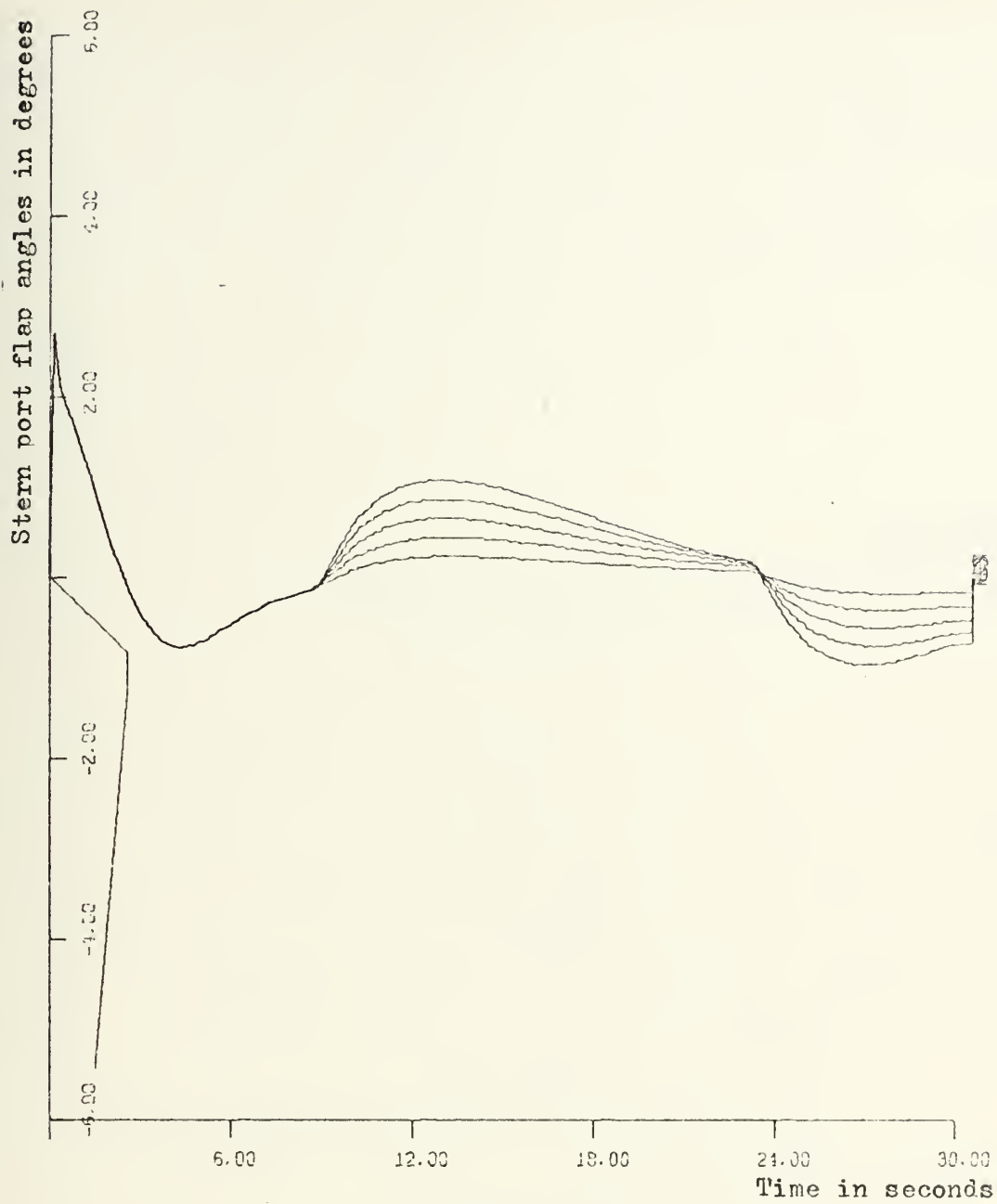


FIGURE 17D

DISTURBANCE : HELM

SPEED=36 KNOTS

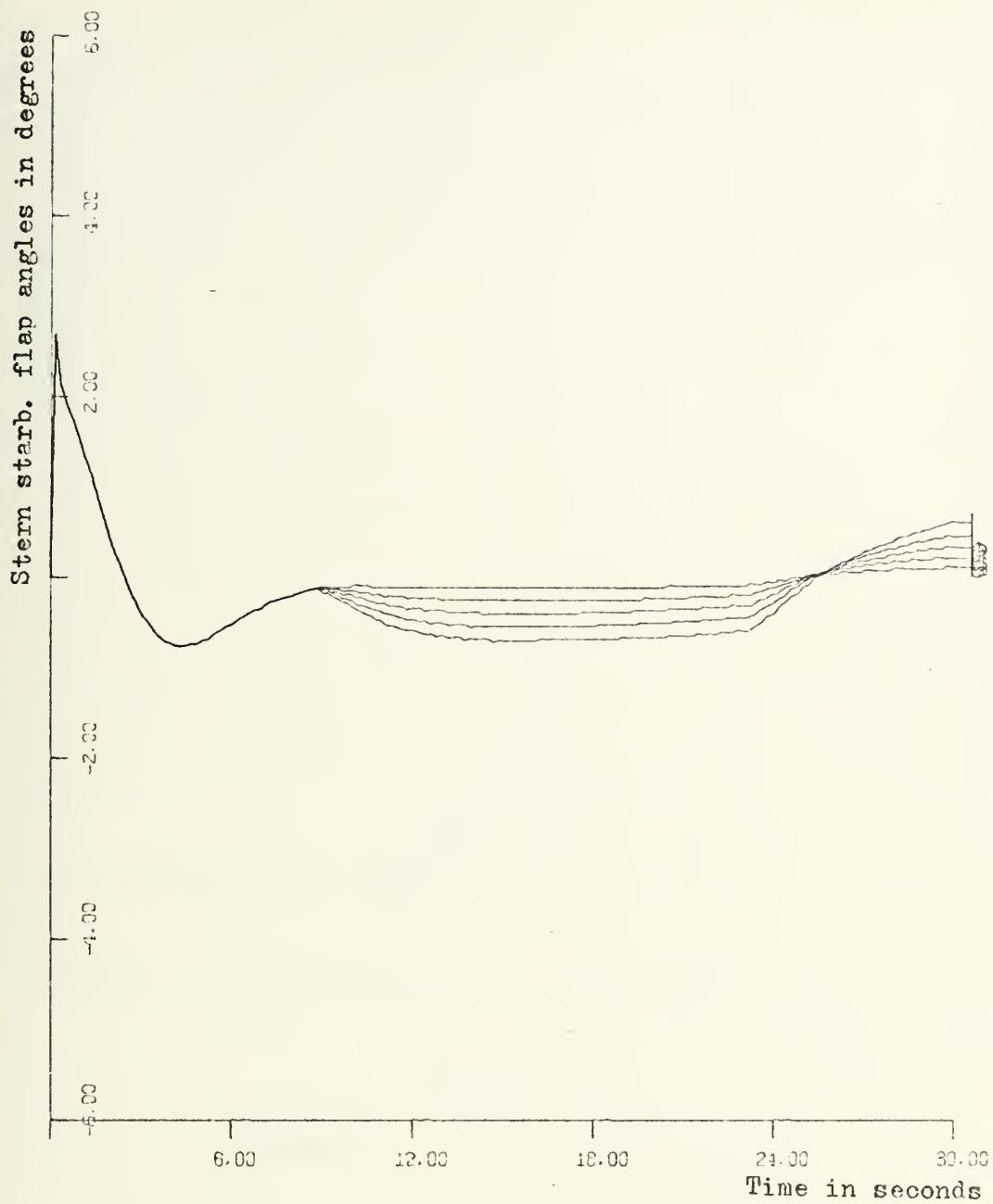


FIGURE 17E

DISTURBANCE : HELM

SPEED=36 KNOTS

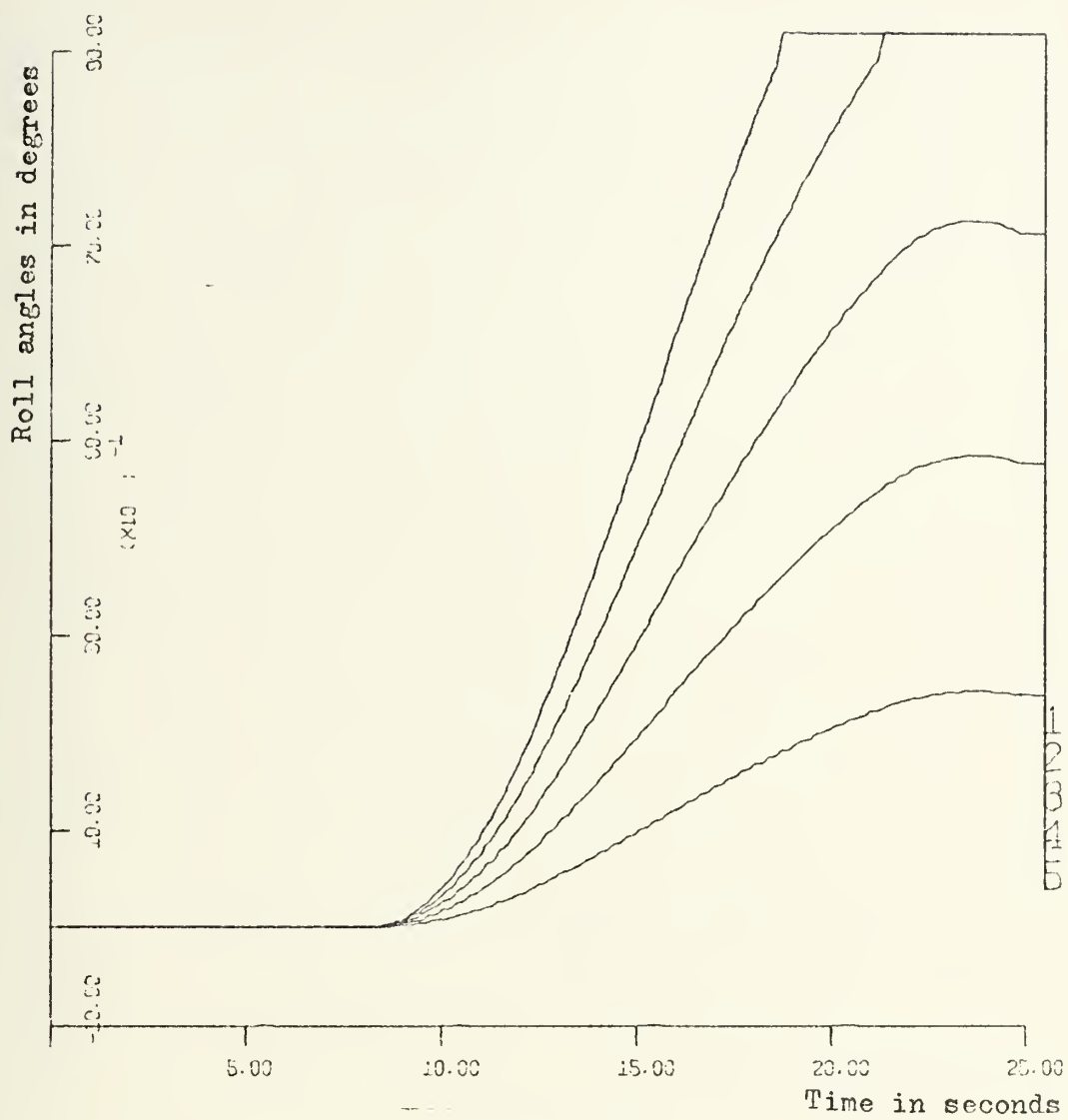


FIGURE 18A

DISTURBANCE : HELM

SPEED=40 KNOTS

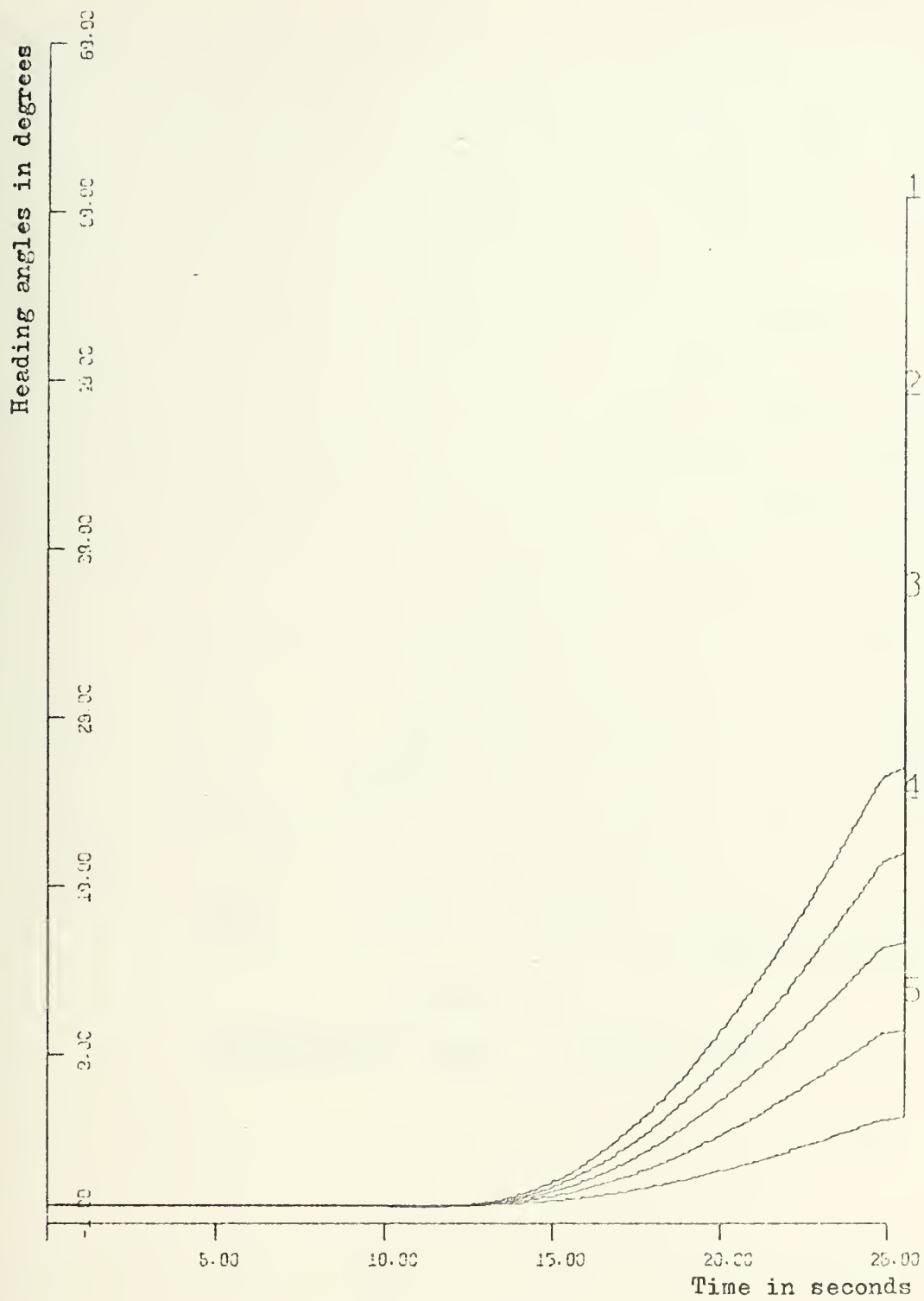


FIGURE 18B

DISTURBANCE : HELM

SPEED=40 KNOTS

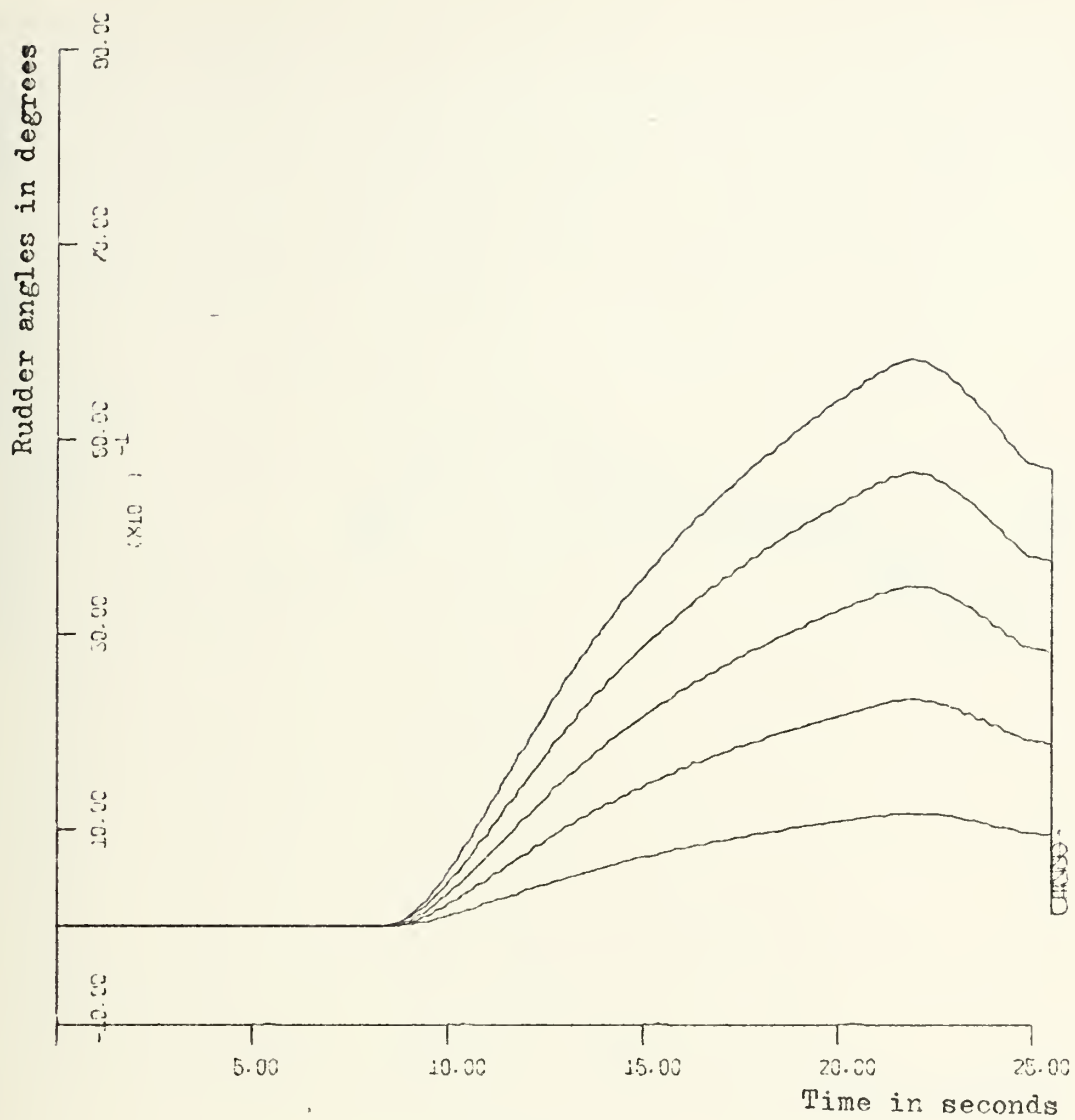


FIGURE 18C

DISTURBANCE : HELM

SPEED=40 KNOTS

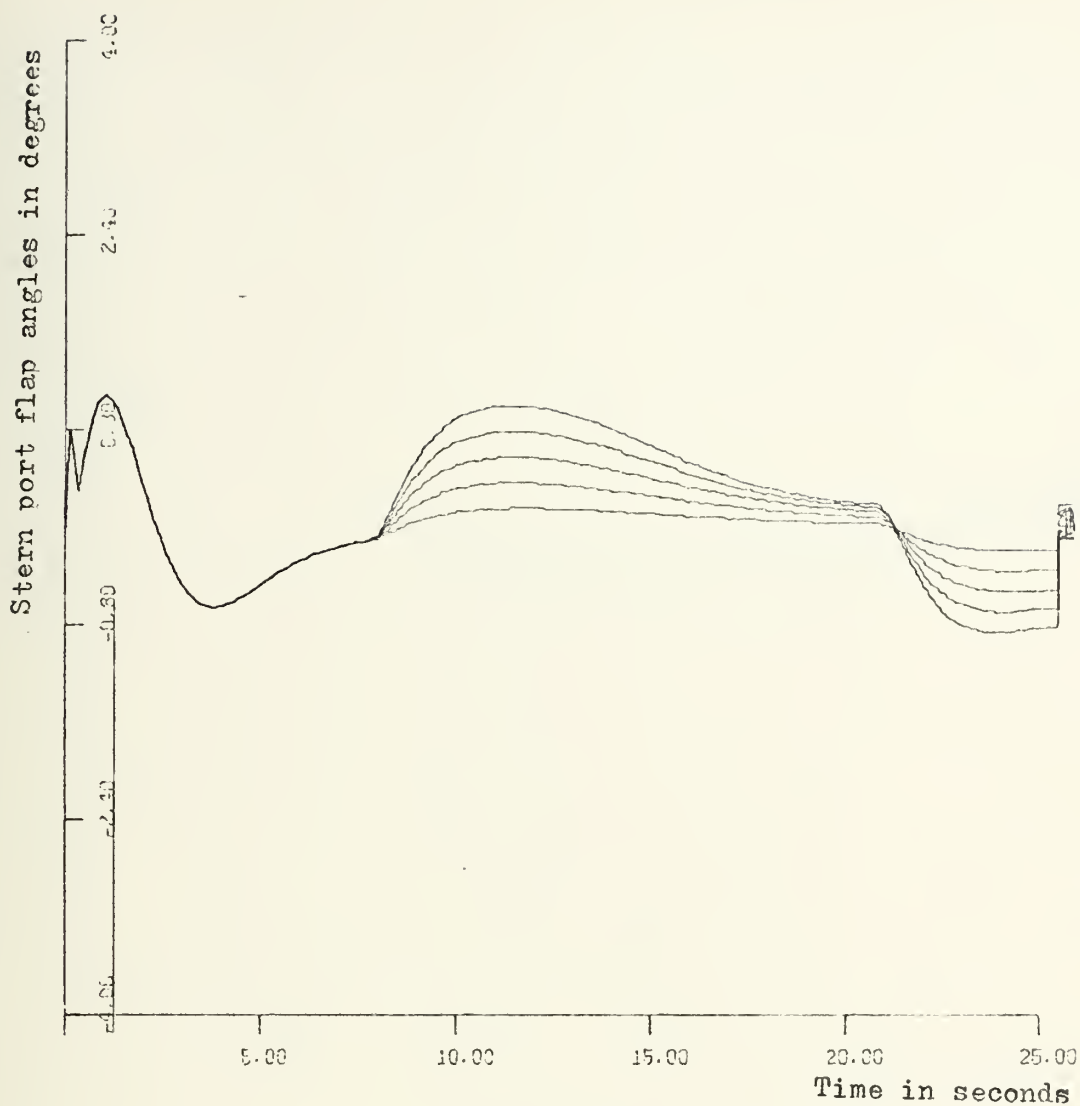


FIGURE 18D

DISTURBANCE : HELM

SPEED=40 KNOTS

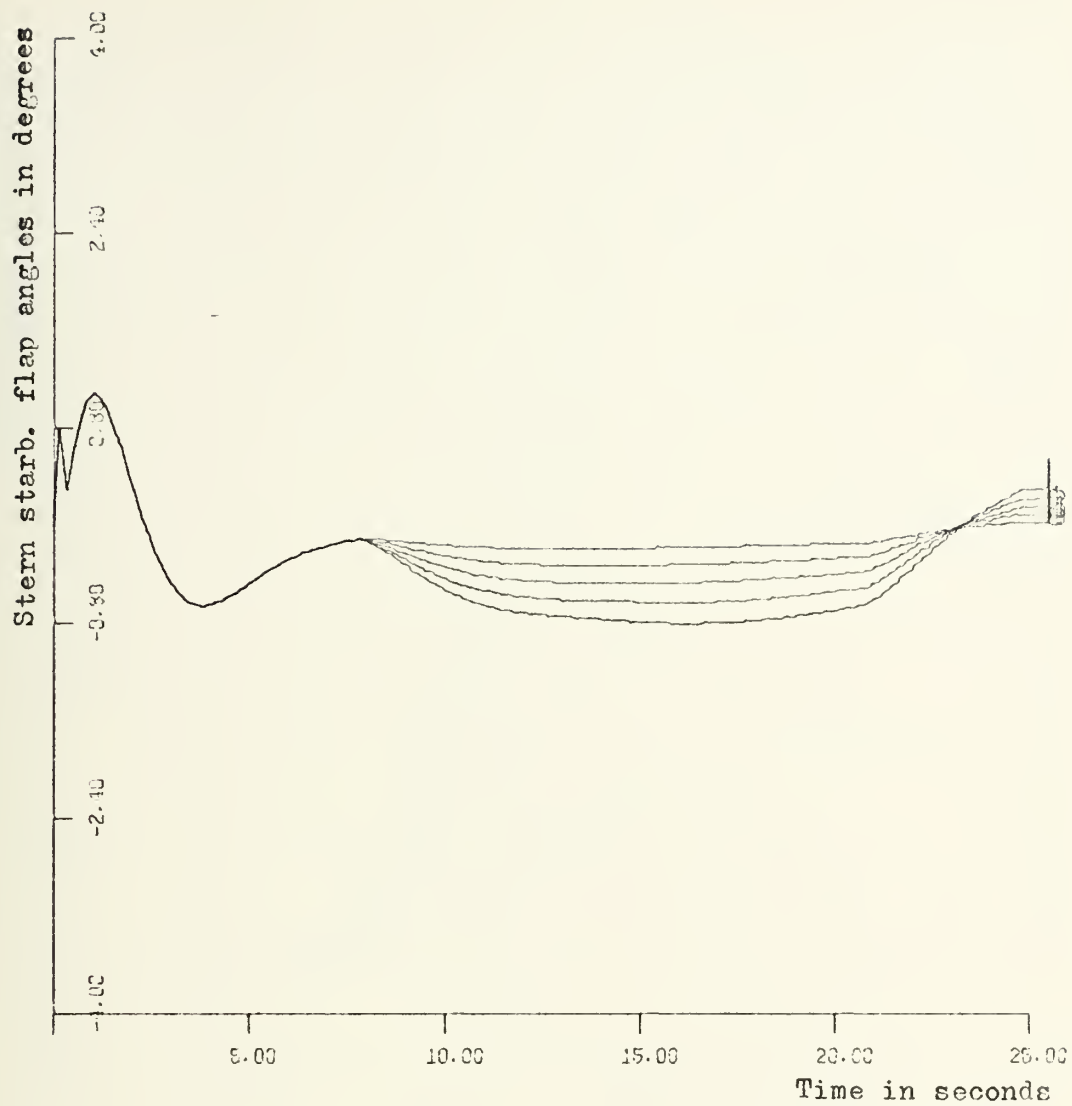


FIGURE 18E

DISTURBANCE : HELM

SPEED=40 KNOTS

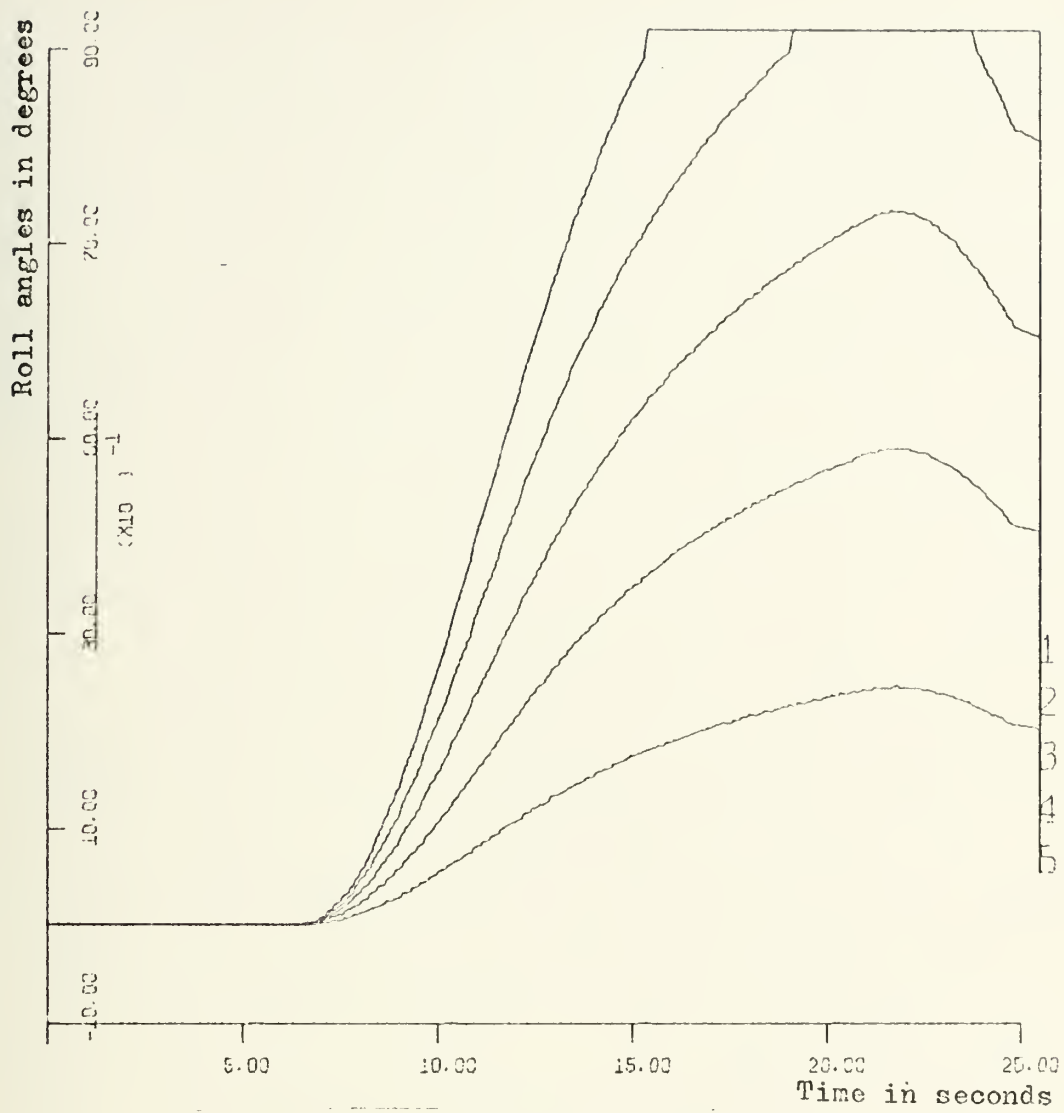


FIGURE 19A

DISTURBANCE : HELM

SPEED=50 KNOTS



FIGURE 19B

DISTURBANCE : HEIM

SPEED=50 KNOTS

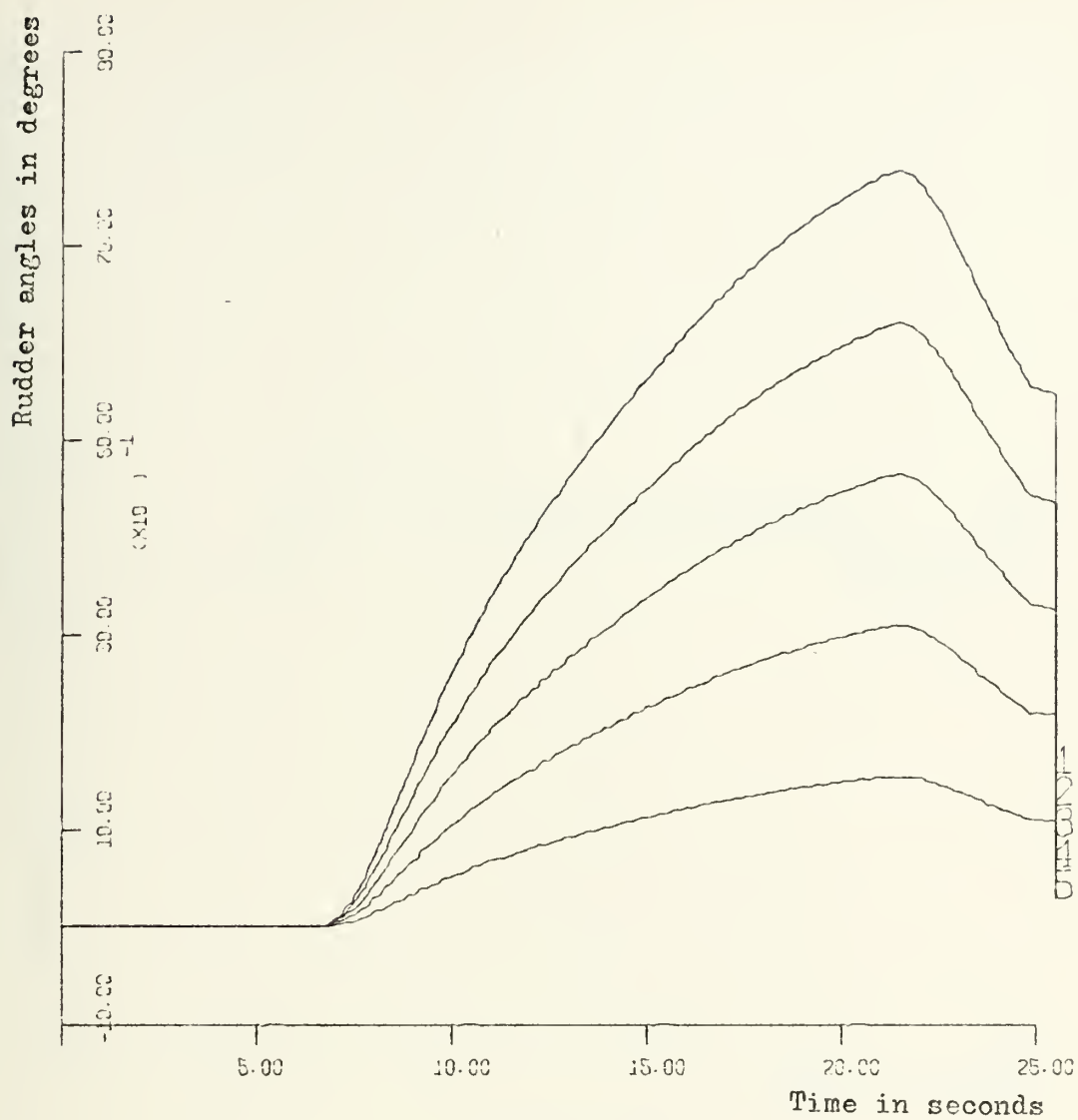


FIGURE 19C

DISTURBANCE : HELM

SPEED=50 KNOTS

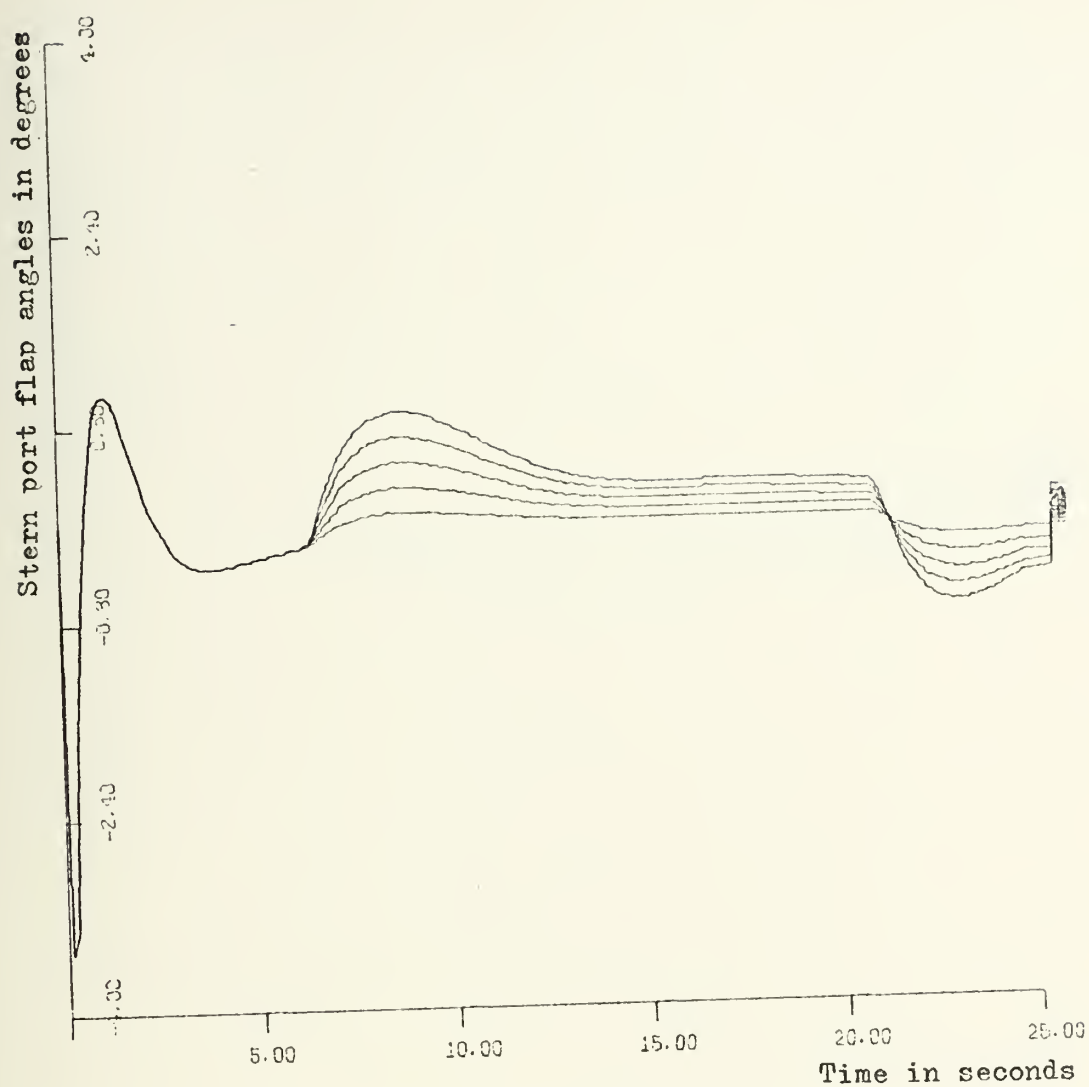


FIGURE 19D

DISTURBANCE : HELM

SPEED=50 KNOTS

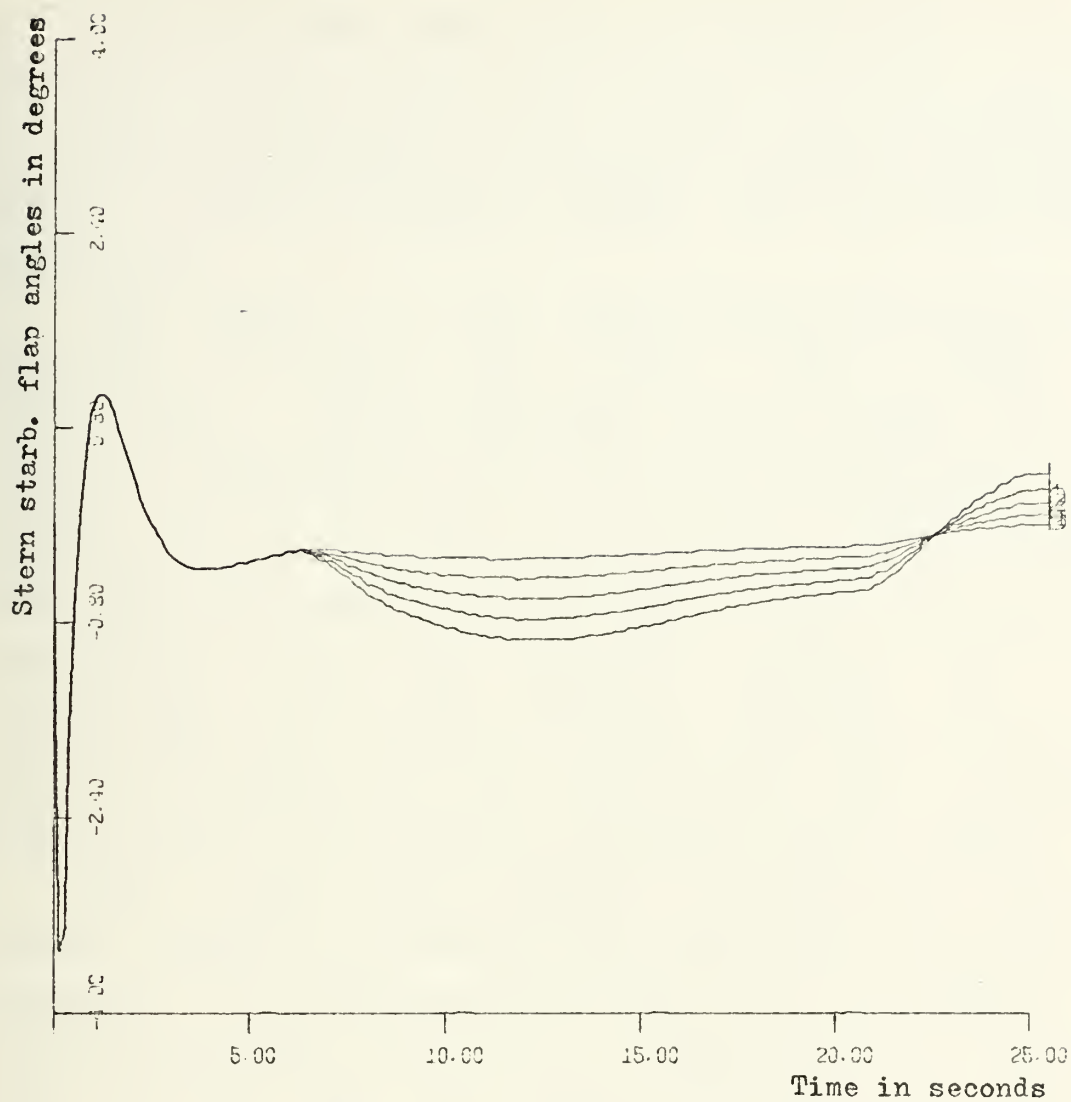


FIGURE 19E

DISTURBANCE : HELM

SPEED=50 KNOTS

C. RESULTS WITH THE SPLITTING OF THE FORWARD FOIL

The forward foil was split in two parts to analyze how it improves or prejudices the craft's pitching, the craft's rolling and the craft's turning rate in the desired directions.

Some changes in the computer simulation program were necessary to achieve this trial. Thus, instead of considering a unique submergence for the forward foil, two different submergences, Secp and Secs, corresponding to the forward port foil and to the forward starboard foil were considered. These two foils were moved independently, thus, two different forward flap angles, Elv1 and Elv3 were considered. Also two different forward foil drag coefficients and two different forward foil lift coefficients were introduced. Finally the block diagram of Ref.5 was adapted to an extra forward foil, provoking a small change on the simulated automatic control system.

With a helm step command to starboard, the craft started turning to starboard and it also started rolling to starboard. As was explained in part B of this chapter, the two forward flaps were moved in a manner similar to that of the aft port flap and the aft starboard flap, thus, the forward port flap went down provoking an upward lift force on the port side and the forward starboard flap went up provoking a downward force on the starboard side. Several runs with different speeds and different helm angles were done. In a general way, the roll angle in the desired direction was improved by 10% and the turning rate was improved by 8%, but the pitch angle had values 3% smaller than the values obtained with a single forward foil, because with half of the forward foil in the upward direction, there are two lift forces, (one positive and the other negative), prejudicing the craft's bow lift.

Finally, the forward flaps were moved in opposite directions to those of the preceding paragraph, thus, the

forward port flap went up and the forward starboard flap went down. The results were worse than those of the preceding paragraph.

D. CALCULATION OF THE CORRECT ROLL ANGLE

Many runs with the craft exposed to several disturbances were made. Different roll angles according to the existent conditions were obtained, but now a question arises : are these roll angles sufficiently near the optimum value?

A block called Calculation of the Correct Roll Angle was introduced in the computer simulation program to answer this question. Knowing the craft's turning radius for a certain speed and a certain helm angle, the craft's centrifugal force can be calculated. The craft's gravitational force in the Z direction was already known, then, the force perpendicular to the deck, called net force, can be calculated, by the gravitational and centrifugal forces. The angle between the gravitational force and the net force perpendicular to the deck is the correct roll angle.

In Figures 20A and 20B the craft's trajectories in the X-Y plane for a speed of 40 knots and helm step commands of 20 and 60 degrees respectively were represented. The craft's turning radius was calculated at the point where the heading angle was reversed 180 degrees in relation with the initial heading angle at the beginning of the run, since this will be approximately the steady state value.

In Figure 20C the craft's turning path, for a helm command of 160 degrees, a speed of 50 knots (extreme conditions) and a run time of 156 seconds was represented. The turning path was approximately a circle, with an approximate turning radius of 410 feet.

The values of the actual roll angle matched closely with the values of the correct roll angle, for the steady state period, although there were differences during the transient period. These values are represented in Table II.

In Figure 20D the craft's turning path for a helm angle of 160 degrees and a speed of 30 knots was represented. The

turning radius was smaller, approximately 300 feet.

The values of the actual roll angle matched again with the values of the correct roll angle, for the steady state period. These values are shown in Table III.

TABLE II

Roll angles for helm=160 degrees and speed=50 knots

Time (Seconds)	Actual roll angle (Degrees)	Correct roll angle (Degrees)
17.3	13.98	5.65
26.0	17.08	10.22
34.7	18.33	14.07
43.4	18.86	18.19
52.0	19.14	19.31
60.7	19.27	19.39
70.3	19.36	19.46
78.1	19.39	19.52
86.8	19.39	19.53
95.4	19.39	19.53

TABLE III

Roll angles for helm=160 degrees and speed=30 knots

Time (Seconds)	Actual roll angle (Degrees)	Correct roll angle (Degrees)
19.2	10.77	7.32
28.9	14.53	10.51
38.5	14.88	13.84
48.2	15.29	14.59
57.8	15.47	15.12
66.9	15.47	15.72
75.2	15.47	15.72

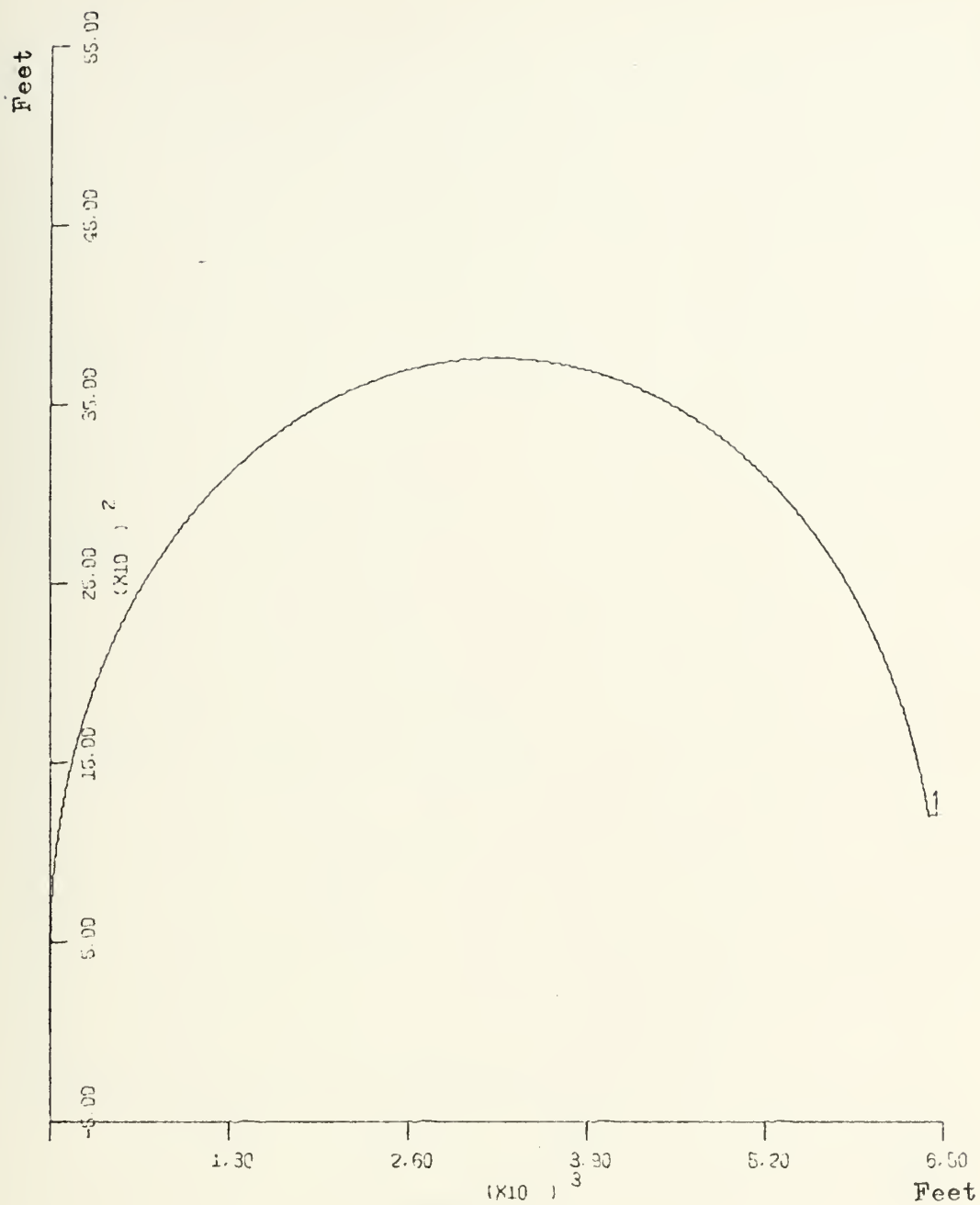


FIGURE 20A

TURNING PATH OF THE HYDROFOIL
HELM=20 DEGREES SPEED=40 KNOTS

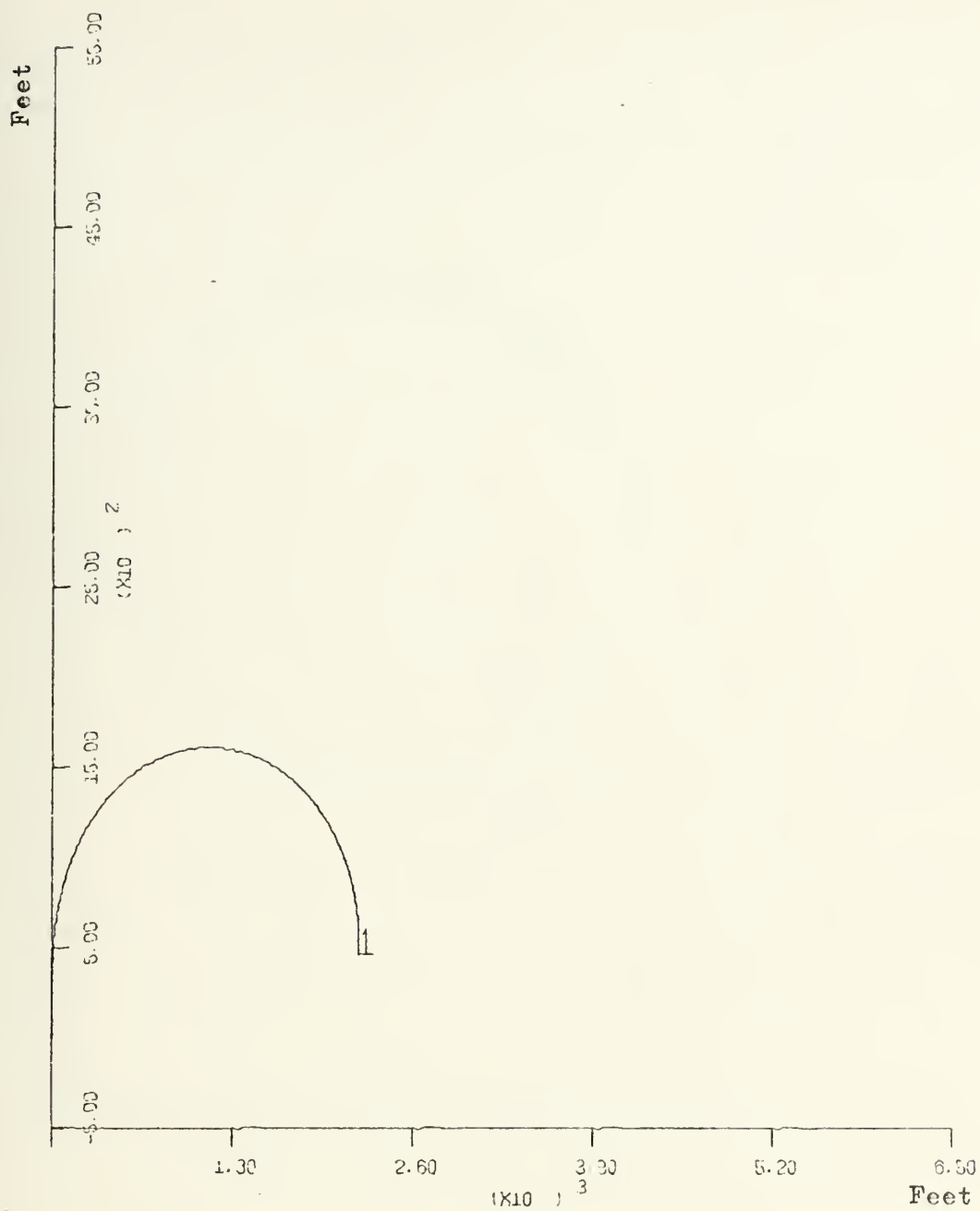


FIGURE 20B

TURNING PATH OF THE HYDROFOIL

HELM=60 DEGREES

SPEED=40 KNOTS

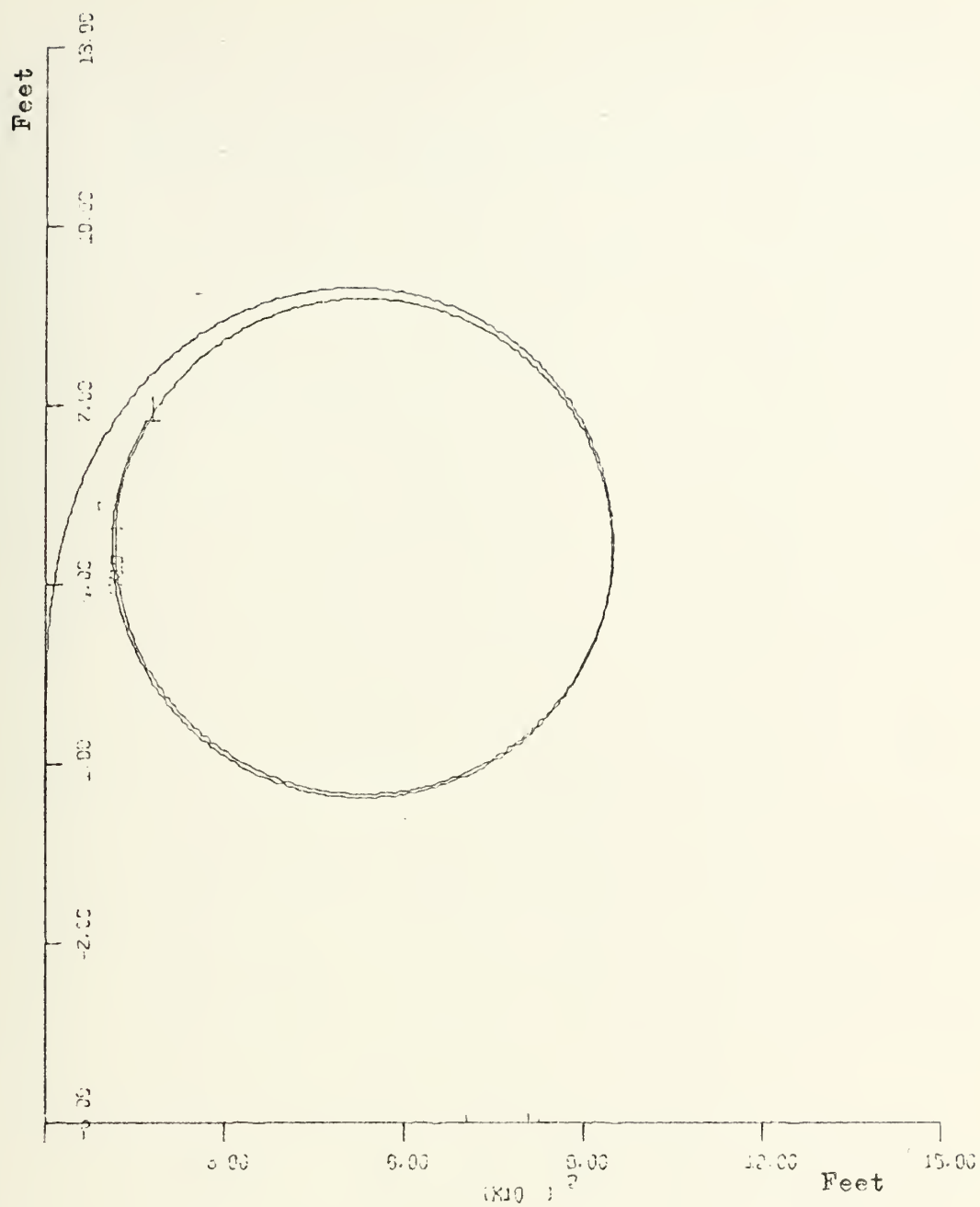


FIGURE 20C

TURNING PATH OF THE HYDROFOIL

HELM=160 DEGREES

SPEED=50 KNOTS

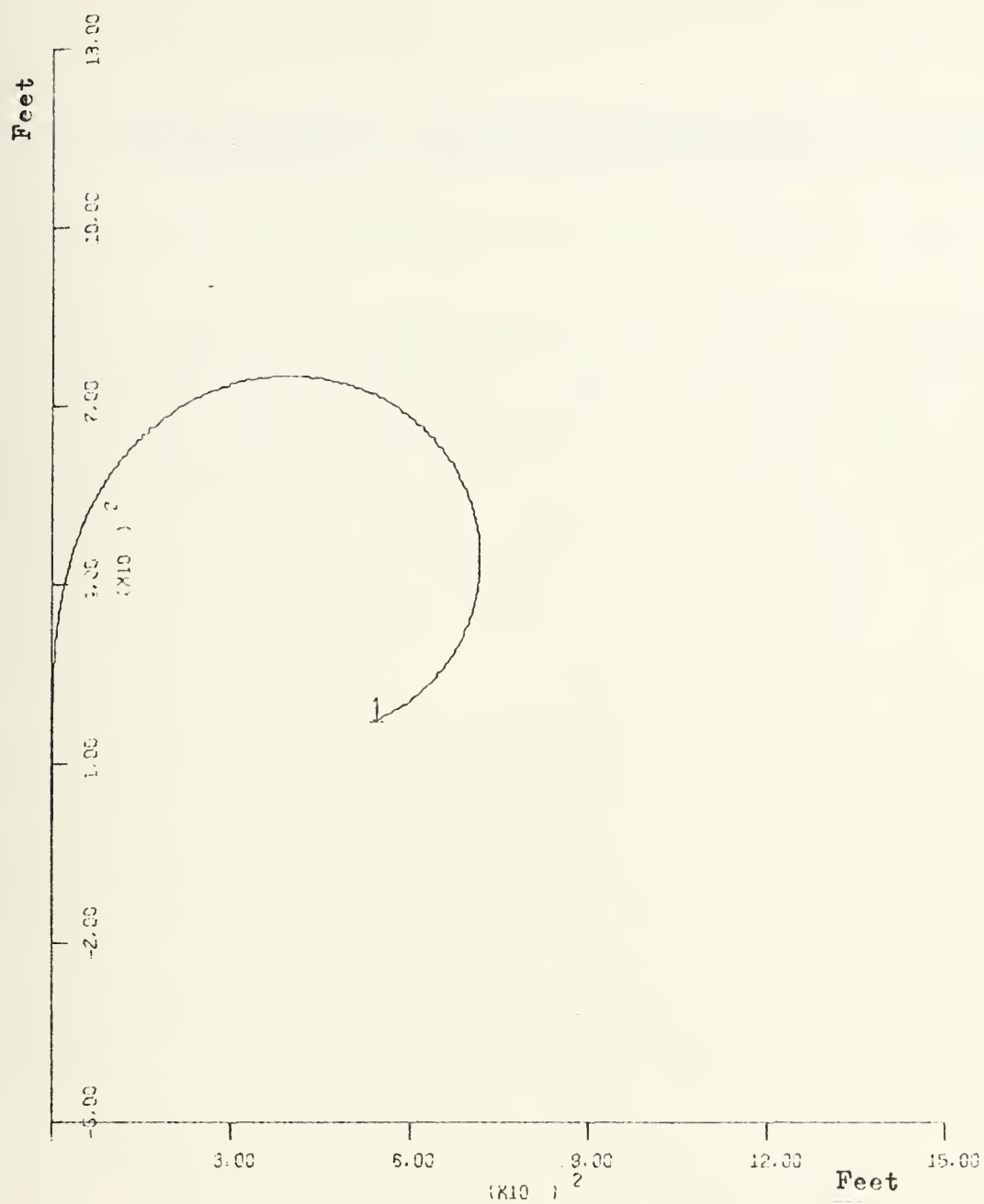


FIGURE 20D

TURNING PATH OF THE HYDROFOIL

HELM=160 DEGREES SPEED=30 KNOTS

V. CONCLUSIONS AND RECOMMENDATIONS FOR FURTHER STUDIES

The system was made stable in six degrees of freedom, with the following limitation : the dimensions, the foil areas, the weight and the thrust of the model PC(H)-1 were used in References 1 and 2 and in the computer simulation program. Due to a lack of information, because only very general information was available, certain values of the automatic control system of the model PHM, instead of the PC(H)-1, had to be used.

A study of the craft turning characteristics was made in this thesis. The simulated automatic control system was improved and adapted to perform this study.

Roll was controlled by differential displacements of the aft flaps, actuated by the helm control, while pitch was essentially controlled by the forward flap.

The rudder has negative effects on the hydrofoil's rolling direction, which should be the same as the turning direction, due to the high speeds of operation.

It was not worth while to split the forward foil.

Recommendations for further studies include :

1. Explore more deeply the advantages or the disadvantages of the splitting of the forward foil, combining it with the motions of the aft flaps and the rudder.

2. Study the response of the craft in a sinusoidal sea and in a random sea. Design improved control systems for sea state operation.

3. Simulate the transformation from hullborne operation to foilborne operation.

APPENDIX A

SUMMARY OF COMPLETE EQUATIONS

EQUATIONS FOR ACCELERATION IN BODY AXIS

$$\dot{U} = \frac{1}{m}F_X + RV - QW \quad (A-1)$$

$$\dot{V} = \frac{1}{m}F_Y + PW - RU \quad (A-2)$$

$$\dot{W} = \frac{1}{m}F_Z + QU - PV \quad (A-3)$$

$$\dot{P} = \frac{1}{I_{XX}}[L - QR(I_{ZZ} - I_{YY}) + (\dot{R} + QP)I_{XZ}] \quad (A-4)$$

$$\dot{R} = \frac{1}{I_{YY}}[N - PQ(I_{YY} - I_{XX}) - (QR - \dot{P})I_{XZ}] \quad (A-5)$$

VELOCITY IN BODY AXES

$$U = \int \dot{U} dt \quad (A-6)$$

$$V = \int \dot{V} dt \quad (A-7)$$

$$W = \int \dot{W} dt \quad (A-8)$$

$$P = \int \dot{P} dt \quad (A-9)$$

$$Q = \int \dot{Q} dt \quad (A-10)$$

$$R = \int \dot{R} dt \quad (A-11)$$

TRANSFORMATION OF VELOCITIES FROM BODY TO EARTH AXES

$$U_E = U \cos \theta \cos \psi + V(\cos \psi \sin \theta \sin \phi - \sin \psi \cos \phi) + W(\cos \psi \sin \theta \cos \phi + \sin \psi \sin \phi) \quad (A-12)$$

$$V_E = U \cos \theta \sin \psi + V(\cos \psi \cos \phi + \sin \psi \sin \theta \sin \phi) + W(\sin \psi \sin \theta \cos \phi - \cos \psi \sin \phi) \quad (A-13)$$

$$W_E = -U \sin \theta + V \cos \theta \sin \phi + W \cos \theta \cos \phi \quad (A-14)$$

$$\dot{\phi} = P + \dot{\psi} \sin \theta \quad (\text{A-15})$$

$$\dot{\theta} = Q \cos \phi - R \sin \phi \quad (\text{A-16})$$

$$\dot{\psi} = (Q \sin \phi + R \cos \phi) \cos \theta + (\dot{\phi} - P) \sin \theta \quad (\text{A-17})$$

POSITION IN EARTH AXES

$$X_E = \int U_E dt \quad (\text{A-18})$$

$$Y_E = \int V_E dt \quad (\text{A-19})$$

$$Z_E = \int W_E dt \quad (\text{A-20})$$

$$\phi = \int \dot{\phi} dt \quad (\text{A-21})$$

$$\theta = \int \dot{\theta} dt \quad (\text{A-22})$$

$$\psi = \int \dot{\psi} dt \quad (\text{A-23})$$

EXPANSION OF FORCE AND MOMENT EQUATIONS

$$F_X = \Sigma F_{XIF} + \Sigma F_{XIS} + mg_X^{+T} X \quad (\text{A-24})$$

$$F_Y = \Sigma F_{YIS} + mg_Y \quad (\text{A-25})$$

$$F_Z = \Sigma F_{ZIF} + mg_Z \quad (\text{A-26})$$

$$L = (F_Z L_Y)_{PF} + (F_Z L_Y)_{SF} - (F_Y L_Z)_{PS} - (F_Y L_Z)_{SS} - (F_Y L_Z)_{CS} \quad (\text{A-27})$$

$$M = \Sigma (F_Z L_X)_{IF} + \Sigma (F_X L_Z)_{IF} + \Sigma (F_X L_Z)_{IS} + T_X L_{ZT} \quad (\text{A-28})$$

$$N = \Sigma (F_Y L_X)_{IS} \quad (\text{A-29})$$

EXPANSION OF GRAVITY TERMS

$$mg_X = -mg \sin \theta \quad (\text{A-30})$$

$$mg_Y = mg \cos \theta \sin \phi \quad (\text{A-31})$$

$$mg_Z = mg \cos \theta \sin \phi \quad (\text{A-32})$$

FOIL VELOCITY COMPONENTS IN BODY AXES

Center Foil:

$$U_C = U + L_{ZCF} \cdot Q \quad (A-33)$$

$$V_C = V - L_{ZCF} \cdot P + L_{XCF} \cdot Q \quad (A-34)$$

$$W_C = W - L_{XCF} \cdot Q \quad (A-35)$$

Port Foil:

$$U_P = U + L_{ZPF} \cdot Q - L_{YPF} \cdot R \quad (A-36)$$

$$V_P = V - L_{ZPF} \cdot P + L_{XPF} \cdot R \quad (A-37)$$

$$W_P = W + L_{YPF} \cdot P - L_{XPF} \cdot Q \quad (A-38)$$

Starboard Foil:

$$U_S = U + L_{ZSF} \cdot Q - L_{YSF} \cdot R \quad (A-39)$$

$$V_S = V - L_{ZSF} \cdot P + L_{XSF} \cdot R \quad (A-40)$$

$$W_S = W + L_{YSF} \cdot P - L_{XSF} \cdot Q \quad (A-41)$$

Mid Foil:

$$U_M = U + L_{XMF} \cdot Q \quad (A-42)$$

$$V_M = V - L_{ZMF} \cdot P + L_{XMF} \cdot R \quad (A-43)$$

$$W_M = W - L_{XMF} \cdot Q \quad (A-44)$$

TRANSFORMATION OF WATER PARTICLE ORBITAL VELOCITY FROM EARTH
TO BODY AXES

$$U_{WI} = U_{EWI} \cos \psi \cos \theta + V_{EWI} \sin \psi \cos \theta - W_{EWI} \sin \theta \quad (A-45)$$

$$V_{WI} = U_{EWI} (\cos \psi \sin \theta \sin \phi - \sin \psi \cos \phi) + V_{EWI} (\sin \psi \sin \theta \sin \phi + \cos \psi \cos \phi) \\ + W_{EWI} \cos \theta \sin \phi \quad (A-46)$$

$$W_{WI} = U_{EWI} (\cos \psi \sin \theta \cos \phi + \sin \psi \sin \phi) + V_{EWI} (\sin \psi \sin \theta \cos \phi - \cos \psi \sin \phi) \\ + W_{EWI} \cos \theta \cos \phi \quad (A-47)$$

Each of these equations must be repeated for each foil.

RELATIVE VELOCITY COMPONENTS

$$U_{RI} = U_I - U_{WI} \quad (A-48)$$

$$V_{RI} = V_I - V_{WI} \quad (A-49)$$

$$W_{RI} = W_I - W_{WI} \quad (A-50)$$

One set of equations for each foil.

ANGLES OF ATTACK AND SIDE SLIP

$$\alpha_I = \arctan W_{RI}/U_{RI} + \alpha_{I-FIXED} \quad (A-51)^*$$

$$\beta_I = \arcsin \frac{V_{RI}}{\sqrt{U_{RI}^2 + V_{RI}^2 + W_{RI}^2}} \quad (A-52)^*$$

* One set of equations for each foil. Angles of attack and side slip are calculated in radians.

TOTAL RELATIVE VELOCITY AT A PARTICULAR FOIL OR STRUT

$$V = \sqrt{U_R^2 + V_R^2 + W_R^2} \quad (A-53)$$

HYDRODYNAMIC FORCES IN WATER AXES

(Each foil equation and strut equation must be repeated for foil and strut, respectively)

Foil Lift:

$$F_L = \frac{1}{2} \rho V^2 A_F C_F \quad (A-54)$$

Foil Drag:

$$F_{DF} = \frac{1}{2} \rho V^2 A_F C_F \quad (A-55)$$

Strut Drag:

$$F_{DS} = \frac{1}{2} \rho V^2 A_S C_{DS} \quad (A-56)$$

Strut Side Force:

$$F_S = \frac{1}{2} \rho V^2 A_S C_S \quad (A-57)$$

TRANSFORMATION OF FOIL FORCES FROM WATER AXES TO BODY AXES

$$F_{XIF} = -F_{IDF} \cos \alpha \cos \beta + F_{LIF} \sin \alpha \quad (A-58)$$

$$F_{YIF} = -F_{DIF} \sin \beta \quad (A-59)$$

$$F_{ZIF} = -F_{DIF} \sin \alpha \cos \beta - F_{LIF} \cos \alpha \quad (A-60)$$


```

// EXEC DSL, PARM.C='NOSOURCE,NOMAP'
//DSL.INPUT DD *
D      COMMON MATRIX(539)
CONTRL FINTIM=30.0,DELT=0.025,DELS=0.1
INTEG RKSFX
INTEGER IFLAG,IFLAG1,NPLOT,NUM,NCUR
CONST NFLOT=1,NCUR=1,IFLAG=0
CONST WEIGHT=262527, IXX=601200, IYY=4286000,...
IZZ=4174000,G=32.2
CONST ACF=32.7,APF=36.8,ASF=36.8,AMF=76.0,...
PI=3.141593
CONST LXCF=41.59,LXCS=41.59,LXPF=-16.98,LXPS=-16.98,...
LXSF=-16.98,LXSS=-16.98,LXMF=-16.98,LYCP=-5.0,LYCS=5.0,...
LYPF=-12.42,LYPS=-8.0,LYSF=12.42,LYSS=8.0,LZCF=15.5,...
LZCS=13.25,LZPF=17.14,LZPS=14.0,LZSF=17.14,LZSS=14.0,...
LZMF=17.14,LXT=-16.9,LZT=17.7,LXH=68.0
CONST K1=5.0,K2=-98.0,K3=-82.0
CONST K4=1.5,K5=10.0,K6=3.5,K7=1.42,K8=1.5,K9=-2.0,...
K10=0.4,K11=-13.0,K12=3.0,K13=3.0,K14=0.014
CONST RST=0.0
STORAG IC1(3),NU1(3),DEN1(4),IC2(2),NU2(2),DEN2(3),...
IC3(3),NU3(2),DEN3(4)
TABLE IC1(1-3)=3*0.0,NU1(1-3)=1.0,3.01,0.03,...
DEN1(1-4)=1.0,110.1,3011.0,300.0,IC2(1-2)=2*0.0,...
NU2(1-2)=1.0,1.0,DEN2(1-3)=1.0,87.7,1885.0,IC3(1-3)=3*0.0,...
NU3(1-2)=30.0,58.5,DEN3(1-4)=1.0,30.25,0.015,0.45
PARAM UZERO=40.0
PARAM RUZR=0.0
PARAM HELMR=2.79
PREPAR .1,RTIME,PHI1,PSI1,XE,YE
GRAPH XE,YE
PRPLCT
LABEL RESPONSES WITH HELM STEP COMMAND
PRINT 0.5,RTIME,PHI,PHI3,PHI1,PHI4,PSI,PSI1,XE,YE,UE,VE,...
RGIR,FGRZ,FCENT,FNET
*
INITIAL
*
DENSE=2.0
UINIT=UZERO*2000.0*3.0*1.0/3600.0
U=UINIT
TX=3960.0
ALM=0.074269
ALS=0.074269
ALP=0.074269
ALF=0.037111
PREF=0.0
TREF=0.0
THETA2=0.0
PHI2=0.0
PSI2=0.0
MASS=WEIGHT/G
CONV=PI/180.0
HREF=11.5
HREF2=-11.5
LENGTH=115.75
FLAG=0.0
IFLAG1=0
EPS=25.0
IF(IFLAG.EQ.0) CALL SETUP(FLAG)
IFLAG=1
IF(FLAG.EQ.1) CALL ENDRUN
*
DERIVATIVE
*
NOSORT
*
*   ANGLES OF ATTACK AND SIDE SLIP
*
VRC=V-LZCF*P+LXCF*R
VRS=V-LZSF*P+LXSF*R
VRM=V-LZMF*P+LXMF*R

```



```

VRP=V-LZPF*P+LXPF*R
WRP=W+LYPF*P-LXPF*Q
WRS=W+LYSF*P-LXSF*Q
WRM=W-LXMF*Q
WRC=W-LXCF*Q
ALFC=WRC/U+ALF
ALFAP=WRP/U+ALP
ALFAS=WRS/U+ALS
ALFAM=WRM/U+ALM
BETAC=WRC/U
BETAP=VRP/U
BETAS=WRS/U

```

*
*
*
CALCULATION OF EULER ANGLES

```

PHID1=P
THETD1=Q
PSID1=R

```

*
SORT

```

THETA=INTGRL(THETA2,THETD1)
PHI=INTGRL(PHI2,PHID1)
PSI=INTGRL(PSI2,PSID1)
WE=-U*SIN(THETA)+V*COS(THETA)*SIN(PHI)+W*COS(THETA)*...
*COS(PHI)
ZE=INTGRL(HREF2,WE)
ZE1=ZE-HREF2

```

*
NOSORT

*
*
*
SUBMERGENCE TERMS

```

SECF=ZE-LXCF*THETA+LZCF*COS(PHI)
SEPF=ZE-LXPF*THETA+LYPF*SIN(PHI)+LZPF*COS(PHI)
SESF=ZE-LXSF*THETA+LYSF*SIN(PHI)+LZSF*COS(PHI)
SEMF=ZE-LXMF*THETA+LZMF*COS(PHI)

```

*
*
*
HYDRODYNAMIC COEFFICIENTS

```

HELMR1=STEP(RST)
HELM=HELMR*HELMR1
RUD11=K7*PHI+K9*R
RUD=REALPL(0.0,0.159,RUD11)
ELV1=ELV*CONV
ELVD=LIMIT(-5.0,5.0,ELV1)
FLAD=FLAP*CONV
FDEG=LIMIT(-5.0,5.0,FLAD)
ARPD=ARP*CONV
ARPL=LIMIT(-5.0,5.0,ARPD)
ARSD=ARS*CONV
ARS11=LIMIT(-5.0,5.0,ARSD)
CALL INTERP(ALFC,ELVD,COEFC,2)
CALL INTERP(ALFAP,ARPL,COEFPX,3)
CALL INTERP(ALFAS,ARS11,COEFSX,3)
CALL INTERP(ALFAM,FLAP,COEFMX,1)
CALL INTRP1(BETAC,SECF,CFDS,2,THETA,THETA1)
CALL INTRP1(BETAP,SEPF,CPDS,1,THETA,THETA1)
CALL INTRP1(BETAS,SESF,CSDS,1,THETA,THETA1)

```

*
*
*
FORCES IN THE WATER AXES

```

FGRAX=-MASS*G*SIN(THETA)
FGRAY=MASS*G*SIN(PHI)
FGRAZ=MASS*G*COS(PHI)
CCS=-0.04375*BETAC+0.04375*RUD
ACCS=CCS*4.25*SECF
FSC=0.5*DENSE*(U**2)*ACCS
FDSC=0.5*DENSE*(U**2)*CFDS
PCS=-2.15*BETAP
APCS=PCS*4.25*SEPF
FPS=0.5*DENSE*(U**2)*APCS
FDPS=0.5*DENSE*(U**2)*CPDS

```



```

SCS=-2.15*BETAS
ASCS=SCS*4.25*SESF
FSS=0.5*DENSE*(U**2)*ASCS
FCSS=0.5*DENSE*(U**2)*CSDS
CLCF=5.15*ALFC+0.036*ELV+0.13
FLC=0.5*DENSE*(U**2)*ACF*CLCF
FDC=0.5*DENSE*(U**2)*ACF*COEFC
CLPF=4.10*ALFAP+0.018*ARP
FLP=0.5*DENSE*(U**2)*APF*CLPF
FDP=0.5*DENSE*(U**2)*APF*COEFPX
CLSF=4.10*ALFAS+0.018*ARS
FLS=0.5*DENSE*(U**2)*ASF*CLSF
FDS=0.5*DENSE*(U**2)*ASF*COEFSX
CLMF=5.15*ALFAM+0.036*FLAP
FLM=0.5*DENSE*(U**2)*AMF*CLMF
FDM=0.5*DENSE*(U**2)*AMF*COEFMX
FLCZ=0.5*DENSE*(U**2)*ACF*CLCF
FDCZ=0.5*DENSE*(U**2)*ACF*COEFC
FLPZ=0.5*DENSE*(U**2)*APF*CLPF
FDPZ=0.5*DENSE*(U**2)*APF*COEFPX
FLSZ=0.5*DENSE*(U**2)*ASF*CLSF
FDSZ=0.5*DENSE*(U**2)*ASF*COEFSX
FLMZ=0.5*DENSE*(U**2)*AMF*CLMF
FDMZ=0.5*DENSE*(U**2)*AMF*COEFMX

```

TRANSFORMATION TO BODY AXES

```

FXCF=-FDC+ALFC*FLC
FXPF=-FDP+ALFAP*FLP
FXSF=-FDS+ALFAS*FLS
FXMF=-FDM+ALFAM*FLM
FXCS=-FDC*BETAC*BETAS*FSC
FXPS=-FDC*BETAP*BETAS*FPS
FXSS=-FDC*BETAS*FSS
FYCS=-BETAC*FDC*BETAS*FSC
FYPS=-BETAP*FDC*BETAS*FPS
FYSS=-BETAS*FDC*BETAS*FSS
FZCF=-FDC*ALFC-FLCZ
FZPF=-FDPZ*ALFAP-FLPZ
FZSF=-FDSZ*ALFAS-FLSZ
FZMF=-FDMZ*ALFAM-FLMZ
LZCS=LZCF-0.4*SECF
LZPS=LZPF-0.4*SEPF
LZSS=LZSF-0.4*SESF

```

```

FXCNE=FXCF+FXPF+FXSF+FXMF+FXCS+FXPS+FXSS

```

SUMMATION OF FORCES AND MOMENTS

```

FX=FXONE+FGRAX+TX
UDOT=(1./MASS)*FX-Q*W
IF (IFLAG1.EQ.0) UDOT=0.0
FY=FYCS+FYPF+FYSS+FGRAY
FZ=FZCF+FZPF+FZSF+FZMF+FGRAZ
L=FZPF*LYPF+FZSF*LYSF-FYPS*LZPS-FYSS*LZSS-FYCS*LZCS
MFWD=FZCF*LXCF
M=-MFWD-FZPF*LXPF-FZSF*LXSF-FZMF*LXMF+...
FXCF*LZCF+FXPF*LZPF+FXSF*LZSF+FXMF*LZMF+FXCS...
*LZCS+FXPS*LZPS+FXSS*LZSS+TX*LZT
N=FYCS*LXCS+FYPF*LXPS+FYSS*LXSS

```

VELOCITY INTEGRALS

```

VDOT=(1./MASS)*FY-R*U
WDOT=(1./MASS)*FZ+Q*U
PDOT=(1.0/IXX)*L
QDOT=(1.0/IYY)*M
RDOT=(1.0/IZZ)*N
U=INTGRL(UNIT,UDOT)
V=INTGRL(0.0,VDOT)

```



```

W=INTGRL(0.0,WDOT)
P=INTGRL(0.0,PDOT)
Q=INTGRL(0.0,QDOT)
R=INTGRL(0.0,RDOT)

```

SENSED ACCELERATIONS

```

AZC=FZ/MASS-LXCF*QDOT
AZS=FZ/MASS+LXSF*QDOT+LYSF*PDOT
AZP=FZ/MASS+LXPF*QDOT-LYPF*PDOT

```

AUTOMATIC CONTROL BLOCK

```

HACT=-ZE+LXH*THETA
DELH=HREF-HACT
DELHC=REALPL(0.0,0.04,DELH)
DETH=TREF-THETA
FLAP=K2*DETH
B=AZC+K14*(PHI**2)
AZCC=TRNFR(2,3,IC3,NU3,DEN3,B)
AZSC=REALPL(0.0,0.033,AZS)
AZPC=REALPL(0.0,0.033,AZP)
THETAC=TRNFR(2,3,IC1,NU1,DEN1,1000.0*THETA)
PHIC=TRNFR(1,2,IC2,NU2,DEN2,1885.0*PHI)
HELMC=REALPL(0.0,1.0,HELM)
ELV11=K11*THETAC+K12*THETA+K13*DELHC+K4*AZCC
ELV=REALPL(0.0,0.159,ELV11)
ARS2=K4*AZSC+K5*THETAC+K6*PHIC-K10*HELMC
ARP2=K4*AZPC+K5*THETAC-K6*PHIC+K10*HELMC
ARS=REALPL(0.0,0.159,ARS2)
ARP=REALPL(0.0,0.159,ARP2)
THETA3=(THETA-THETA2)*180.0/PI
PHI1=(PHI-PHI2)*180.0/PI
PSI1=(PSI-PSI2)*180.0/PI
RUD1=RUD*180.0/PI

```

CALCULATION OF THE CORRECT ROLL ANGLE

```

UE=U*CCS(THETA)*COS(PSI)+V*(COS(PSI)*SIN(THETA)*...
SIN(PHI)-SIN(PSI)*COS(PHI))+W*(COS(PSI)*SIN(THETA)*...
COS(PHI)+SIN(PSI)*SIN(PHI))
VE=U*COS(THETA)*SIN(PSI)+V*(COS(PSI)*COS(PHI)+...
SIN(PSI)*SIN(THETA)*SIN(PHI))+W*(SIN(PSI)*SIN(THETA)*...
CCS(PHI)-COS(PSI)*SIN(PHI))
YE=INTGRL(0.1,UE)
XE=INTGRL(0.1,VE)
RGIR=((XE**2)+(YE**2))/XE
FCENT=MASS*((UE**2)+(VE**2))/RGIR
FNET=SQRT((FGRAZ**2)+(FCENT**2))
PHI3=ATAN2(FCENT,FGRAZ)
PHI4=PHI3*180.0/PI

```

CALCULATION OF REAL TIME

```

RTIME=(LENGTH/UINIT)*TIME

```

DYNAMIC

SAMPLE

```

CALL DRWG(1,1,XE,YE)

```

TERMINAL

```

CALL ENDRW(NPLOT)

```

END

STOP

FORTRAN

C

C

C

C

C

C

C

C

SUBROUTINE SETUP

THIS SUBROUTINE FORMS THE DATA POINTS COMPRISING THE CURVES OF FOIL AND STRUT DRAG COEFFICIENTS AND SIDE SLIP COEFFICIENTS INTO MATRACES.

C

```

SUBROUTINE SETUP(FLAG)
COMMON COEFMX,COEFCX,COEFOX,CFDS1,CADS1
DIMENSION COEFCX(3,33),COEFOX(3,33),COEFMX(3,33),
1CFDS1(11,11),CADS1(11,11),INFO(8)
REAL INFO
IC=0
IFLAG=0
IFLAG1=0
MATRIX=1
J=0
K=1
ICCOUNT=0
2 READ(5,100) INFO
100 FORMAT(7F10.8)
I1=1
IF(IFLAG1.EQ.1) GO TO 51
GO TO (4,5,6,7,8),MATRIX
4 CONTINUE
DO 1 I=1,8
J=J+1
IF(J.GT.3) K=K+1
IF(J.GT.3) J=1
COEFOX(J,K)=INFO(I)
ICCOUNT=ICCOUNT+1
IC=IC+1
IF(ICCOUNT.EQ.99) GO TO 3
1 CONTINUE
GO TO 2
3 I1=I
IF(I1.LE.8) I1=I1+1
J=0
K=1
ICCOUNT=0
MATRIX=2
5 IF(I1.GT.8) GO TO 2
DO 9 I=I1,8
J=J+1
IF(J.GT.3) K=K+1
IF(J.GT.3) J=1
COEFCX(J,K)=INFO(I)
ICCOUNT=ICCOUNT+1
IC=IC+1
IF(ICCOUNT.EQ.99) GO TO 10
9 CONTINUE
GO TO 2
10 I1=I
IF(I1.LE.8) I1=I1+1
J=0
K=1
ICCOUNT=0
MATRIX=3
6 IF(I1.GT.8) GO TO 2
DO 11 I=I1,8
J=J+1
IF(J.GT.3) K=K+1
IF(J.GT.3) J=1
COEFMX(J,K)=INFO(I)
ICCOUNT=ICCOUNT+1
IC=IC+1
IF(ICCOUNT.EQ.99) GO TO 12
11 CONTINUE
GO TO 2
12 I1=I
IF(I1.LE.8) I1=I1+1
J=0
K=1
ICCOUNT=0
MATRIX=4
7 IF(I1.GT.8) GO TO 2
DO 13 I=I1,8
J=J+1

```



```

      IF(J.GT.11) K=K+1
      IF(J.GT.11) J=1
      CADSI(J,K)=INFO(I)
      ICCUNT=ICOUNT+1
      IC=IC+1
      IF(ICOUNT.EQ.121) GO TO 15
13  CONTINUE
      GO TO 2
15  I1=I
      IF(I1.LE.8) I1=I1+1
      J=0
      K=1
      ICCUNT=0
      MATRIX=5
8   IF(I1.GT.8) GO TO 2
      DO 14 I=I1,8
      J=J+1
      IF(J.GT.11) K=K+1
      IF(J.GT.11) J=1
      CFDSI(J,K)=INFO(I)
      ICOUNT=ICOUNT+1
      IC=IC+1
      IF(ICOUNT.EQ.121) GO TO 16
14  CONTINUE
      GO TO 2
16  IFLAG1=1
50  IFLAG=1
      IF((IFLAG.EQ.1).AND.(IFLAG1.EQ.1)) GO TO 52
51  WRITE(6,104) ICOUNT,MATRIX,IC
104  FORMAT(' ','JOB FAILURE',1X,'COUNT=',I6,1X,'MATRIX=',
116,1X,'NO.PTS=',I6)
      FLAG=1
      RETURN
52  WRITE(6,105) IC
105  FORMAT(' ','JOB COMPLETE',1X,'POINTS STORED=',I6)
      RETURN
      END

```

FORTRAN

SUBROUTINE INTERP

C
C
C
C

```

SUBROUTINE INTERP(ALFAC,FLAP,COEF,M)
COMMON COEFMX,COEFCX,COEFOX
DIMENSION COEFMX(3,33),COEFCX(3,33),COEFOX(3,33)
DATA CONDEG/57.295773/
ALFA=ALFAC*CONDEG
IF(ALFA.GT.10.0) WRITE(6,100)ALFAC,M
IF(ALFA.GT.10.0) ALFA=10.0
100  FORMAT('O','ERROR.ALFA EXCEEDED LIMITS.ALFA=',E14.8,
12X,'M=',I1)
IF(ALFA.LT.-6.0) WRITE(6,100) ALFAC,M
IF(ALFA.LT.-6.0) ALFA=-6.0
ALPHA=2.0*ALFA
IF(ALPHA.LT.0.0) GO TO 1
IF(ALPHA.GT.0.0) GO TO 2
IA=13
WTA=0.0
GO TO 3
1  IA1=-ALPHA
IA=13-IA1
ALPHA1=-IA1
WTA=ALPHA-ALPHA1
GO TO 3
2  IA1=ALPHA
IA=13+IA1
ALPHA1=IA1
WTA=ALPHA-ALPHA1
3  IF(FLAP.LT.-5.0) WRITE(6,101) FLAP
IF(FLAP.LT.-5.0) FLAP=-5.0
IF(FLAP.GT.5.0) WRITE(6,101) FLAP
IF(FLAP.GT.5.0) FLAP=5.0

```



```

101 FORMAT('0','ERROR.FLAP EXCEEDED LIMITS.FLAP=',E14.8)
   IF (FLAP) 4,5,6
4    IB=1
    WTB=-((5.0+FLAP)/5.0)
    GO TO 7
5    IB=2
    WTB=0.0
    GO TO 7
6    IB=3
    WTB=(5.0-FLAP)/5.0
7    IF (WTA) 8,9,10
8    IA2=IA-1
    GO TO 11
9    IA2=IA
    GO TO 11
10   IA2=IA+1
11   IF (WTB) 12,13,12
12   IB2=2
    GO TO 14
13   IB2=IB
14   GC TO (15,16,17),M
15   COEF1=COEFMX(IB,IA)
    COEF2=COEFMX(IB2,IA)
    GO TO 18
16   CCEF1=CCEFCX(IB,IA)
    CCEF2=CCEFCX(IB2,IA)
    GO TO 18
17   COEF1=COEFOX(IB,IA)
    COEF2=COEFOX(IB2,IA)
18   COEF3=(COEF2-COEF1)*ABS(WTB)+COEF1
    GO TO (19,20,21),M
19   CCEF1P=COEFMX(IB,IA2)
    COEF2P=COEFMX(IB2,IA2)
    GO TO 22
20   CCEF1P=CCEFCX(IB,IA2)
    COEF2P=CCEFCX(IB2,IA2)
    GO TO 22
21   COEF1P=COEFOX(IB,IA2)
    COEF2P=COEFOX(IB2,IA2)
22   CCEF3P=(CCEF2P-COEF1P)*ABS(WTB)+CCEF1P
    CCEF=(CCEF3P-COEF3)*ABS(WTA)+COEF3
    RETURN
END

```

FORTRAN

SUBROUTINE INTRP1

C
C
C
C

```

SUBROUTINE INTRP1(BETA1,SOB,COEFS,M,THETA,THETA1)
COMMON JUNK,CFDS1,CADS1
DIMENSION JUNK(297),CFDS1(11,11),CADS1(11,11)
DATA CONDEG/57.295773/
SUB=SOB
BETA=BETA1*CONDEG
IF (BETA.GT.15.0) WRITE(6,100) BETA1,M
IF (BETA.GT.15.0) BETA=15.0
100 FORMAT('0','ERROR.BETA EXCEEDS LIMITS.BETA=',E14.8,2X,
1'N=',I1)
IF (BETA.LT.-15.0) WRITE(6,100) BETA1,M
IF (BETA.LT.-15.0) BETA=-15.0
IF (BETA.LT.0.0) GO TO 1
IF (BETA.GT.0.0) GO TO 2
IA=6
WTA=0.0
GC TO 3
1 IA1=-BETA
IA=6-IA1
BETAG=-IA1
WTA=BETA-BETAG
GC TO 3
2 IA1=BETA
IA=6+IA1

```



```

      BETAG=IA1
      WTA=BETA-BETAG
3     IF(SUB.LT.0.0) SUB=0.0
      IF(SUB.GT.10.0) SUB=10.0
      IF(SUB.GT.0.0) GO TO 5
      IS=1
      WTS=0.0
      GO TO 7
5     IS1=SUB
      IS=IS1+1
      SUB1=IS1
      WTS=SUB-SUB1
7     IF(WTA) 8,9,10
8     IA2=IA-1
      GO TO 11
9     IA2=IA
      GO TO 11
10    IA2=IA+1
11    IF(WTS.GT.0.0) GO TO 12
      IS2=IS
      GO TO 15
12    IS2=IS+1
15    IF(M.EQ.2) GO TO 16
      COEF1=CADS1(IS,IA)
      CCEF2=CADS1(IS2,IA)
      GO TO 18
16    CCEF1=CFDS1(IS,IA)
      CCEF2=CFDS1(IS2,IA)
18    COEF3=(COEF2-COEF1)*WTS+COEF1
      IF(M.EQ.2) GO TO 20
19    CCEF1P=CADS1(IS,IA2)
      CCEF2P=CADS1(IS2,IA2)
      GO TO 22
20    CCEF1P=CFDS1(IS,IA2)
      CCEF2P=CFDS1(IS2,IA2)
22    CCEF3P=(CCEF2P-COEF1P)*WTS+COEF1P
      COEF3=(COEF3P-COEF3)*ABS(WTA)+COEF3
      THETA1=THETA*CONDEG
      RETURN
      END
//L.SYSUT1 DD SPACE=(3500,(100,10))
//L.SYSLMOD DD SPACE=(3500,(100,10,1))
//G.FT06F001 DD SPACE=(CYL,(3))
//G.AUXDATA DD *
0.018
0.024
0.019
0.017
0.024
0.0135
0.017
0.023
0.016
0.016
0.022
0.0165
0.016
0.022
0.017
0.015
0.021
0.017
0.015
0.020
0.017
0.014
0.020
0.0175
0.014
0.019
0.018
0.013

```


0.018
0.018
0.013
0.018
0.019
0.013
0.018
0.020
0.013
0.018
0.020
0.013
0.019
0.021
0.013
0.020
0.022
0.0135
0.020
0.023
0.014
0.022
0.025
0.014
0.023
0.026
0.015
0.024
0.028
0.016
0.026
0.030
0.0175
0.0275
0.032
0.020
0.030
0.035
0.021
0.032
0.0375
0.023
0.034
0.040
0.025
0.037
0.044
0.028
0.040
0.0475
0.030
0.044
0.052
0.034
0.047
0.055
0.036
0.051
0.059
0.040
0.054
0.068
0.044
0.058
0.067
0.047
0.063
0.070
0.050
0.065
0.074
0.025

0.026
0.027
0.024
0.025
0.026
0.023
0.023
0.024
0.020
0.021
0.022
0.018
0.019
0.021
0.0165
0.0185
0.020
0.015
0.017
0.018
0.014
0.015
0.0175
0.013
0.0145
0.013
0.013
0.014
0.017
0.011
0.013
0.018
0.010
0.012
0.018
0.008
0.012
0.019
0.007
0.012
0.020
0.006
0.012
0.021
0.005
0.013
0.023
0.005
0.0135
0.028
0.005
0.014
0.026
0.0055
0.015
0.027
0.006
0.016
0.030
0.0065
0.0175
0.0325
0.007
0.020
0.035
0.008
0.022
0.038
0.010
0.0245
0.043
0.012

0.0265
0.047
0.014
0.0295
0.054
0.016
0.033
0.060
0.018
0.037
0.070
0.021
0.042
0.078
0.028
0.048
0.084
0.026
0.056
0.093
0.032
0.067
0.10
0.036
0.08
0.11
0.021
0.021
0.0215
0.0205
0.0205
0.021
0.020
0.020
0.0205
0.018
0.018
0.019
0.017
0.0175
0.018
0.0165
0.017
0.0175
0.015
0.0155
0.016
0.014
0.0145
0.0155
0.0135
0.014
0.015
0.0125
0.013
0.0145
0.010
0.012
0.015
0.0095
0.011
0.015
0.008
0.0105
0.016
0.0075
0.010
0.017
0.006
0.0105
0.0195
0.005

0.011
0.022
0.0045
0.012
0.024
0.0045
0.013
0.028
0.005
0.0145
0.031
0.005
0.0165
0.035
0.006
0.020
0.041
0.008
0.023
0.048
0.010
0.027
0.055
0.012
0.031
0.064
0.015
0.036
0.078
0.019
0.044
0.093
0.022
0.051
0.10
0.028
0.060
0.10
0.035
0.075
0.10
0.039
0.084
0.10
0.045
0.092
0.10
0.05
0.095
0.10
0.056
0.10
0.10
0.25
0.30
0.345
0.41
0.46
0.52
0.56
0.62
0.65
0.70
0.78
0.25
0.295
0.34
0.38
0.425
0.47
0.52
0.55

0.60
0.63
0.68
0.25
0.29
0.325
0.36
0.40
0.43
0.47
0.50
0.545
0.575
0.62
0.25
0.28
0.32
0.345
0.37
0.41
0.44
0.47
0.50
0.54
0.57
0.25
0.28
0.31
0.34
0.36
0.40
0.43
0.45
0.48
0.51
0.54
0.25
0.28
0.31
0.34
0.36
0.39
0.42
0.45
0.47
0.50
0.53
0.25
0.28
0.31
0.34
0.36
0.40
0.43
0.45
0.48
0.51
0.54
0.25
0.28
0.32
0.345
0.37
0.41
0.44
0.47
0.50
0.54
0.57
0.25
0.29
0.325

0.36
0.40
0.43
0.47
0.50
0.54⁵
0.57⁵
0.62
0.25
0.29⁵
0.34
0.38
0.42⁵
0.47
0.52
0.55
0.60
0.63
0.68
0.25
0.30
0.34⁵
0.41
0.46
0.52
0.56
0.62
0.65
0.70
0.78
0.05
0.11
0.17
0.23
0.29
0.35
0.40
0.46
0.52
0.58
0.64
0.05
0.10
0.15
0.19⁵
0.24⁵
0.29
0.34
0.38
0.44
0.48
0.54
0.05
0.09⁵
0.14
0.17
0.21
0.25
0.28
0.33
0.36
0.40
0.45
0.05
0.08
0.13
0.15
0.18
0.22
0.25
0.28
0.32

0.35
0.38
0.05
0.08
0.11
0.14⁵
0.17
0.20
0.23
0.26
0.29
0.33
0.35
0.05
0.07
0.11
0.14
0.17
0.19⁵
0.22
0.25
0.32⁵
0.30
0.33
0.05
0.08
0.11
0.14⁵
0.17
0.20
0.23
0.26
0.29
0.33
0.35
0.05
0.08
0.13
0.15
0.18
0.22
0.25
0.28
0.32
0.35
0.38
0.05
0.09⁵
0.14
0.17
0.21
0.25
0.28
0.33
0.36
0.40
0.45
0.05
0.10
0.15
0.19⁵
0.24⁵
0.29
0.34
0.38
0.44
0.48
0.54
0.05
0.11
0.17
0.23

0.29
0.35
0.40
0.46
0.52
0.58
0.64

//PLCT.SYSIN DD *
RESPONSES WITH HELM STEP COMMAND

RIBEIRO

0.0	300.0	-500.0	300.0	5.0	6.0	5
-----	-------	--------	-------	-----	-----	---

LIST OF REFERENCES

1. A thesis, Simulation of Hydrofoil Performance in Calm Water, by Gary Dee Hickox.
2. A thesis, The Simulation of Hydrofoil Performance, by Jitt Na Nagara.
3. The Boeing Company Report U 141949, Hydrofoil Simulation Equations Study, by J.J.Jamieson, December 1966.
4. The Boeing Company Report U 141948, Performance Criteria and Test Report for Hydrofoil Craft, by J.J.Jamienson, December 1966.
5. The Boeing Company Report U 150981, PHM Foilborne Ship Motion Simulation Equations, by R.H.Mitchell and I.A. Hirsch, August 1972.

INITIAL DISTRIBUTION LIST

	No. Copies
1. Defense Documentation Center Cameron Station Alexandria, Virginia 22314	2
2. Library, Code 0212 Naval Postgraduate School Monterey, California 93940	2
3. Department Chairman, Code 52 Department of Electrical Engineering Naval Postgraduate School Monterey, California 93940	2
4. Professor George J. Thaler, Code 52Tr Department of Electrical Engineering Naval Postgraduate School Monterey, California 93940	5
5. Professor Alex Gerba, Jr., Code 52Gz Department of Electrical Engineering Naval Postgraduate School Monterey, California 93940	1
6. Lieutenant Jose A. Ribeiro, Portuguese Navy Avenida Paris, 4, 4 Lisbon-1, Portugal	3



Thesis
R3737
c.1
Ribeiro
Hydrofoil simulation
in six degrees of free-
dom.

103971

18 MAY 83

24030

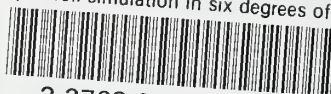
28355

Thesis
R3737
c.1
Ribeiro
Hydrofoil simulation
in six degrees of free-
dom.

103971

thesR3737

Hydrofoil simulation in six degrees of f



3 2768 000 99045 1

DUDLEY KNOX LIBRARY